UNIVERSITY OF CALIFORNIA
SANTA CRUZ

SLEEPING WHILE DIVING: TOOLS TO DETECT, ANALYZE, AND VISUALIZE SLEEP IN WILD SEALS

A dissertation submitted in partial satisfaction
of the requirements for the degree of

DOCTOR OF PHILOSOPHY

in

ECOLOGY AND EVOLUTIONARY BIOLOGY

by

Jessica M. Kendall-Bar

June 2022

The Dissertation of
Jessica M. Kendall-Bar is approved:

_____
Professor Terrie M. Williams, Chair

_____
Professor Daniel P. Costa

_____
Professor Craig Heller

_____
Professor Peter Tyack

_____
Professor Peter Raimondi

_____
Peter Biehl
Vice Provost and Dean of Graduate Studies

TABLE OF CONTENTS

LIST OF TABLES

LIST OF FIGURES

SLEEPING WHILE DIVING: TOOLS TO DETECT, ANALYZE, AND VISUALIZE SLEEP IN WILD SEALS

Jessica M. Kendall-Bar

ABSTRACT

Wild animals have evolved extreme physiological adaptations to balance the risks of starvation, predation, and exhaustion. Sleeping animals sacrifice food while vulnerable to predators. Marine mammals at sea balance the need to feed with the added challenge of surfacing to breathe, where predators lie in wait. Northern elephant seals (*Mirounga angustirostris*) travel thousands of kilometers, performing long dives to gather sustenance before returning to land to fast while they breed or molt. For my dissertation, I engineered a device that measures when, how, and how much these animals sleep at sea- the first recording of sleep in a wild marine mammal. Across their amphibious habitat, seals slept as much as 14 hours per day on land in the lab and as little as 0 hours per day at sea. Analytical methods derived from these results allow us to interpret hundreds of diving records over a 20-year dataset to find that seals sleep about 2 hours per day during >220-day foraging trips. At sea, elephant seals leverage their extreme breath-holding capacity to create a safe sleeping niche, up to 377 meters below the surface. I developed a process to transform data into animated 3D visualizations that display physiology alongside behavior. As new technology facilitates the collection of large ecophysiology datasets, we must also advance sensor technology, analytical workflows, and visualization techniques to better interpret this data. My dissertation creates and implements novel instruments and techniques that record, characterize, and visualize the physiology and behavior of wild animals to facilitate comparative neurophysiology research within conservation and translational medicine.

DEDICATION

To my parents and brother for their endless support and patience

ACKNOWLEDGEMENTS

I would like to begin by extending my deepest gratitude to my two advisors, Drs. Terrie Williams and Dan Costa, for their support and mentorship. My work and the network and community I have built during my time at UCSC would not have been possible without them. I am very grateful to Dan for the opportunity to be a part of the long-term elephant seal research program at Año Nuevo State Park and glean information from its unique long-term dataset. Likewise, I am thankful to Terrie for the opportunity to collaborate with trainers and animals with the Marine Mammal Physiology Project. I am very fortunate to have two advisors who are personally invested in the intersection of art and science and who have supported and initiated artistic collaborations, including scientific animations and the design of the "Photos from the Field" exhibit at the Seymour Center.

The research community at UC Santa Cruz and beyond has brought many other wise advisors into my life. First and foremost, I would like to thank Dr. Mike Beck for welcoming me into his lab group, with whom I've contemplated science communication strategies for over four years during my PhD. I'll never forget the heated discussions about mortgages, climate change, Nature-Based Solutions, and color palettes. Thank you for the careful emphasis you place on communication, effective team management, and brilliantly concise writing (not my forté). Your team has been like a family to me (not just because I live with some of them) and has been an energy-giving interdisciplinary melting pot of ideas and inspiration.

Next, I would like to thank the other interdisciplinary advisors and organizations at UCSC that have encouraged me to find a niche outside of biology at the intersection of

art, programming, and science. My committee member Dr. Pete Raimondi has tolerated (and even supported) my artistic meanderings, allowing me to distract myself from my PhD by drawing figures for his students with my favorite (don't tell the seals) study system- giant kelp! Drs. Karen Holl & Juniper Harrower have created fertile grounds for art-science collaboration within the Norris Center at UCSC. My art-science residency with Dr. Paloma Medina led me to illustrate a precious children's book where we shared a queer underwater world with a similarly beautiful queer community within Santa Cruz. This rippled into fruitful science communication workshops for queer and trans youth at the Diversity Center of Santa Cruz and the Exploratorium. Dr. Angus Forbes of UCSC's Creative Coding Lab introduced me to the field of data visualization, encouraging me to devote a whole chapter to animation- a dream come true. Jennifer Parker & Erika Check-Hayden, Directors of UCSC OpenLab and the Science Communication Program, have provided steadfast support and advocacy for my desire to teach data-driven animation– I look forward to this journey with both of you.

Beyond UCSC, I have found inspiration, support, and mentorship from experts around the world, who specialize in sleep and whales. Thank you to the ~whale people~ for your insights on processing large datasets and for your generosity in welcoming me (a seal person) into your cetacean behavioral-ecophysiology community, especially my committee member Dr. Peter Tyack, Drs. Jeremy Goldbogen, Matt Schalles, Jim Finneran, Dorian Houser, Dave Cade, and Max Czapanskiy. Within the sleep science community, Drs. Oleg Lyamin & Jerry Siegel graciously offered an opportunity to learn about marine mammal sleep in Russia, where unihemispheric sleep in dolphins was first discovered. Without that experience in 2016, I wouldn't be where I am today.

Thank you, Oleg, for patiently answering my questions ever since, providing measured skepticism, and pushing my science to be as bulletproof as I can make it. The students, trainers, scientists, and caretakers at Utrish Marine Mammal Station warmly welcomed me into their community and homes with borscht, French music, Russian lessons, and tales from decades of cetacean ecophysiology research. Thank you to the broader sleep science community for your help in advancing new tools and interesting discussions about the future of sleep science: Drs. John Lesku, Niels Rattenborg, Paul-Antoine Libourel, Michael Harris, Sam Ridgway, and my committee member Dr. Craig Heller.

I would like to thank several mentors and peers for their collaboration and assistance. Thank you to Julie Pitman for hooking me up to EEG machines, in and out of the ocean, for your wit and humor, and for teaching me the ropes of sleep science. Thank you to senior Costa lab members for your patience as I bombard you with questions: to Dr. Rachel Holser for demonstrating how to elegantly navigate crowded seal colonies during breeding season procedures and how to manage time, teams, and the stress of a PhD with grace; to Ana Valenzuela Toro for geeking out over seal skulls, data visualization, and maps with me; to Arina Favilla for being in it with me- from lugging bulky objects to cleaning seal poop- while expertly and gracefully juggling a million other things; to Dr. Roxanne Beltran for being an inspirational early career role model and sharing your coding and mind-mapping expertise; and to Dr. Patrick Robinson for allowing me to learn from your excellent interpretive science outreach and seal herding magic. Thank you to other Costa, Williams, and Beltran lab mates for all the laughs, troubleshooting, and solidarity: Emily, Andrew, Lilian, Philippine, Joffrey,

Theresa ('T1'), Logan, Steph, Kelly, Theresa ('T2'), Jordann, Luis, Flo, Haley, Allison, and Dan (P.).

I would like to acknowledge the students, volunteers, and researchers who have all contributed to the long-term Año Nuevo elephant seal research program. I thank Año Nuevo State Park and the Año Nuevo UC Natural Reserve for their ongoing support. I am thankful for the opportunity to work with and learn from an incredible crew of field researchers including G. McDonald, D. Crocker, R. Jones, L. Keehan, and J. Mulsow. TMMC veterinarians and volunteers were instrumental in the pilot testing for my project, and I am grateful for the time and efforts of E. Whitmer, S. Whoriskey, E. Trumbull, D. Whittaker, F. Gulland, and S. Pattison. I also want to thank Long Marine Lab staff and volunteers for facilitating lab-based studies, especially D. Casper, R. Skrovan, N. Moore, C. Reichmuth of the Pinniped Lab, and T. Kendall of the Marine Mammal Physiology Project. I would like to thank P. Guerrero, E. Slattery, J. Bielke, colleagues at Ocean Innovations, Scripps Institution of Oceanography, and the Shorter lab at University of Michigan for engineering support and mentorship.

I want to acknowledge my many mentees, a group of dedicated bright minds that bring joy and purpose to my life. This list includes my team of sleep scoring mentees: Ritika Mukherji, Catherine Lopez, and Jordan Nichols. I've had the pleasure of mentoring other intelligent, creative, and motivated UCSC undergraduates through the Center to Advance Mentored, Inquiry-Based Opportunities (CAMINO 2020) and other programs including D. Lozano, C. Munro, M. Krieg, R. Cuthbertson, A. Conklin, A. Manriquez, I. Shukla, and A. Gutierrez. I am thankful to have worked with smart and motivated high

school student mentees interested in programming and visualization through the Science Internship Program (SIP 2021) including J. Das, H. Li, and R. Srinivasan.

Funding for instrumentation and field work was provided by the National Science Foundation (NSF) (grant no. 1656282), the Strategic Environmental Research and Development Program (SERDP) (grant no. RC20-C2-1284), Office of Naval Research (ONR) (grant no. N00014-18-1-2822), ONR Defense University Research Instrumentation Program (DURIP) (grant no. N00014-19-1-2178), Women Diver's Hall of Fame's Laurel Clark Sea to Space Physiology Research Grant, National Geographic Early Career Grant, Steve & Rebecca Sooy Graduate Research Fellowship, the Achievement Rewards for College Scientists (ARCS), the NSF Graduate Research Fellowship Program, and the Special Research Grant (SRG) from the Committee on Research at UC Santa Cruz.

Equally critical was the emotional support that I received from my family, friends, and the EEB community. Thank you for the early-morning writing accountability sessions (Julia, Matt, Merly, & Laura), mid-morning pep talks with EEB staff (Stephanie, Judy, and Jacqueline), mid-day coding interventions (Matt, Tanya, Calvin, Mallarie, Merly), and of course the sunset surfs and beers (Julia, Rae, & Christa). To friends and my loved ones: Papa- nos conversations quotidiennes m'apprennent la belle complexité du monde, dans l'académie et en dehors ; Maman- nos bébés (la maison de Nicolas et ma thèse) nous ont couté de l'amour et de la peine, mais célèbrerons leur aboutissement ensemble cet été ; Nicolas- merci d'être la "colle" qui nous connecte (ni collé ni cola), le remède immédiat qui adoucit l'anxiété et la tristesse ; Nicole- your screenwriting approach to science communication works wonders, we are grateful to learn from your

creative mind; Taylor- from sailboats, to the kelp forests beneath them and tiny islands that can barely fit the trees they house, thank you for being there for me; Jacey, Lindsay, & Sky- thanks for jumping in the ocean with me, wherever and whenever- the threads you three weave between art and science amaze and inspire me; Kalina- since 7th grade, thank you for sharing your warmth and curiosity for the world; casa 212 (Erin, Megan, Pelayo, Patricio, & more)- thank you for providing a quiet nest by the sea for me to write this thing; the ladies of 112 Kennan (Kelsey, Sophie, Haley, Pravina, Emmy, Rose, Jacey, Gaby, & more)- thank you for the dance parties, home-improvement projects, and skeleton decorations (and for putting up with the ~sprawl~ of my seal-sleep-recording equipment); the Hebardians (Dan, Dray, Dani, Ken, & more)- thank you for the delicious meals, long meandering walks, peaceful moments with the chickens, and for bringing music back into my life.

My family has lovingly supported me in pursuing science. They recognized the magnetic pull the ocean had on me at an early age and they indulged me by letting me explore the Pacific coast through backpacking trips and marine biology summer research camps in Alaska, Catalina, and Santa Cruz. My grandpa, a physicist, periodically sends news clippings and generous research grants. My cousins, aunts, and uncles patiently listen to me find the words to explain what I do in French. Since attending a Seymour Center summer camp together when we were kids, my brother has teased me about the obsession I have with dolphins and seals- figuring out what they do and where they go. Today, he teases me still, but I think I've unlocked his curiosity a bit. He has generously shared his industry animation programming expertise (and even co-authored one of my chapters). Thank you, Nick, for indulging me and for sharing your

wisdom with me. My parents have provided unwavering support of my academic interests, messy art projects, and wacky experiments. They both strongly value education and generously contribute their own unique and artistic perspectives; my dad as a hacker telecommunications professor/social justice advocate and my mom as a sustainability-focused architect. Thank you, Papa and Maman, for the love, creativity, patience, and wisdom you generously offer, day to day.

I also want to acknowledge the extent to which my work has been facilitated by my privilege, including the financial support of my family. The privilege to explore coastal ecosystems, engage in summer research programs, and extracurricular research opportunities, is not universal. The onus is on those holding this privilege to tackle the systemic hurdles to underserved communities by reducing financial burdens and creating more inclusive learning environments. These systemic barriers silence and erase the experience, contributions, and knowledge of underserved groups, including the Indigenous people on whose land we work. The work I performed as part of my dissertation, at Año Nuevo State Park and at UC Santa Cruz, unfolded within the unceded territory of the Awaswas-speaking Uypi Tribe. The Amah Mutsun Tribal Band, comprised of the descendants of Indigenous people taken to missions Santa Cruz and San Juan Bautista during Spanish colonization of the Central Coast, is today working hard to restore traditional stewardship practices on these lands and heal from historical trauma (UC Santa Cruz, 2022). This UCSC land acknowledgment and the ongoing work by the university with the Amah Mutsun Tribal Band is a first step.

There is more work to be done, by myself, and everyone in academia to increase diversity, equity, and inclusion in STEM. As part of the course I am developing, I am

pursuing funding to compensate female, queer, trans, and/or people of color guest speakers who are domain experts at the intersection of art and science. This includes a native Alaskan artist who will speak on the importance of place-based storytelling. We have secured funding to offset several students' tuitions to promote participation for queer, Latinx, and African American art-science communicators. As part of an ongoing collaboration with the North Pacific Research Board and Sitka Tribe of Alaska, we will be working to weave together illustrations and narrations from native Alaskan artists and storytellers, into animations alongside western science, to share a more complete view of the ecology of local ecosystems. I acknowledge that there is more work to do to educate myself and to pursue this work ethically and effectively. "Quyana" to Ilgavak (Peter Williams), Taylor White, the North Pacific Research Board, and the Sitka Tribe of Alaska, for the opportunity to work together, learn from you, and share your knowledge.

INTRODUCTION

BACKGROUND

Extreme divers such as seals, penguins, and cetaceans have independently evolved physiological adaptations to resist severe oxygen depletion (venous O_2 partial pressure <2mmHg in elephant seals) (*1*) and constant vigilance with little sleep (>2 months of high vigilance and low sleep in new dolphin mothers) (*2*). By investigating the behavior and mechanisms underlying these physiological extremes, we can guide the development and application of technologies that treat humans suffering from oxygen- and sleep-mediated pathology. To ensure the validity of this translational research, we can leverage the similarity in neuropathological presentation between humans and cognitively advanced marine mammals, such as similarities in epileptic pathology in humans and sea lions. However, we need to develop biosensing tools, analytical workflows, and visualization frameworks to study animals that push the limits of their physiological capacity. My dissertation presents an integrative approach to answer a central question: **how does the mammal brain survive (and sleep) at sea?**

Captive sleep studies relying primarily on invasive methods (Figure 1.1 & Table 1-3) have uncovered two unusual adaptations to allow sleep at sea (*3*, *4*). While in water, eared seals and dolphins exhibit unihemispheric slow-wave sleep (SWS) (sleep in one hemisphere and wakefulness in the other) and an apparent lack of rapid-eye-movement (REM) sleep that allows animals to surface and breathe while sleeping (*5*–

13). On the other hand, true seals and walruses leverage superior breath-holding capabilities to perform prolonged sleep apneas underwater (*14–19*).

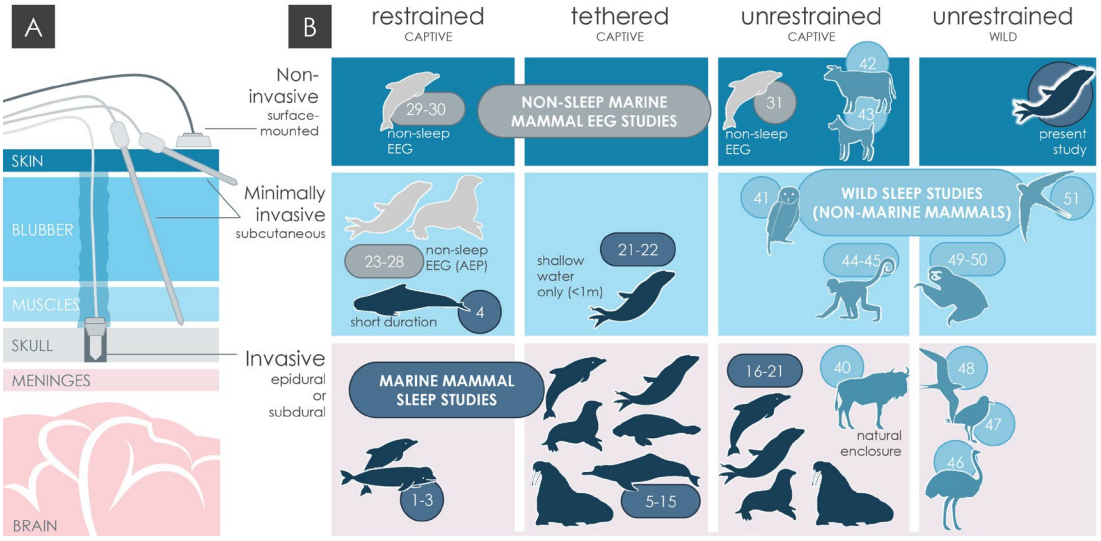

Figure 0.1. Electrophysiological methods over time, highlighting the need for non-invasive sleep studies of wild marine mammals. (A) Schematic diagram showing progressive invasiveness from surface-mounted electrodes (least invasive) to needle electrodes, epidural electrodes placed on the surface of the skull or dura, and subdural electrodes placed beneath the dura in the cortex or inside the brain (most invasive). (B) Diagram showing where the electrophysiological studies from Chapter 2 fall in terms of invasiveness and animal mobility, demonstrating that no sleep studies have used non-invasive methods in the wild. Numbers refer to the citations in Chapter 2.

STUDY SYSTEM

This dissertation examines sleep in the deepest diving pinniped. Northern elephant seals (*Mirounga angustirostris*) routinely undergo near-complete oxygen depletion (*20*). They spend 98% of their time underwater over 7-month foraging trips (*21*, *22*). 2 studies in the 1990s recorded electrophysiological sleep in northern elephant seal pups using minimally invasive needle electrodes and a tethered system. They found that most sleep occurred while the animal was holding its breath. While at

sea, elephant seals perform drift dives where they passively float at depth, either upwards or downwards, depending on their buoyancy. I designed a portable EEG logger to detect brain activity through an iterative design process to search for conclusive, electrophysiological evidence of sleep at sea.

DISSERTATION SUMMARY

Chapter 1 describes my iterative design process by providing material recommendations, technical illustrations, and signal processing techniques (*23*, *24*). After refining our methods with anesthetized northern elephant seals (*Mirounga angustirostris*) (N=11), I engineered a custom headcap and encapsulation for a Neurologger3 (©Evolocus) device to record several days of brain, eye, muscle, and heart activity, 3-axis inertial motion sensing, and environmental data (pressure, temperature, GPS, and illumination). I describe the system's performance over multiple days in 12 freely moving northern elephant seals, sleeping on land, in shallow water, on the continental shelf (< 250 m), and in the open ocean (> 250 m – 444 m). We leverage advances in signal processing by applying Independent Components Analysis (ICA) and inertial motion sensor calibrations to maximize signal quality across large, multi-day datasets. Our study adds to the suite of animal-borne sensors available to scientists seeking to understand the physiology and behavior of wild animals in the context in which they evolved.

In Chapter 2, I characterize the sleep patterns of northern elephant seals from land to sea, highlighting the comparative implications of their sleep, representing an

extreme form of natural sleep apnea. Periods of electrophysiological sleep (slow-wave sleep and rapid-eye-movement sleep) were recorded in seals on land, floating in shallow water, on the ocean floor in shallow water and on the continental shelf, and during open ocean drift dives (N=13 seals). While there was considerable variation in sleep patterns across individuals, total sleep time was lowest while sleeping at sea (as little as 0 h/day) and highest while sleeping on land (as much as 14 h/day). Levels of sleep at sea are the lowest recorded in any wild mammal (*25*). This integrative study of natural sleep apnea in northern elephant seals can provide insights into human sleep pathology and set the stage for translational studies of sleep science.

In Chapter 3, to maximize the translational potential of these comparative studies, I developed new analytical software to create data-driven visualizations of physiology and behavior (*26*, *27*). I established a creative pipeline to incorporate physiological and behavioral data from contemporary marine mammal research into data-driven animations, leveraging industry tools and custom scripts to promote scientific insights, public awareness, and conservation outcomes. These visualizations help scientists identify responses to disturbance, compare diverse study systems, increase public awareness of human-caused disturbance, and help build momentum for targeted conservation efforts backed by scientific evidence.

REFERENCES

1. P. J. Ponganis, T. K. Stockard, J. U. Meir, C. L. Williams, K. V. Ponganis, R. P. van Dam, R. Howard, Returning on empty: extreme blood O_2 depletion underlies dive capacity of emperor penguins. *J Exp Biol*. **210**, 4279–4285 (2007).

2. O. Lyamin, J. Pryaslova, P. Kosenko, J. Siegel, Behavioral aspects of sleep in bottlenose dolphin mothers and their calves. *Physiology & Behavior*. **92**, 725–733 (2007).

3. O. I. Lyamin, J. M. Siegel, in *Handbook of Behavioral Neuroscience* (Elsevier, 2019; https://linkinghub.elsevier.com/retrieve/pii/B9780128137437000256), vol. 30, pp. 375–393.

4. O. I. Lyamin, P. R. Manger, S. H. Ridgway, L. M. Mukhametov, J. M. Siegel, Cetacean sleep : An unusual form of mammalian sleep. **32**, 1451–1484 (2008).

5. L. M. Mukhametov, A. Ya. Supin, I. G. Polyakova, Interhemispheric asymmetry of the electroencephalographic sleep patterns in dolphins. *Brain Research*. **134**, 581–584 (1977).

6. L. M. Mukhametov, O. I. Lyamin, I. G. Polyakova, Interhemispheric asynchrony of the sleep EEG in northern fur seals. *Experientia*. **41**, 1034–1035 (1985).

7. L. M. Mukhametov, A. L. Supin, An EEG study of different behavioral states of freely moving dolphins. *Zhurnal Vysshei Nervnoi Deiatelnosti Imeni I P Pavlova*. **25**, 396–401 (1975).

8. O. I. Lyamin, I. S. Chetyrbok, Unilateral EEG activation during sleep in the Cape fur seal, Arctocehalus pusillus. *Neuroscience Letters*. **143**, 263–266 (1992).

9. O. I. Lyamin, P. O. Kosenko, S. M. Korneva, A. L. Vyssotski, L. M. Mukhametov, J. M. Siegel, Fur Seals Suppress REM Sleep for Very Long Periods without Subsequent Rebound. *Current Biology*. **28**, 2000-2005.e2 (2018).

10. O. I. Lyamin, P. O. Kosenko, J. L. Lapierre, L. M. Mukhametov, J. M. Siegel, Fur seals display a strong drive for bilateral slow-wave sleep while on land. *Journal of Neuroscience*. **28**, 12614–12621 (2008).

11. O. I. Lyamin, J. L. Lapierre, P. O. Kosenko, L. M. Mukhametov, J. M. Siegel, Electroencephalogram asymmetry and spectral power during sleep in the northern fur seal. *Journal of Sleep Research*. **17**, 154–165 (2008).

12. S. H. Ridgway, Asymmetry and symmetry in brain waves from dolphin left and right hemispheres: Some observations after anesthesia, during quiescent hanging behavior, and during visual obstruction. *Brain, Behavior and Evolution*. **60**, 265–274 (2002).

13. J. M. Kendall-Bar, A. L. Vyssotski, L. M. Mukhametov, J. M. Siegel, O. I. Lyamin, Eye state asymmetry during aquatic unihemispheric slow wave sleep in northern fur seals (*Callorhinus ursinus*). *PLoS ONE*. **14**, 1–13 (2019).

14. S. H. Ridgway, R. J. Harrison, P. L. Joyce, Sleep and Cardiac Rhythm in the Gray Seal. *American Association for the Advancement of Science*. **187**, 553–555 (1975).

15. W. Milsom, M. Castellini, M. Harris, J. Castellini, D. Jones, R. Berger, S. Bahrma, L. Rea, D. Costa, Effects of hypoxia and hypercapnia on patterns of sleep-associated apnea in elephant seal pups. *The American journal of physiology*. **271**, R1017–R1024 (1996).

16. M. A. Castellini, W. K. Milsom, R. J. Berger, D. P. Costa, D. R. Jones, J. M. Castellini, L. D. Rea, S. Bharma, M. Harris, Patterns of respiration and heart rate during wakefulness and sleep in elephant seal pups. *American Physiological Society*, R863–R869 (1994).

17. A. A. Karamanlidis, O. I. Lyamin, S. Adamantopoulou, P. Dendrinos, First Observations of Aquatic Sleep in the Mediterranean Monk Seal (*Monachus monachus*). *Aquatic Mammals*. **43**, 82–86 (2017).

18. O. I. Lyamin, Sleep in the harp seal (*Pagophilus groenlandica*). Comparison of sleep on land and in water. *Journal of Sleep Research*. **2**, 170–174 (1993).

19. L. M. Mukhametov, A. Supin, I. Poliakova, Sleep of Caspian Seals. *Zhurnal Vysshei Nervnoi Deiatelnosti Imeni I P Pavlova*. **34**, 259–264 (1984).

20. J. U. Meir, C. D. Champagne, D. P. Costa, C. L. Williams, P. J. Ponganis, Extreme hypoxemic tolerance and blood oxygen depletion in diving elephant seals. *American Journal of Physiology-Regulatory, Integrative and Comparative Physiology*. **297**, R927–R939 (2009).

21. P. W. Robinson, D. P. Costa, D. E. Crocker, J. P. Gallo-Reynoso, C. D. Champagne, M. A. Fowler, C. Goetsch, K. T. Goetz, J. L. Hassrick, L. A. Hückstädt, C. E. Kuhn, J. L. Maresh, S. M. Maxwell, B. I. McDonald, S. H. Peterson, S. E. Simmons, N. M. Teutschel, S. Villegas-Amtmann, K. Yoda, Foraging behavior and success of a mesopelagic predator in the northeast Pacific Ocean: insights from a data-rich

species, the northern elephant seal. *PloS one*. **7** (2012), doi:10.1371/journal.pone.0036728.

22. P. W. Robinson, S. E. Simmons, D. E. Crocker, D. P. Costa, Measurements of foraging success in a highly pelagic marine predator, the northern elephant seal. *Journal of Animal Ecology*. **79**, 1146–1156 (2010).

23. J. M. Kendall-Bar, R. Mukherji, J. Nichols, C. Lopez, D. A. Lozano, J. K. Pitman, R. R. Holser, R. S. Beltran, M. Schalles, C. L. Field, S. P. Johnson, A. L. Vyssotski, D. P. Costa, T. M. Williams, Eavesdropping on the brain at sea: development of a surface-mounted system to detect weak electrophysiological signals from wild animals. *Animal Biotelemetry*. **10**, 16 (2022).

24. J. Kendall-Bar, Eavesdropping on the Brain at Sea - Github Repository. *GitHub* (2021), (available at https://github.com/jmkendallbar/Eavesdropping-on-the-Brain-at-Sea).

25. N. Gravett, A. Bhagwandin, R. Sutcliffe, K. Landen, M. J. Chase, O. I. Lyamin, J. M. Siegel, P. R. Manger, Inactivity/sleep in two wild free-roaming African elephant matriarchs – Does large body size make elephants the shortest mammalian sleepers? *PLoS ONE*. **12**, e0171903 (2017).

26. J. Kendall-Bar, N. Kendall-Bar, A. G. Forbes, G. McDonald, P. J. Ponganis, C. Williams, M. Horning, A. Hindle, H. Klinck, R. S. Beltran, A. S. Friedlaender, D. Wiley, D. P. Costa, T. M. Williams, Visualizing Life in the Deep: A Creative Pipeline for Data-Driven Animations to Facilitate Marine Mammal Research, Outreach, and Conservation. *IEEE VIS Arts Program*. **2021**, 10 (2021).

27. J. Kendall-Bar, *Visualizing Life in the Deep: code repository for visualizing marine mammal tag data* (2021; https://github.com/jmkendallbar/VisualizingLifeintheDeep).

Chapter 1. **Eavesdropping on the brain at sea: the development of a non-invasive technique to maximize the detection of weak electrophysiological signals from wild animals**

Jessica M. Kendall-Bar[1], Ritika Mukherji[2], Jordan Nichols[1], Catherine Lopez[3], Daniel A. Lozano[1], Julie K. Pitman[4], Rachel R. Holser[5], Roxanne S. Beltran[1], Matt Schalles[6], Cara L. Field[7], Shawn P. Johnson[8], Alexei L. Vyssotski[9], Daniel P. Costa[1], and Terrie M. Williams[1].

Affiliations:

1: Ecology and Evolutionary Biology, University of California Santa Cruz, CA
2: Miranda House, University of Delhi, India
3: Scripps Research Institute, La Jolla, CA
4: Sleep Health MD, Santa Cruz, CA
5: Institute of Marine Sciences, University of California Santa Cruz, CA
6: Neuroscience Institute, Carnegie Mellon University, Pittsburgh, PA
7: The Marine Mammal Center, Sausalito, CA
8: Sea Change Health, Sunnyvale, CA
9: Institute of Neuroinformatics, University of Zurich and Swiss Federal Institute of Technology (ETH), Zurich, Switzerland

The text of this dissertation includes a reprint of the following published material, with permission from its co-authors:

J. M. Kendall-Bar, R. Mukherji, J. Nichols, C. Lopez, D. A. Lozano, J. K. Pitman, R. R. Holser, R. S. Beltran, M. Schalles, C. L. Field, S. P. Johnson, A. L. Vyssotski, D. P. Costa, T. M. Williams, Eavesdropping on the brain at sea: development of a surface-mounted system to detect weak electrophysiological signals from wild animals. *Animal Biotelemetry*. **10,** 16 (2022). DOI: ***10.1186/s40317-022-00287-x***

1.1 ABSTRACT

Despite rapid advances in sensor development and technological miniaturization, it remains challenging to non-invasively record small-amplitude electrophysiological signals from an animal in its natural environment. Many advances in ecophysiology and biologging have arisen through sleep studies, which rely on detecting small signals over multiple days and minimal disruption of natural animal behavior. This paper describes the development of a surface-mounted system that has allowed novel electrophysiological recordings of sleep in wild marine mammals. We discuss our iterative design process by providing sensor-comparison data, detailed technical illustrations, and material recommendations. We describe the system's performance over multiple days in 12 freely-moving northern elephant seals (Mirounga angustirostris) sleeping on land and in water in captivity and the wild. We leverage advances in signal processing by applying Independent Components Analysis and inertial motion sensor calibrations to maximize signal quality across large (>10 gigabyte), multi-day datasets. Our study adds to the suite of biologging tools available to scientists seeking to understand the physiology and behavior of wild animals in the context in which they evolved.

1.2 INTRODUCTION

Technological advances have allowed the creation and refinement of small, sensitive, rugged devices that can record physiological signals from free-moving animals in their natural environment (1–8). Despite these advances, reliable signal detection with minimally invasive methods is challenging. This is especially true in marine mammals, where animals' thick tissue layers and the conductive saltwater environment diminish electrical signals. Researchers often opt for invasive methods that pierce the skin and are placed within tissues, the bloodstream, the skull, or the brain to obtain more reliable signals (4,9,10). Invasive procedures pose greater infection risk, raise ethical concerns, and are especially undesirable in the wild where continuous observation and intervention are impossible. The lack of non-invasive methods for neurophysiological studies has limited our understanding of ecophysiology in the wild. The development of new techniques will allow us to observe the neurophysiological underpinning of animal behavior in the wild.

Recent efforts to record sleep in the wild coincide with significant advances in sensor technology and miniaturization (4,5,10–12). Electrophysiological sleep recordings rely on detecting small changes in brain activity (several orders of magnitude smaller than typical heart signals) and benefit from multiple-day recordings of freely behaving animals in the wild. Sleep studies rely on the use of electroencephalogram (EEG) to record changes in brain activity from "large amplitude" (~75 μV peak-to-peak amplitude in humans) slow-wave sleep (SWS: 0.5-4Hz) to small

amplitude, high-frequency activity during waking or rapid-eye-movement (REM) sleep. Sleep states are distinguished from one another using electrooculogram (eye) activity, electromyogram (muscle) activity, accelerometry, and heart rate variability (13).

In addition to promoting technological advancement, studying sleep in the wild contributes to our knowledge of its function and evolution, with implications for conservation and comparative medicine (14–16). Across the animal kingdom, sleep provides critical restorative functions from energy conservation, immune function, metabolism, memory, and learning (14,17). Sleep quota differences between captivity and wild settings highlight the importance of quantifying in-situ sleep patterns (4,11). In-situ multi-generational sleep recordings have demonstrated that hereditary sleep adaptations can improve reproductive success (12). Marine mammal sleep studies suggest that unihemispheric sleep may provide similar homeostatic functions as REM sleep through the apparent lack of REM sleep in cetaceans and lack of REM rebound in fur seals (18,19). Wild marine mammal sleep studies can further investigate extreme forms of sleep to shed light on sleep phenology, evolution, and pathology.

Although surface recordings for human clinical EEG applications are widespread, most animal EEG studies use implanted electrodes (4,20–23). Only a handful of animal sleep studies have employed non-invasive EEG methods, and none of these studies were performed in the wild (18,20–35) (Figure 1.1 & Supplementary Table 1). While surface sensors are preferable, the signals obtained are 8-fold lower amplitude, accuracy, and precision than implanted electrodes on the skull (36,37). To

maximize signal quality from less sensitive surface sensors, we can leverage improvements in quantitative signal processing that have advanced our ability to identify, filter, and remove sources of electrical noise while identifying and isolating signals of interest. These algorithms, such as Independent Components Analysis (ICA), show promise towards automating artifact identification and removal in human neuroscience studies (38–41).

Beyond maximizing signal quality, we need robust, field-ready dataloggers to enable electrophysiological studies of wild animals. Despite advances in biologging within and outside of sleep science, few if any pressure-proofed devices are equipped to accept several (>2) independent electrophysiological signals (18–35,42–45). The development of pressure-proofed multi-channel electrophysiology loggers will allow us to track multiple bioelectric parameters simultaneously. Our study addresses these knowledge gaps by providing advances along multiple dimensions to create a system for sensitive electrophysiological signal detection in wild marine mammals: (1) the ***validation of surface-mounted electrodes*** to detect brain activity, (2) the ***application of sophisticated signal processing techniques*** to maximize signal quality, and (3) the ***creation of a portable, robust, and pressure-proofed device*** for multi-channel electrical recordings. We developed a method to record electrophysiological sleep over multiple days in a wild animal with a thick blubber layer amidst conspecifics and in a deep ocean environment. We discuss our iterative process from selecting electrode types, configurations, and materials to engineering a portable system in captive and

wild environments. We provide a systematic framework that capitalizes on technological advances to facilitate future sleep studies on wild marine mammals.

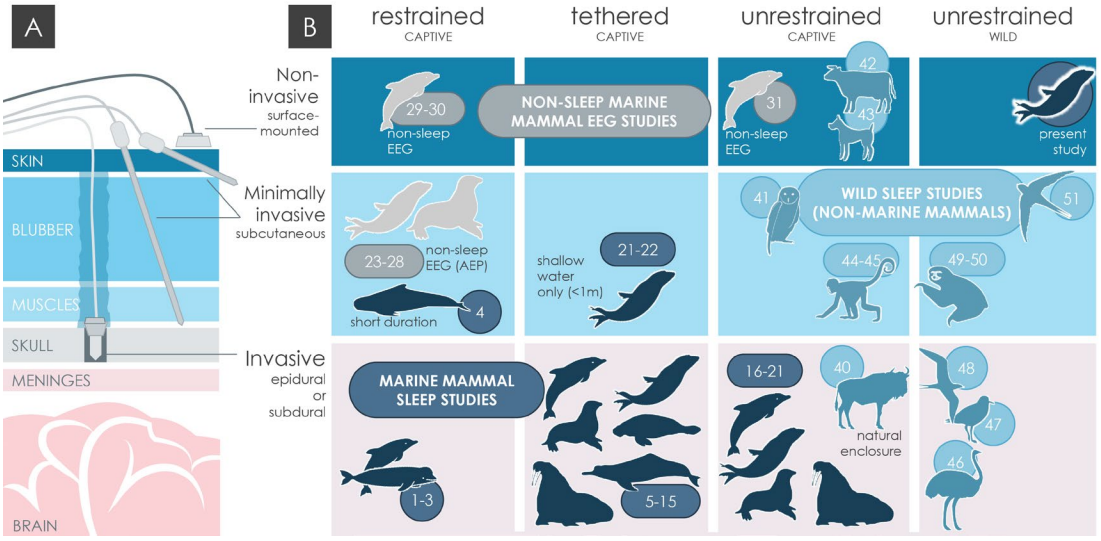

Figure 1.1. Electrophysiological methods over time, highlighting the need for non-invasive sleep studies of wild marine mammals. (A) Schematic diagram showing progressive invasiveness from surface-mounted electrodes (least invasive) to needle electrodes, epidural electrodes placed on the surface of the skull or dura, and subdural electrodes placed beneath the dura in the cortex or inside the brain (most invasive). (B) Diagram showing where the electrophysiological studies from Table 1 fall in terms of invasiveness and animal mobility, demonstrating that no sleep studies have used non-invasive methods in the wild. Numbers refer to the reference number.

1.3 METHODS

We developed a system for long-term electrophysiological recordings in wild, free-swimming northern elephant seals, Mirounga angustirostris. First, we recorded EEG from anesthetized northern elephant seal pups at The Marine Mammal Center (TMMC- Sausalito, CA) (Table 1-1) (**Phase 1; N=11**). Second, we developed a portable EEG datalogger to record sleep in freely moving juvenile northern elephant seals (**Phase 2; N=12**). We recorded EEG from freely moving seals (**2a**) in the controlled lab

environment at Long Marine Lab (University of California Santa Cruz) and (**2b**) on the beach at Año Nuevo State Park (California, USA). This iterative design process allowed us to test and compare electrode performance (**Phase 1**) and then apply these results to developing our portable device (**Phase 2**). All animal procedures were approved at the federal and institutional levels under National Marine Fisheries Permits #19108, #23188, and #18786 (TMMC), and by the Institutional Animal Care and Use Committee (IACUC) of the University of California Santa Cruz (Costd1709 and Costd2009-2) and The Marine Mammal Center (TMMC #2019-2). All animals were sedated following standard protocols (1,33–34,46–47). Briefly, an induction injection of intramuscular Telazol® [tiletamine and zolazepam] (1 mg/kg) was maintained with doses of Telazol/ketamine/valium as needed.

1.3.1 *Phase 1: Stationary Recordings*

We tested and refined electrode configuration during stationary EEG recordings with 11 anesthetized northern elephant seal weanlings (weaned pups ~3-4 months old) undergoing rehabilitation at TMMC (Table 1-1). Each recording lasted less than an hour and coincided with routine veterinary procedures. Of the 11 anesthetized seals, 2 were deemed unfit for release to the wild by TMMC veterinarians due to congenital defects unrelated to the study and were euthanized via lethal injection (Euthasol® [pentobarbital sodium and phenytoin sodium]). Euthanasia recordings provided an opportunistic assessment of brain wave attenuation. They demonstrated that our electrodes could detect brain activity despite ambient electrical noise.

Table 1-1. Description of animals involved in this study, denoting animal ID, recording location (TMMC: The Marine Mammal Center, LML: Long Marine Lab, and ANO: Año Nuevo State Park), date of recording (between 2-May-2019 and 27-Apr-2021), age class and age estimate in years (weanling (post-nursing): 1-6 months, yearling: 6-12 months, juvenile: 1-3 years old), sex (determined visually as male [M] or female [F]), standard length (cm), axillary girth (cm), mass (in kilograms), study phase and tag design iteration (V1/V2/V3), type of recording (during euthanasia or release exam procedure (at TMMC) or deployment in captivity or the wild), and the total recording duration in hours (h) and days (d).

#	Location	Age Class & Estimate (yrs)	Sex	Length (cm)	Girth (cm)	Mass (kg)	Phase	Recording Type	Record Duration (hrs)
1	TMMC	Weanling (0,1]	M	161	-	43.0	1	Euthanasia; deemed unreleasable	<1 h
2	TMMC	Weanling (0,1]	F	115	-	26.5	1	Euthanasia; deemed unreleasable	<1 h
3	TMMC	Weanling (0,1]	F	138	-	57.0	1	Release Exam	<1 h
4	TMMC	Weanling (0,1]	M	128	-	61.0	1	Release Exam	<1 h
5	TMMC	Weanling (0,1]	F	147	-	63.5	1	Release Exam	<1 h
6	TMMC	Weanling (0,1]	F	139	-	52.5	1	Release Exam	<1 h
7	TMMC	Weanling (0,1]	F	137	-	50.5	1	Release Exam	<1 h
8	TMMC	Weanling (0,1]	F	138	-	55.5	1	Release Exam	<1 h
9	TMMC	Weanling (0,1]	M	146	-	57.0	1	Release Exam	<1 h
10	TMMC	Weanling (0,1]	M	141	-	74.5	1	Release Exam	<1 h
11	TMMC	Weanling (0,1]	F	130	-	54.5	1	Release Exam	<1 h
12	LML	Yearling (0,1]	F	152	132	118	2a / V1	Captive Deployment	81.86 h
13	LML	Yearling (0,1]	F	165	139	148	2a / V2	Captive Deployment	79.71 h
14	LML	Juvenile (1,2]	F	188	124	141	2a / V2	Captive Deployment	116.85 h
15	LML	Juvenile (1,2]	F	206	147	196	2a / V2	Captive Deployment	115.86 h
16	LML	Juvenile (1,2]	F	206	129	177	2a / V2	Captive Deployment	69.62 h
17	ANO	Weanling (0,1]	F	165	143	200	2b / V2	Wild Deployment	73.81 h
18	ANO	Weanling (0,1]	F	157	130	116	2b / V3	Wild Deployment	120.90 h
19	ANO	Weanling (0,1]	F	151	129	118	2b / V3	Wild Deployment	120.04 h
20	ANO	Juvenile (1,2]	F	170	140	157	2b / V3	Wild Deployment	119.19 h
21	ANO	Juvenile (2,3]	F	187	102	~120	2b / V2	Wild Deployment	75.16 h
22	ANO	Juvenile (2,3]	F	177	134	154	2b / V3	Wild Deployment	98.81 h
PHASE 1 TOTAL (N=11)							1	Stationary Recordings (TMMC)	<12h
PHASE 2A TOTAL (N=5)							2a	Captive Deployments (LML)	464 h (19.3 d)
PHASE 2B TOTAL (N=6)							2b	Wild Deployments (ANO)	608 h (25.3 d)

1.3.1a *Instrumentation & Data Collection*

We tested several surface-mounted electrode types: (1) soft-dry electrodes (DRYODE™ by IDUN Technologies), (2) dry electrodes (SoftPulse™ by Dätwyler), and

goldcup), and (3) Genuine GRASS® reusable goldcup electrodes. We used non-invasive, surface-mounted Genuine Grass® goldcup electrodes to measure 9 differential electrophysiological channels (4 electroencephalogram [EEG], 2 electrooculogram [EOG], 2 electromyogram [EMG], and 1 electrocardiogram [ECG]). EEG electrodes were placed over the frontal and parietal derivations of each cerebral hemisphere, EOG electrodes were placed approximately 5 centimeters posterior to the outer canthus, EMG electrodes were placed above the nuchal muscles, ECG electrodes were placed on either side of the body near the fore flippers, and ground electrodes were placed on the forehead between the supraorbital vibrissae (Figure 1.2). This electrode configuration closely matches montages used for implanted polysomnography in other pinnipeds (21,28,30,45). We trimmed the fur and attached all electrodes to clean skin using conductive paste and kinesiology tape. We recorded EEG with a stationary amplifier (PowerLab™) (#1-11) (Table 1-1) and tested multiple electrode types and configurations to optimize signal detection. We collected and visualized data in LabChart (ADInstruments).

1.3.2 ***Phase 2: Recordings of Freely Moving Animals***

1.3.2a *Phase 2a: Deployments in Temporary Captivity – Long Marine Lab (LML)*

Given Phase 1 results (see Results: Phase 1 for more details), we used Genuine Grass goldcup electrodes and a differential electrode montage to build our EEG logger. We recorded sleep in five female juvenile northern elephant seals (#12-16: 2 yearlings [~8 months old] and 3 juveniles [~1 year and 8 months old]) in the lab, where we could

monitor the instrument and seal and establish sleep signal quality over multiple days. Following initial chemical immobilization, we transported seals using established procedures from Año Nuevo State Park to the Long Marine Lab marine mammal facility 21 miles south at the University of California, Santa Cruz (Table 1-1) (46,47). Shortly after transport, we re-anesthetized and instrumented the seals with the portable EEG datalogger (see "Instrument Attachment").

We released the seals into a dry enclosure measuring 6.1m by 3.0m for at least 48 hours after sedation. The animals were then released into a seawater pool measuring 4.9m by 3.0m by 1.4m (water volume 21m^3) with an adjoining haul-out area (1.2m by 3.0m). After an acclimatization period of 30 minutes to 2 days, the seals learned to exit the pool and freely transitioned between the two media. If needed, seals were sedated to modify instrument attachments. We removed instrumentation during a final sedation and transported seals back to Año Nuevo State Park.

1.3.2b *Phase 2b: Wild Deployments – Año Nuevo State Park (ANO)*

We anesthetized and instrumented six seals at Año Nuevo State Park (#17-22: 3 weanlings [~75 days old] and 3 juveniles [14 or 24 months old]) (Table 1-1). These animals were left in the wild for 3-5 days and then instruments were recovered. Seals were instrumented during the molt haulout when animals of all age classes were present at the colony, but before most newly weaned pups had departed to sea on their first foraging trip.

1.3.3 ***Portable Datalogger Instrumentation***

We recorded 21 electrophysiological signals, pressure, illumination, temperature, 3D accelerometer, 3D gyroscope, and 3D magnetic compass using the Neurologger3 (©2016 Evolocus LLC). We created a portable, waterproof, and ruggedized housing for the Neurologger3 to withstand the pressure experienced by an elephant seal in the wild (up to 2000 meters of seawater; pressure equivalent of 200 atmospheres or ~3000 psi as below). The housing had external sensor ports to record pressure and illumination and to display recording status via a small LED. The logger transmitted snapshots of electrophysiological data via Bluetooth.

We created a housing for the device that accommodated several concerns: (1) the illumination sensor must be against a transparent wall, (2) the pressure sensor (KELLER 4LD) must be machined between an internal lip and external retaining wall or clip, (3) attenuation of Bluetooth signals by the aluminum housing material, and (4) 21 electrical signals must exit the housing, each of which is a potential conduit for water.

We selected a robust SubConn® Micro Circular 21-pin underwater connector to transmit electrophysiological signals into the housing. After several design iterations, our third and final iteration (V3) was a cylindrical aluminum housing with one rounded end and a threaded cap at the other side that integrates pressure and illumination sensors, an acrylic window, and the SubConn® Micro Circular 21-pin underwater connector (Figure 1.2 & Table 1-2). The acrylic window allowed light detection by the illumination sensor, visualization of the LED status, and reception of Bluetooth signals to verify signal quality.

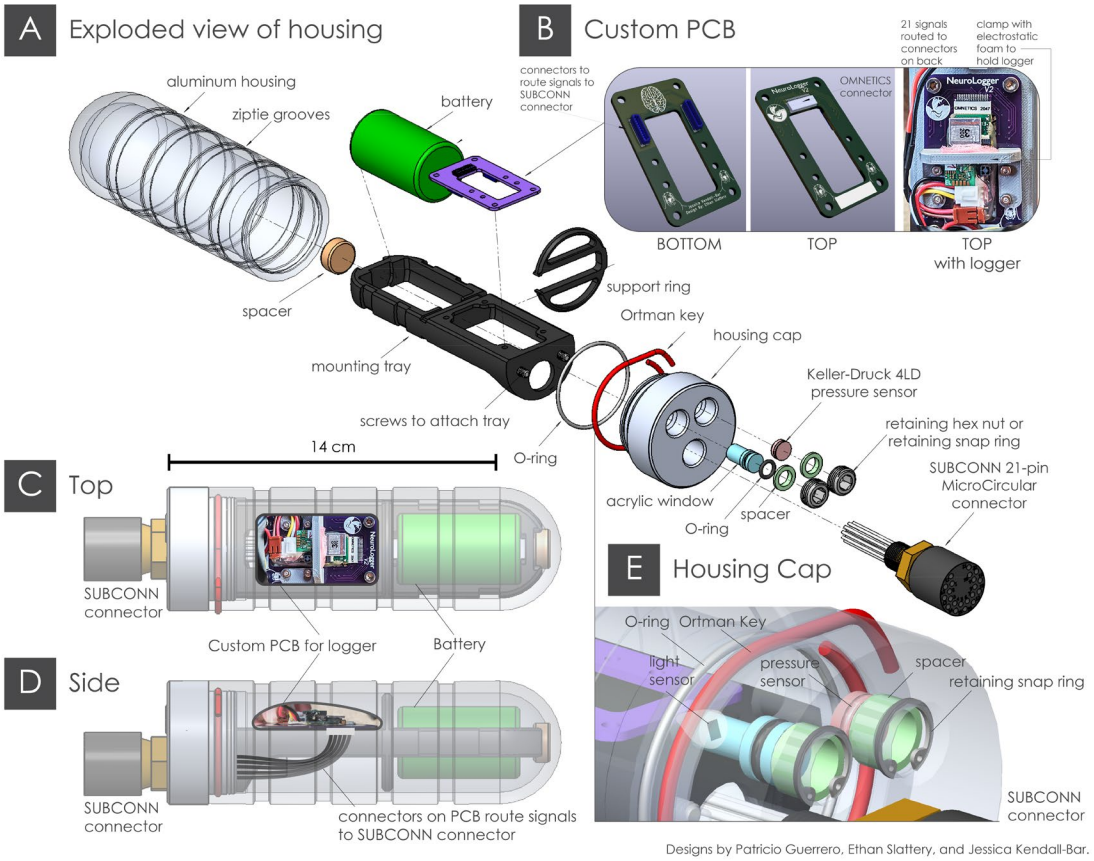

Figure 1.2. Final iteration of custom datalogger housing design (V3). (A) Exploded view of logger housing demonstrates each component of the encapsulation. (B) Inset to show the custom printed circuit board (PCB), which holds the logger and routes 21 signals to connectors on its underside to connect signals to the waterproof 21-pin connector. (C) The top and side (D) views of the logger demonstrate the position of the logger when mounted on the custom PCB. (E) Detailed view of housing cap showing retaining systems for illumination and pressure sensors.

1.3.4 *Headcap and patch design*

We designed the EEG headcap and patches by embedding electrodes between two layers of neoprene (Figure 1.3A). After several design iterations, we found that the most effective configuration embedded electrodes between an outer layer of durable, flexible neoprene rubber (3mm thick, 40A durometer) with a second, inner layer of thin neoprene foam (3mm thick) to hold electrodes in place against the skin. This design facilitated the reuse of the equipment by preventing tearing in the upper neoprene layer. We fixed the electrodes into place between the two layers of neoprene using a silicone room-temperature-vulcanizing (RTV) adhesive (Permatex® Adhesive Sealant) to protect the wires and maintain wire configuration across deployments. The sealant created a robust mechanical bond to abraded neoprene rubber, a chemical bond to silicone-insulated electrode sheathing, and no bond to the neoprene cement (added after the full cure time of the silicone RTV) that peeled off easily upon each retrieval of the instrument.

Table 1-2. Design iteration summary (V1, V2, and V3). Table summarizes features of each design iteration of the housing and frontend (including the headcap, patches, and wires) and assesses water intrusion and signal quality for each (Good vs. Scorable vs. Unscorable ECG – subjective judgment of accuracy level for automated peak detection [always accurate, not always accurate, apnea vs. eupnea not readily distinguishable]; Good vs. Scorable vs. Unscorable EEG – subjective judgment of ability to visually and quantitatively distinguish between SWS and REM [both distinguishable, visual but not quantitative, not readily distinguishable]).

		Features	Design Iteration		
			V1	V2	V3
Logger Housing		Material	High-density polycarbonate	6061-T6 Aluminum	7075-T6 Aluminum
		Pressure test	>10 msw (failed test at 1310 msw [1900 psi])	>2000 msw (passed test to 2068 msw [3000 psi])	>2000 msw (passed test to 2068 psi [3000 psi])
		Solution for light and Bluetooth transmission	Transparent housing	High-density polycarbonate window	High-density polycarbonate window
		Pressure sensor retaining strategy	Stainless steel retaining plate	Stainless steel retaining plate	Stainless steel retaining snap ring
Frontend (Headcap, patches, and wires)	Headcap & patches	Material - bottom layer	Neoprene foam	Neoprene foam	Neoprene foam
		Electrode brand (inside headcap)	Genuine Grass reusable goldcup	Genuine Grass reusable goldcup	Genuine Grass reusable goldcup
		Electrode insulation (inside headcap)	"Light-weight" Teflon®	"Light-weight" Teflon®	"No-tangle" Silicone
		Wire configuration maintenance	Hot glue	None	Permatex® Silicone RTV Sealant
		Material - top layer	Neoprene foam	Neoprene rubber (40A durometer)	Neoprene rubber (40A durometer)
	Wire exit from patch	Wire exit strategy	Wires exit side of patch through abraded marine-grade heat shrink	Wires exit top of patch through 3D mold	Wires exit top of patch through 3D mold
		Chemical bond at wire exit	No	No	Yes
		3D mold potting material	No 3D molds used	Polyurethane resin	Polyurethane resin
		Electrode brand (outside headcap)	Genuine Grass reusable goldcup	Genuine Grass reusable goldcup	Technomed goldcup
		Electrode insulation (outside headcap)	"Light-weight" Teflon®	"Light-weight" Teflon®	Thermoplastic polyurethane
	Wires	Wire shielding	Copper braided	None	Ultra-lightweight Stainless steel
		Wire fortification - EEG	4-ft standard heat shrink (1/4")	Liquid electrical tape or nylon braided sheathing	4-ft standard heat shrink (3/4"), liquid electrical tape
		Wire fortification - ECG	4-ft standard heat shrink (1/4")	Liquid electrical tape	4-ft standard heat shrink (1/4"), liquid electrical tape
Design assessment		Headcap Water intrusion	Most (N=1)	Minimal (N=4); None (N=1)	Minimal (N=4); None (N=1)
		Land EEG Signal Quality	Good (N=1)	Good (N=5)	Good (N=5)
		Pre-ICA In-Water EEG Signal Quality	Unscorable (N=1)	Unscorable (N=4); Good (N=1)	Good (N=5)
		Post-ICA In-Water EEG Signal Quality	Good (N=1)	Scorable (N=4); Good (N=1)	Good (N=5)
		ECG Signal Quality	Good (N=1)	Scorable (N=5)	Good (N=5)

We took precautions to minimize water intrusion where each electrode exited the upper layer of neoprene rubber. We designed custom 3D-printed molds (Figure 1.3C) through which we routed electrode wires and then through holes we created in the upper neoprene rubber. We potted this mold with a two-part Epoxies® urethane resin potting compound (Part No.: 20-2180). We placed an extra layer of neoprene foam on either side of the rigid mold to better conform to the curve of the head. Earlier iterations had problems with water intrusion at the base of the headcap, which this design resolved. Twice, patches remained completely watertight using this method, as evidenced by the persistence of conductive paste under the electrode and water-contact indicator tape placed adjacent to the electrode. In all cases, V3 resulted in a nearly waterproof seal where any water intrusion was minimal and slow, such that signal quality remained adequate for sleep stage characterization throughout the recording (see "Signal Quality Analysis").

To further prevent water intrusion, we created a chemical bond at the top of the 3D mold to avoid slow water intrusion along the wire and into the 3D mold (as in V2). We spliced Genuine Grass reusable goldcup electrodes with "no-tangle" wire insulation to a Technomed goldcup electrode's thermoplastic polyurethane wire (Part No.: 20-2180) to achieve a chemical bond between the electrode wire and potting compound. We prevented water intrusion to this splice joint through several sequential layers: a) standard heat shrink, b) ScotchKote™, c) marine-grade heat shrink, d) ScotchKote™, e) marine-grade heat shrink, f) urethane potting compound (mentioned earlier), and g)

silicone RTV Permatex® Adhesive Sealant (only on the silicone-insulated inner end) (Figure 1.3C). The abraded marine-grade heat shrink created a chemical bond with the urethane potting compound. The silicone RTV created a chemical bond with the silicone insulation and held the wires in place. We repeated this process for each patch, using smaller 3D molds for the 1- and 2-wire outputs from EMG and ECG patches. For creating waterproofed electrode patches, we recommend carefully waterproofing the bottom lip of the patch and creating a chemical bond at the wire's exit point.

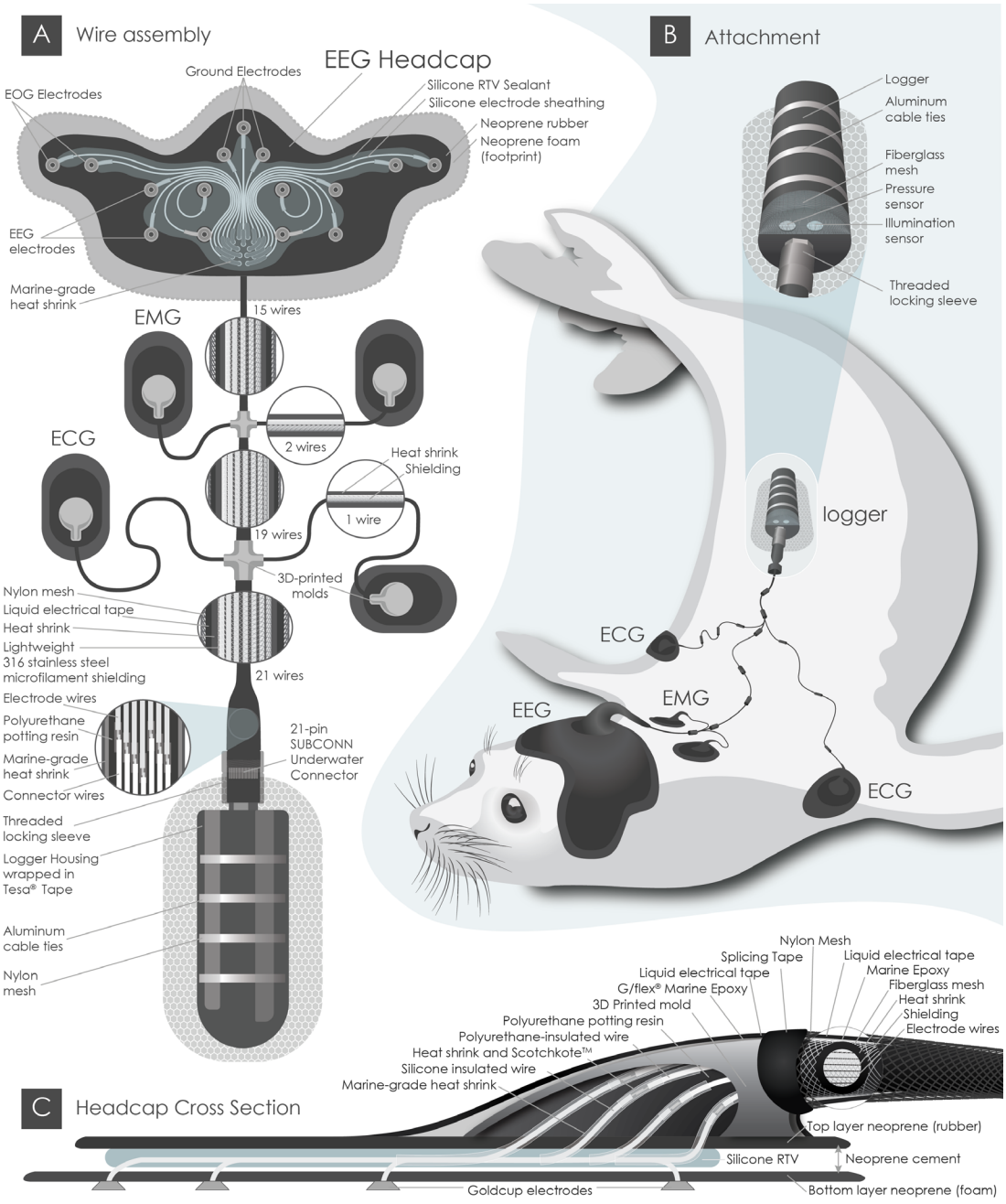

Figure 1.3. Final design iteration (version 3) demonstrating custom wire assembly, attachment, and headcap cross-section. (A) Wiring schematic from electrodes to the 21-pin

underwater connector with callouts showing wire shielding and sheathing and the internal structure of the plotted splice joint between electrode and connector wires. (B) Diagram showing attachment placement and method for each component, including logger, ECG, EMG, and headcap patches. (C) Headcap cross-section showing internal components of the headcap, including the splice joints within the 3D-printed mold and each successive layer of shielding and sheathing until the outer layer of nylon mesh.

We surrounded cable bundles with ultra-lightweight braided microfilament 316L stainless steel shielding material, heat shrink, liquid electrical tape, and nylon braided sheathing (Figure 1.3A). We soldered electrode cables to the leads of a 21-pin underwater connector which routed the electrical signals into the portable datalogger (Figure 1.3A). These solder joints were staggered to maximize space efficiency and strength, covered in heat-shrink, potted in polyurethane, and covered with large-diameter marine-grade heat shrink to minimize water intrusion at mechanically vulnerable connections. We used a threaded locking sleeve to reduce the risk of the connector becoming disconnected during the experiment.

1.3.5 *Instrument attachment*

Once animals were immobilized, we trimmed the fur and cleaned the skin with alcohol or acetone at electrode attachment sites to promote signal conduction and adhesion. We applied neoprene adhesive (Aquaseal™) onto the headcap and patches and the animal's skin. Several minutes later, we applied a second layer of adhesive. After the second layer had dried, we lowered the patches and headcap onto each adhesive footprint (Figure 1.3B). We attached small cable bridges to the fur in several places to minimize cable tension and entanglement potential. We used Velcro® cable organizers attached with neoprene adhesive (Figure 1.3C).

The datalogger was wrapped in Tesa® tape and attached to a flexible nylon mesh with stainless steel zip ties. The flexible nylon mesh was epoxied to the animal's fur, consistent with established best practices for external attachment of animal telemetry tags (Horning et al. 2019) (Figure 1.3B). For each design iteration, combined instrumentation did not exceed 10% of the animal's cross-sectional area and 2% of the animal's body mass (0.87% of body mass and 2.31% cross-sectional area). When time allowed, we verified datalogger signal quality by examining 20-second raw-signal snapshots via Bluetooth.

After the recording, we removed the datalogger by disconnecting the zip ties from the nylon mesh. We separated the top layer of neoprene rubber from the bottom layer of neoprene foam, removing all electrodes and wires from the animal. The animal molted off the nylon mesh and any residual neoprene foam in its next molt.

1.3.6 *Data Processing*

A total of 1224 hours (51 days) of electrophysiological data were collected from the 12 animals in *Phase 2* of this study, of which 564 hours (23.5 days) were from free-moving animals at Long Marine Lab, and 660 hours (27.5 days) were from free-moving animals at Año Nuevo Reserve. In addition, one animal instrumented at Año Nuevo Reserve spent 44 hours (1.9 days) at sea.

The Neurologger3 sampled electrophysiological data at 500 Hz and inertial motion and environmental sensors at approximately 36Hz (250/7 = 35.7142857Hz). We down-sampled inertial motion data to 25Hz using the 'resample' function in

MATLAB to obtain an integer sampling frequency. Binary data was stored on a 200 GB microSD card in the Neurologger3, processed using a custom MATLAB script (Neurologger Converter & Visualizer © Evolocus LLC), and then converted into .MAT (MATLAB file) and .EDF (European Data Format) formats.

ECG artifacts were sometimes present in EEG channels when animals entered the water, complicating visual and quantitative scoring methods. To minimize ECG artifacts and enable visual and quantitative EEG scoring, we applied the "runica" Independent Component Analysis function in the open-source EEGLAB v2020.0 toolbox in MATLAB. Independent Component Analysis (ICA) is now standard practice in EEG signal processing and refers to a collection of unsupervised learning algorithms that decompose multivariate signals into maximally independent components (ICs) (48). We trained the ICA algorithm with a subset of electrophysiological data collected from animals while stationary underwater. This training data (training data durations: median- 12 min; minimum- 5.5 min; maximum- 20.2 min) was selected as a representative section where movement artifacts were minimal, and SWS, REM, and heart rate artifacts were present. We visualized ICA weights for manual review. If the heart rate decomposed separately from EEG signals into at most 2 or 3 ICs, these ICA weights were selected and applied across the entire recording for that animal.

We compared spectral density profiles and the ability to discriminate between SWS and REM across (A) the raw signal, (B) the independent component (IC) that maximally expresses brain activity, and (C) the raw signals pruned with ICs that

minimally express brain activity (e.g. heart signals or electrical noise). We determined the maximal brain IC visually by selecting the IC that 1) allowed discrimination between SWS and neighboring periods of REM, 2) was generated by one of four EEG electrode locations in the 2D topographic maps for each IC, and 3) fit patterns of elevated delta spectral power during quantitative spectral analysis and spectrogram visualization. We always kept the intact ECG channel (without the ECG IC(s) removed) and the IC that maximally expressed heart activity for heart rate analysis. We determined the maximal heart IC by locating the highest amplitude ECG signal generated by the posterior ECG location in 2D topographic maps. Because the ECG waveform is often separated into two or more ICs, the ECG channel often yielded the cleanest heart rate signal.

Inertial motion sensor data were calibrated and processed using the Customized Animal Tracking Systems (CATS) toolbox in MATLAB to measure overall dynamic body acceleration, pitch, roll, and heading (49). We applied rotation matrices and spherical calibrations for each animal to transform the tag's reference frame to that of the animal and account for differences in attachment orientation.

We combined raw electrophysiological data (500Hz), electrophysiological data pruned with ICA, ICs (which maximally expressed brain and heart activity), and processed motion and environmental sensor data (25Hz) into a single EDF file using the *writeeeg* function in EEGLAB. We then inspected the resulting file in LabChart (©ADInstruments). Instantaneous heart rate was calculated using the cyclic measurement peak detection algorithm in LabChart®, with ECG peak detection

parameters consistent with those used for large mammals, exceeding a minimum of 2 standard deviations with a QRS width of 60 milliseconds across normalized 4-second windows.

1.3.7 *Qualitative Signal Analysis*

To prepare the raw data for visual sleep scoring, we bandpass filtered electrophysiological signals according to the standard outlined in the American Academy of Sleep Medicine sleep scoring manual (50): EEG/EOG: 0.3-30Hz; EMG: 10-100Hz; ECG: 0.3-75Hz. We visualized signals using standard temporal and voltage scales (100μV for EEG/EOG, 40μV for EMG, 2mV for ECG, [-1.5,1.5] G-forces (g) for accelerometer data). We visualized spectrograms for two (L & R) of the best EEG channels and the maximal brain IC using Fast Fourier Transform (FFT) using a Hann (cosine-bell) window with a sample size of 1024 points and 50% overlap, examining spectral power from ~20-40 dB for frequencies between 0-15Hz.

Guidelines for visual sleep scoring were based on those set for other marine mammals (21,43,45). We scored sleep according to the following sleep states in 30-second epochs: Active Waking (AW), Quiet Waking (QW), Drowsiness (DW), Slow-Wave Sleep (SWS), Rapid-eye Movement Sleep (REM) (Figure 1.4). Here, we present a brief discussion of the sleep scoring criteria used in this study. In subsequent works, we further expand on our sleep scoring criteria and interscorer reliability (Kendall-Bar, in prep). We provide a summary of these criteria below.

We scored Quiet Waking (QW) when there was low voltage, high-frequency background EEG activity (>50% epoch duration), occasional movement or eye blink artifacts (occupying <50% of the epoch duration), and accelerometer traces demonstrating only subtle breathing or motion (i.e., slowly rolling, grooming, or body repositioning) (Figure 1.4D). We scored Active Waking (AW) when gross movement artifacts appeared in all electrophysiological channels for >50% of the duration of the 30-second epoch and were accompanied by movement in the accelerometer (more activity than behaviors described above for QW) (Figure 1.4E).

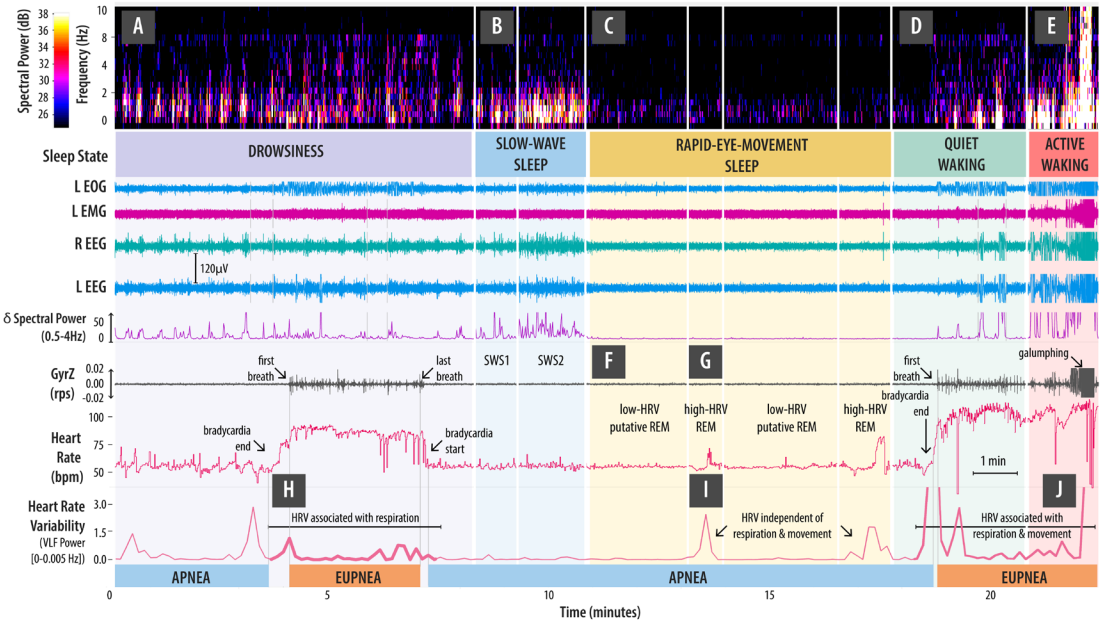

Figure 1.4. Sleep categorization methods. Sleep stages were distinguished from distinct characteristics of the EEG spectrogram, z-axis gyroscope (for breath detection), and heart rate. Spectral power varied across stages from (A) slow (10 s) oscillations between slow waves and waking during Drowsiness (DW), (B) highest amplitude low-frequency activity during SWS (exemplified by hot colors in low frequencies [0.5-4Hz] of the spectrogram), (C) lowest amplitude high-frequency activity during REM (exemplified by dark colors in the spectrogram),

and (D) low amplitude high-frequency activity during quiet waking (QW), and (E) motion artifacts during active waking (AW). We differentiated between periods of REM with (F) low heart rate variability (HRV) and (G) high HRV (independent of changes in respiratory state - apnea [not breathing] & eupnea [breathing consistently]). We demonstrate HRV patterns due to (G) respiration, (H) independent of respiration, and (I) due to both respiration and movement artifacts (due to short-duration inaccuracies in automated peak detection). During active waking, motion artifacts could be caused by large breaths or active forward movement ('galumphing' on land or swimming in water).

We scored SWS when continuous high amplitude (>10μV^2/Hz) slow waves between 0.5 and 4 Hz occupied >50% of the 30-second epoch (Figure 1.4B). The peak-to-peak amplitude of slow waves varied slightly between recordings and recording location (land v. water). On land, SWS amplitude typically reached or exceeded 75μV (a standard threshold for humans). Delta spectral power was >2-fold greater during sleep than during neighboring periods of quiet waking or rapid eye movement sleep (except with extensive water intrusion - see Signal Quality Analysis). SWS occurred independently of breathing and always involved symmetrical high amplitude activity in each hemisphere, low muscle activity in the EMG channels, and no visible eye activity in the EOG channels. We subdivided SWS into two stages for quantitative analysis: SWS1 & SWS2. High amplitude slow-wave sleep (SWS2) was scored when slow waves reached their maximal amplitude (compared to neighboring sleep cycles). In contrast, low-amplitude slow-wave sleep (SWS1) was a transitional state scored when slow waves exceeded the amplitude of EEG activity during waking by at least 1.5X and were not maximal in amplitude compared with neighboring sleep cycles. K-complexes and sleep spindles were present in SWS1 but not in SWS2. We scored drowsiness (DW) when

episodes of fragmented SWS (interrupted by waking EEG activity) occupied >50% of the 30-second epoch (Figure 1.4A).

We scored rapid eye movement sleep (REM) when low voltage, high-frequency EEG activity coincided with an increase in heart rate variability for >50% of the 30-second epoch, consistent with previous sleep studies of walruses during sleep apneas (13). Although our surface-mounted EOG sensors reliably detected eye blinks, we only occasionally detected eye movements (more subtle than eye blinks) during REM. As such, we did not rely on EOG for scoring REM. Instead, we conservatively scored rapid eye movement sleep only when both low voltage activity and heart rate variability were observed. Muscle activity (measured with EMG on the neck) during REM was sometimes lower than during SWS but usually remained unchanged if EMG activity was already low in SWS. The subtle changes in EMG may result from our reduced ability to detect fine-scale changes in muscle tone using non-invasive surface electrodes and the fact that the seals typically sleep with their head outstretched on the ground.

We used very-low frequency heart rate variability (HRV) power (total power between 0-0.005 Hz; 8K FFT Hann (cosine-bell) window with 50% overlap) to subdivide low-amplitude, high frequency EEG periods following slow wave sleep high HRV (high-certainty REM) versus low HRV (putative REM). Both high HRV and low HRV REM episodes coincided with behavioral characteristics of REM such as closed eyes, motionlessness, occasional muscle and whisker twitches, occasional whole-body jerks,

and rapid eye movements. However, we conservatively restricted the quantitative signal analysis (next section) to high HRV REM episodes.

1.3.8 *Quantitative Signal Quality Analysis*

Of several techniques employed to assess signal quality in lab-based experiments, many are not feasible for field experiments with wild animals. For example, our device cannot measure impedance, a measure of effective resistance of the tissues overlying the skull often involved in signal quality assessments (78). Others, such as quantifying alpha-band power due to the Berger effect (79) or theta-band power during REM, are only possible if these signals are detected from the occipital lobe or hippocampus (respectively), outside the scope of our frontoparietal EEG montage. Therefore, we chose to examine delta spectral power (δ) during SWS divided by delta spectral power during REM (SWS δ/REM δ) to measure signal quality over time. Although sleep signal amplitude may vary across animals and age classes, changes in delta power over time can be used to determine the reliability of a novel recording technique over long, multi-day recordings (78). Like these previous studies, we also applied subject-specific linear regression models and group-specific linear mixed-effects models to assess the impact of age (<1, <2, and <3 years old), recording location (land v. water), and design iteration (V1, V2, and V3). The data were analyzed in JMP® Software (Cary, NC) (51) and R (80) and visualized using ggplot2 (81).

We selected one EEG channel per animal (out of 9 channels: 4 raw EEG, 4 EEG pruned with ICA, and one maximal brain IC) with the fewest motion artifacts for

quantitative signal quality analyses. We calculated delta spectral power (0.5-4Hz) for the best EEG channel for 30-second epochs of SWS2 and REM. Spectral power analyses were performed with a Fast Fourier Transform (FFT) using a Hann (cosine-bell) data window with a sample size of 1024 points and 50% window overlap.

1.4 **RESULTS**

1.4.1 ***Phase 1: Stationary Recordings***

1.4.1a *Phase 1a: Electrode types*

We found that Genuine Grass reusable goldcup electrodes and Ten20™ (Weaver and Company) conductive paste produced the most reliable recordings. In addition to allowing continuous signal conduction, conductive paste helped attach electrodes during stationary recordings without adhesive. Among the dry electrode options we tested, each one introduced "popping" artifacts indicating interrupted contact with the skin (Figure 1.5). When we tested soft dry electrodes and flat dry electrodes, we found that the flexible polymer optimized for smooth, human skin did not make good contact with the rough skin of the elephant seals.

We tested a few goldcup electrode alternatives, which performed similarly, but varied greatly in their ability to resist corrosion over time (Genuine Grass outperformed Technomed). When we directly compared goldcup and needle electrodes (similar to those used in the past to record sleep in elephant seals - (27,28)), we detected auditory cortical responses of similar amplitude and time course when comparing auditory evoked potentials of goldcup versus minimally invasive needle electrodes (see

additional file 2). However, the goldcup electrode signals were more susceptible to electrical noise in high-noise lab environments (50-60Hz).

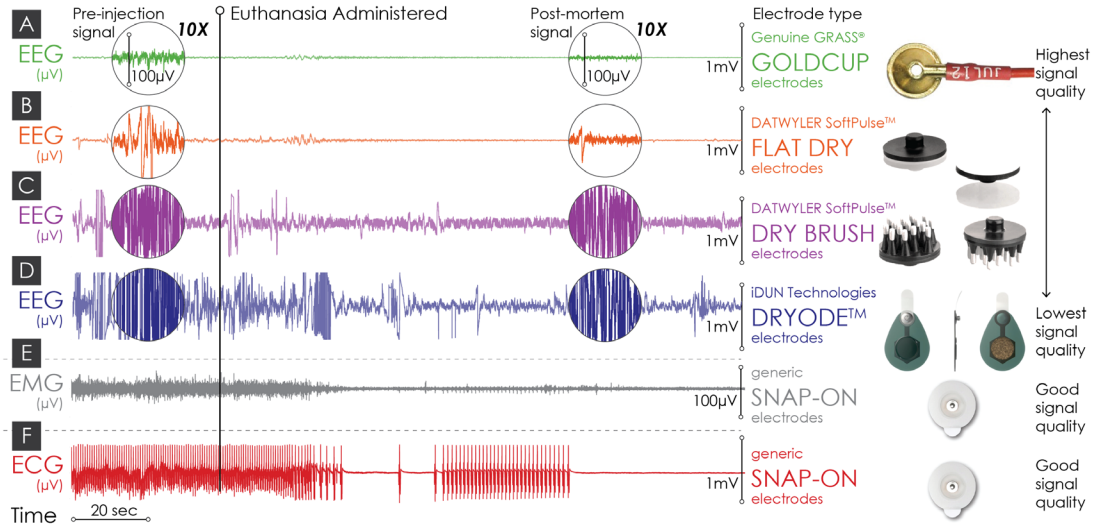

Figure 1.5. Signal quality comparison across several surface-mounted electrodes. This recording demonstrates brain wave attenuation during euthanasia and the superior signal quality of (A) Genuine GRASS® goldcup electrodes, followed by (B) DATWYLER SoftPulse™ flat dry and (C) dry brush electrodes, and then by (D) soft dry DRYODETM electrodes. Snap-on surface mounted electrodes with conductive gel and adhesive reliably detected (E) muscle activity (EMG) and (F) heart rate (ECG) attenuation. The animal was deemed unfit for release by TMMC veterinarians and euthanized due to congenital defects unrelated to this study.

1.4.1b *Phase 1b: Electrode configurations*

We determined ideal electrode configurations for detecting heart (ECG), brain (EEG), and eye (EOG) activity during preliminary stationary recordings at TMMC and preliminary tests at Long Marine Lab. Using a referential montage, we recorded the highest amplitude slow waves with electrodes placed apart >5cm (peak-to-peak slow-wave amplitude >2-fold greater than using a differential montage; Figure 1.6). However, these larger signals were subject to larger artifacts, and the loss of a single reliable

reference electrode occasionally resulted in the loss of any usable signals. We used a differential montage across electrodes placed no more than 5cm apart for the remainder of our recordings. In addition, by placing electrodes closer together, we can decrease the necessary size of the footprint. We found that our selection of a differential montage (as opposed to a montage referenced to a single electrode) allowed us to continue recordings after losing single EEG signals. We found that placing a differential EOG electrode pair approximately 2cm posterior from the outer canthus more selectively detected eye activity than if the reference electrode was placed near the ground electrodes on the forehead. We recorded peak-to-peak ECG amplitudes more than twice as large when using an asymmetrical differential montage (anterior to one fore-flipper, posterior to the other) compared to symmetrical placement anterior to the fore-flippers (Figure 1.6).

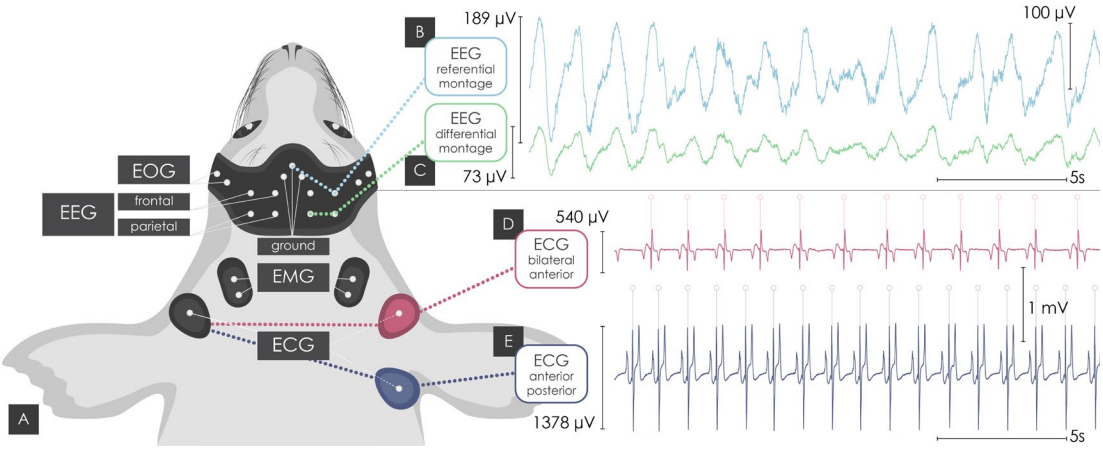

Figure 1.6. Electrode configurations for signal maximization. (A) Electrode configuration for stationary and free-moving recordings showing positions of ground, electrooculogram (EOG), electroencephalogram (EEG), electromyogram (EMG), and electrocardiogram (ECG) electrodes. (B & C) EEG traces during SWS in Seal #4 demonstrate higher peak-to-peak amplitude of slow

waves using the referential montage than recorded simultaneously with a differential montage (green line) (189μV v. 73μV). (D & E) Heart signals derived from the symmetrical anterior placement of both ECG leads (Seal #14) are more than twice as large as heart signals derived from contralateral placement (dark blue line) of ECG leads (Seal #12).

1.4.2 ***Phase 2: Portable datalogger with freely moving animals***

1.4.2a *Raw signal quality*

We recorded reliable electroencephalogram (EEG) and electrocardiogram (ECG) signals in several different settings (Figure 1.7). Overall, we could always extract heart rate peaks, whether the animal was moving or not, and reliably detected changes in EEG activity whenever the animal was calm, including when the animal was resting on the ocean floor from 1 m to 200 m deep, and while drifting at the surface and at depth (~200-300 m) in the open ocean. Here, we present examples of raw signals recorded in these different settings and highlight the ability to discriminate between low-frequency (0.5-4 Hz) and high-amplitude (>50 μV peak-to-peak amplitude) EEG signals during SWS, compared to the high-frequency and low-amplitude signals observed during REM sleep (Figure 1.7). These excerpts also show high heart-rate variability characteristic of REM sleep. We include 1-minute raw signal data excerpts for each setting in our open-source data repository (52).

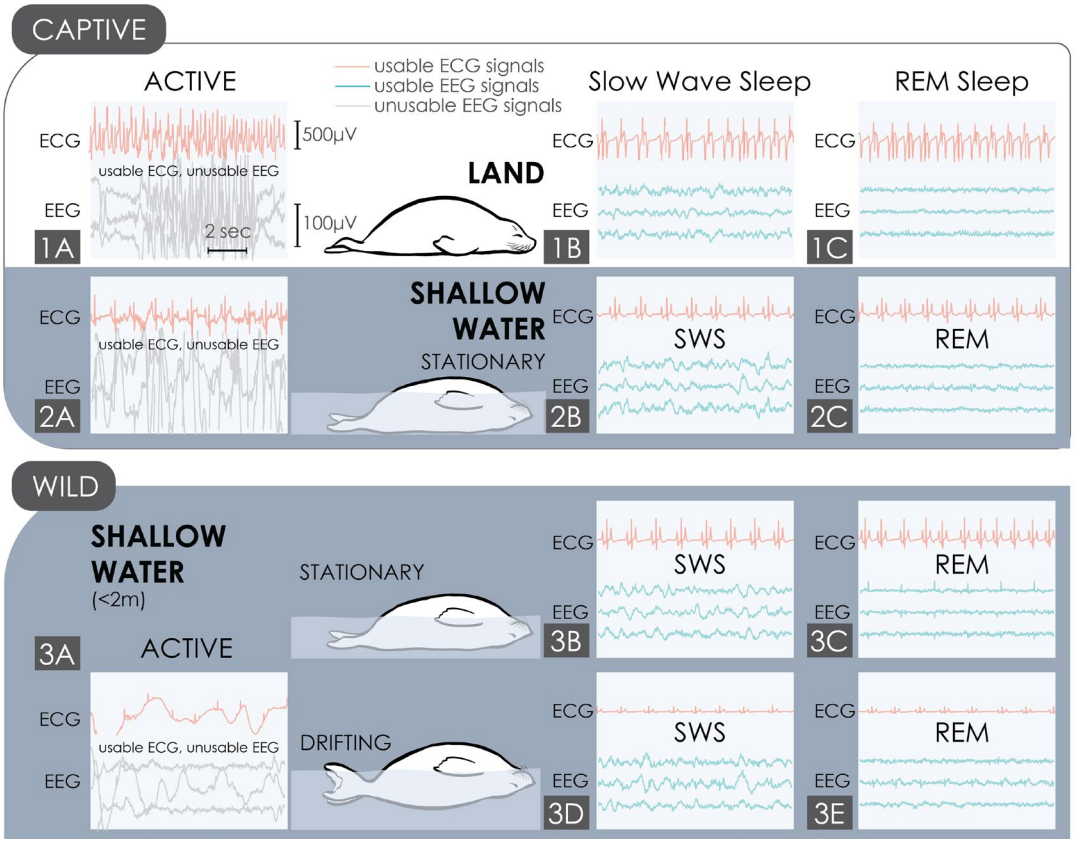

Figure 1.7. Raw signal quality across recording locations. 10-second electroencephalogram (EEG) and electrocardiogram (ECG) data excerpts shown with uniform scaling (EEG 5X magnified compared to ECG) across plots for comparison of signal quality across active behaviors i.e., galumphing [forward movement on land] or swimming in water) and distinct sleep states i.e. slow-wave sleep (SWS) and rapid-eye-movement sleep (REM)). We show usable ECG in red (automated peak-detection possible), usable EEG in blue (no movement artifacts-visual and quantitative sleep state analysis possible with unprocessed raw signals), and unusable EEG in gray (signal processing required to use EEG to distinguish sleep states). We detected heart rate, but not sleep state, while the animal was active on land (1A) and in water (2A, 3A, & 4A). We were able to detect sleep state (difference between SWS & REM) when the animal was calm, whether that was on land (1B-C), stationary in water (2B-C), or drifting at the surface (3D-E).

1.4.2b *Heart rate (ECG) raw signals*

We recorded reliable heart rate signals even while the seal was actively galumphing (forward motion on land) and stroking (swimming back and forth in water) (Figure 1.7). For most recordings, we could locate heartbeats using automated peak-detection using standard settings, consistent with the "large dog" preset using ADInstruments' LabChart software (QRS width=60ms, normalized across a 4-sec window, with a minimum detection period of 180ms). However, when motion was vigorous, and we did not use shielding or heat shrink to reinforce ECG wires, the peaks were not adequately recognized by automated software, although still distinguishable to the human eye (Figure 1.8; 4A&B).

1.4.2c *Brain activity (EEG) raw signals*

As is typical for sleep studies, we could not record artifact-free EEG signals during vigorous forward motion. However, we recorded clean signals when the animal was still or during calm grooming or repositioning. The main obstacle to recording clean EEG signals was contamination by larger ECG signals that usually appeared as soon as the electrodes became wet (Figure 1.8; 1A-B). In early designs, where water intrusion was significant, we could visually discriminate between SWS and REM sleep. Still, artifacts complicated visual analysis and made quantitative analysis impossible. With our final headcap and patch design, we minimized water intrusion and were able to record clean EEG signals with minimal heart rate artifacts. In two recordings, our electrodes stayed dry for the duration of the experiment (verified by water-contact

indicator tape and the persistence of conductive paste), despite the animal going in and out of water for 5 days. However, even in cases where there was some water intrusion, efforts to minimize it seemed to improve signals by helping prevent the flow of saltwater over and between electrodes.

1.4.2d *Electrical contamination*

Electrical recordings amidst other telemetered and transmitting devices presented significant signal detection challenges. Using the standard programming for VHF animal tracking tags, 200ms pulses are transmitted at 148-149 MHz every 1.7 seconds. Since these signals fall well beyond the sampling frequency of our device, noise from a tag such as this collapsed broadly into a mixture of low-frequency and high-frequency noise (Figure 1.8; 2A-B). We recommend configuring a custom VHF transmitter to delay transmission until the end of the experiment to minimize this interference (Figure 1.8; 2C-D). Similarly, satellite tag transmissions briefly interrupted signals detected by the tag, but at a lower transmission frequency (once per 92 seconds) (Figure 1.8; 3A-B). It was possible to remove these large anomalies using methods previously applied to remove ECG artifacts from EMG data (82), similar to manual artifact-removal methods for ECG artifact removal in cetacean EEG papers (41) (Figure 1.8; 3C-D).

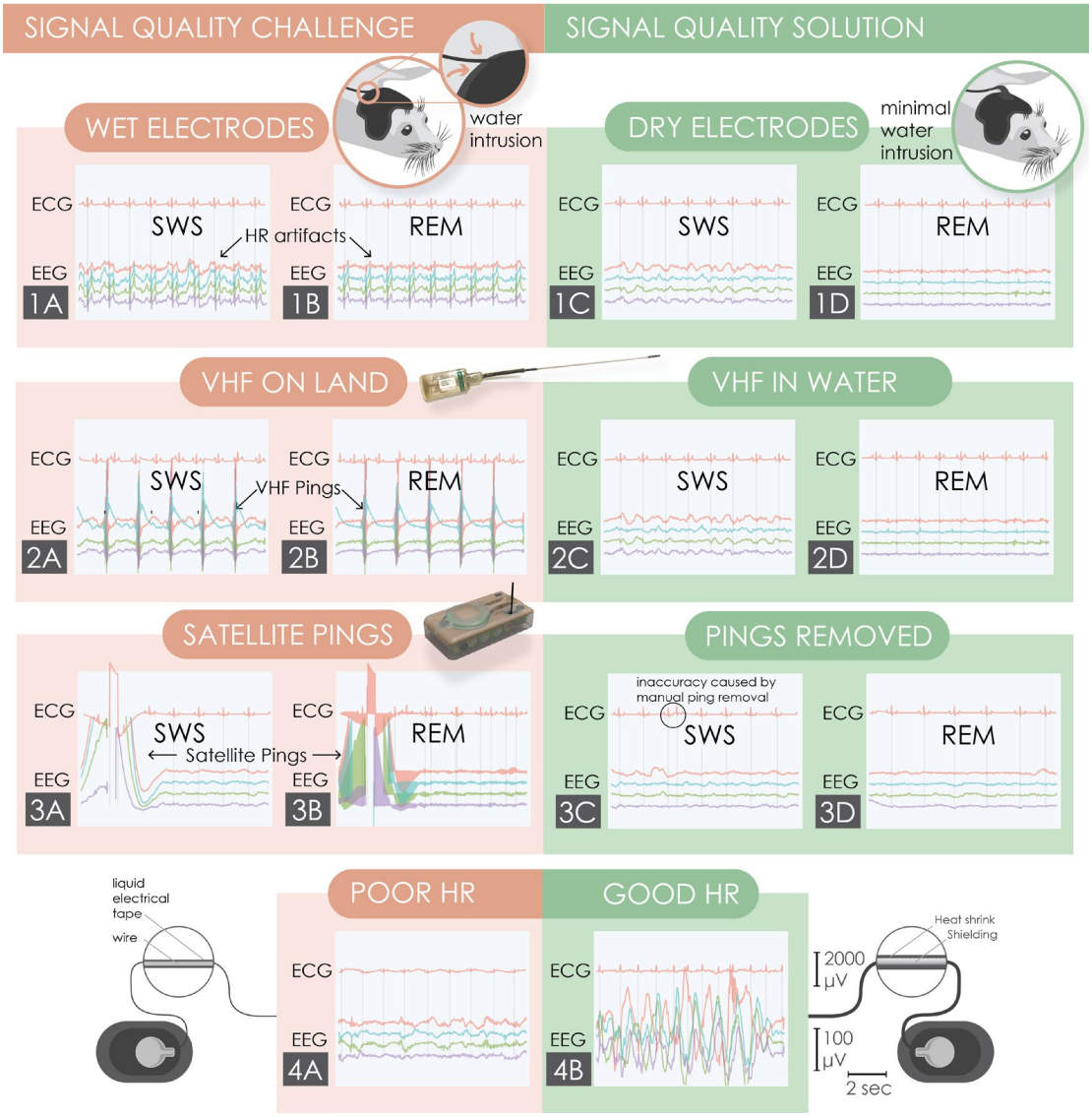

Figure 1.8. Signal quality challenges and solutions. 10-second sequences of ECG and EEG with consistent scaling across plots (EEG 20X magnified compared to EEG). Vertical gray lines represented automated peak detection results. (1A-B) EEG signals with heart rate (HR) artifacts caused by water intrusion, resolved in later iterations that minimized water intrusion (1C-D). (2A-B) VHF transmitter pings obscure ECG peak detection and EEG recordings on land but not in water (2C-D). (3A-B) EEG and ECG signals obscured by satellite pings. (3C-D) We replaced ~5 seconds of data surrounding the ping with data before or after the ping. Manual ping removal can facilitate quantitative analysis by improving automated peak detection but can locally interrupt

fine-scale patterns such as irregular heartbeats (visible in 3B but not 3D). (4A-B) Wires reinforced by shielding and heat-shrink outperform insulated electrode wires covered with liquid electrical tape.

1.4.2e *Signal processing to improve sleep detection*

We were able to recover signal quality using ICA to isolate both contaminating signals (ECG) and signals of interest (EEG). In most cases, our raw signals were improved by the removal of heart rate artifacts via ICA, which facilitated both visual and quantitative scoring (Figure 1.9).

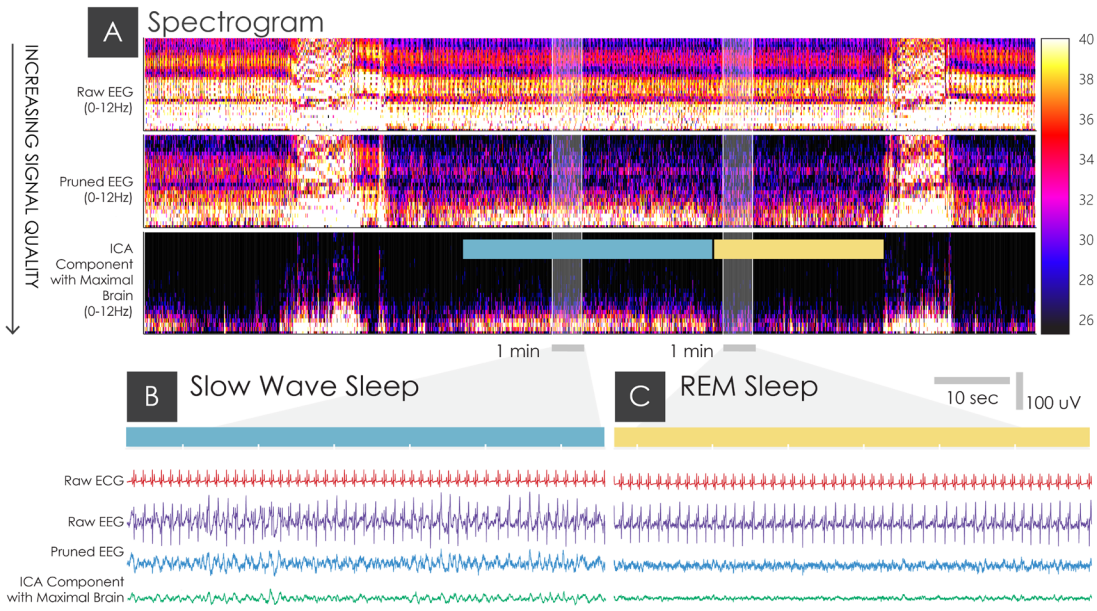

Figure 1.9. SWS vs. REM before and after ICA processing. (A) Three spectrograms (90-minute duration) show the progressive improvement in signal quality for visual discrimination between SWS and REM (designated in the top hypnogram) between the raw EEG signal and the pruned EEG signal contaminating ICs removed, and the IC that maximally expressed brain activity. 1-minute waveforms from SWS (B) and REM (C) show progressively improved signal quality from Raw EEG (purple), Pruned EEG (blue), and the ICs that maximally expressed brain activity (green).

After running ICA on a subset of our data while the animal was stationary in the water, we applied those weights to entire recordings and inspected the resulting ICs. In all cases, we were able to identify ICs that maximally expressed contaminating artifacts (e.g., IC1, IC2, and IC9 in Figure 1.10B) and one IC that maximally expressed brain activity (e.g., IC5 in Figure 1.10B). The maximal heart ICs were identified visually as containing any recognizable component of ECG waveform (e.g., IC1 & IC2 in Figure 1.10B) and confirmed in topographic maps to be tied to the posterior ECG lead (Figure 1.10A & C). We also removed any identifiable contaminating electrical signals (constant frequency; e.g., IC9 in Figure 1.10B). We visually identified the IC that maximally expressed brain activity (IC5) as the one with distinct slow waves during SWS and low-voltage activity during REM. We confirmed this with its topographic map relating to the four EEG electrodes (Figure 1.10D).

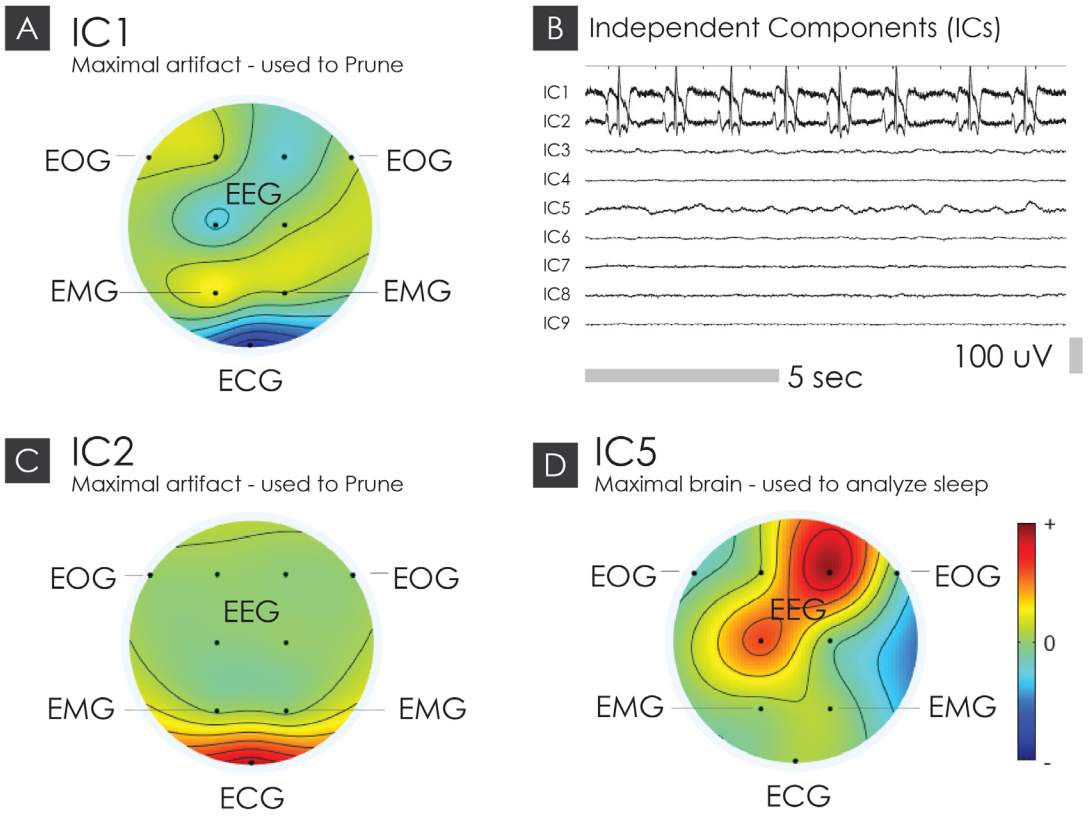

Figure 1.10. ICA outputs over space and time. (A, C, & D) Topographic maps with spherical interpolation (EEGLAB) show each IC's spatial weights based on the relative spatial orientation of sensors on the seal (EEG above cortex, EMG on neck, and ECG near pectoral flippers). Each diagram represents a single IC where red or dark blue (opposite polarity) represents strong spatial weights for each electrode location. IC1 & 2 are opposite polarity components of the heart signal from rear heart rate sensors, while EEG electrode locations above the brain generate IC5. (B) ICs over time, showing the ECG waveform in IC1 & 2 and slow-wave sleep in IC5.

1.4.2f *Signal quality analysis*

Signal quality across Version. We made several adjustments between V1 and V2 to make the frontend lighter and more streamlined, some of which decreased signal quality through water intrusion and the lack of wire reinforcement or shielding. In V3,

we recovered signal quality through more thorough waterproofing and wire fortification of V2's design. We examined delta (δ) spectral power differences between SWS and REM over several days to examine the effects of design iteration (V1, V2, and V3), age (from 0 to 1, 1 to 2, and 2 to 3 years old), and recording location (land versus water) (Figure 1.11; Supplemental File 3). In a mixed-effects model of signal quality over time (individual as a random effect), we found a significant interaction between signal quality over time and version (p=0.0366*). V2 displayed a significant negative trend over time (V2: slope= -3.538±1.016 p=0.032*), V1 and V3 did not significantly degrade over time (V1: slope= -1.807±1.682 p=0.3951; V3: slope= -0.7695±0.5053 p=0.1486) (Figure 1.11A). Because we introduced animals to water later in the experiment, we separately examined the effect of location on signal quality.

Signal quality across Locations. Overall, signal quality was lower in water than on land (Δ SWS δ/REM δ= 3.427±0.5121; p<0.0001*; Figure 1.11C), but that difference varied between versions (p=0.0026*; Figure 1.11& Figure 1.12). Signal quality was significantly lower in water than on land for V1 (p=0.0012*) and V2 (p<.0001*), but we were able to minimize the impact of water intrusion on signal quality by V3 (p=0.9753) (Figure 1.11C-D).

Signal quality across Ages. We found no significant difference in signal quality between oldest (2-3 years old) and youngest (0-1 year old) animals when on land (Δ SWS δ/REM δ= 6.6931±2.812; p=0.1646; Figure 1.11E). The large difference between land and water signal quality seen in 1-2 year-olds is likely due to the predominant use

of V2 on those individuals, which had the greatest decrease in signal quality due to water intrusion (Δ SWS δ/REM δ= 15.002±1.766; p<.0001*; Figure 1.11F).

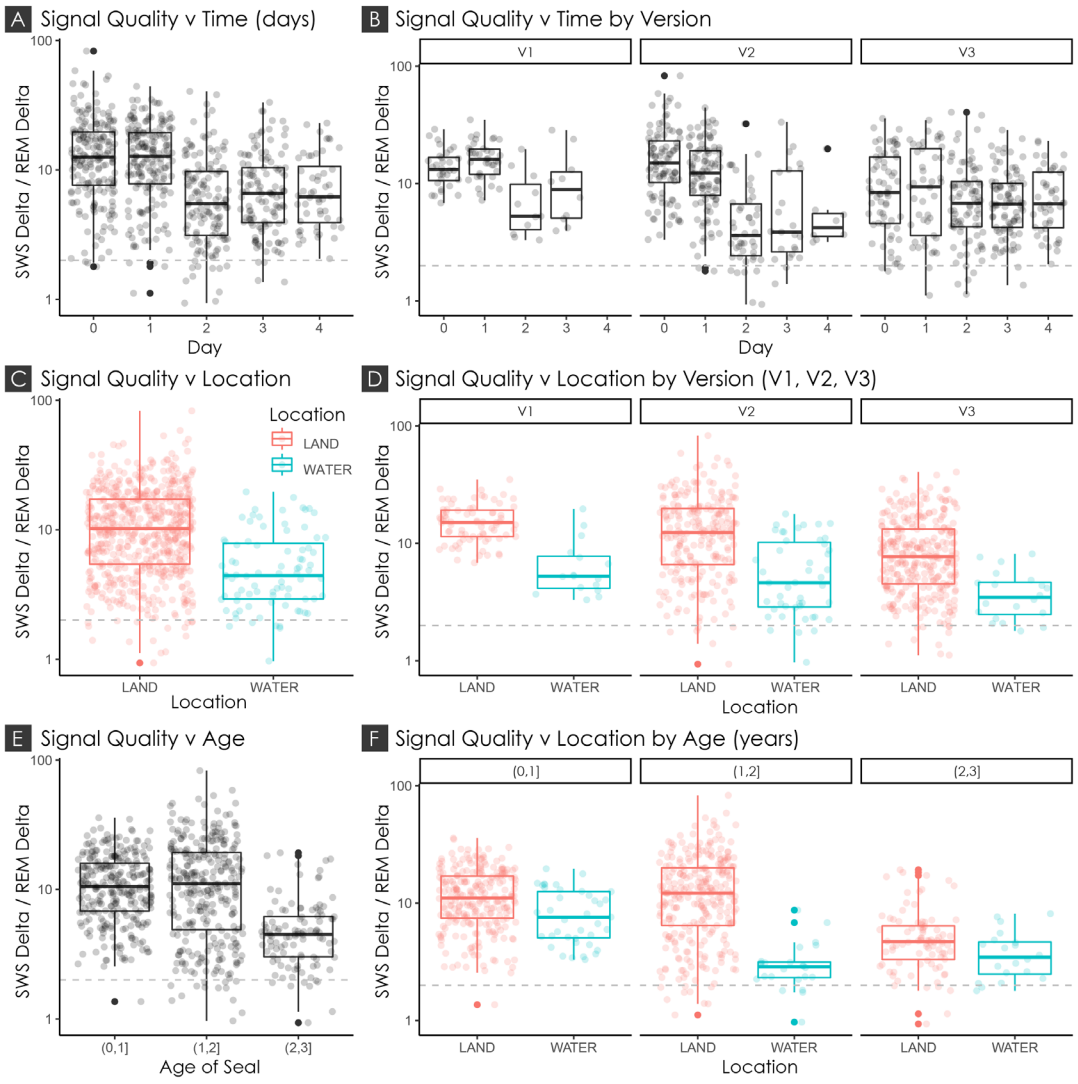

Figure 1.11. Signal quality across time, location, age, and version. Signal quality (delta spectral power during SWS divided by that during REM) presented on a log scale over time, location, age, and version. The horizontal grey line signifies the threshold necessary to quantitatively distinguish between SWS and REM (at least a 2-fold difference). (A) Signal quality over time in days for all animals, showing a slight decrease in signal quality (due to the inclusion

of earlier versions). (B) Signal quality over time in days across subsequent versions of the instrument (V1, V2, V3), showing more consistent signal quality for V3. (C) Signal quality over location for all animals, showing overall lower signal quality in water than on land. (D) Signal quality over location across each version, showing improved resistance to water intrusion and resulting signal quality decrease. (E) Signal quality over age in years across all animals, showing the lowest signal quality in the oldest animals. (F) Signal quality over age in years shows the smallest signal quality decrease due to water in recordings with yearlings and 2-3 year-olds.

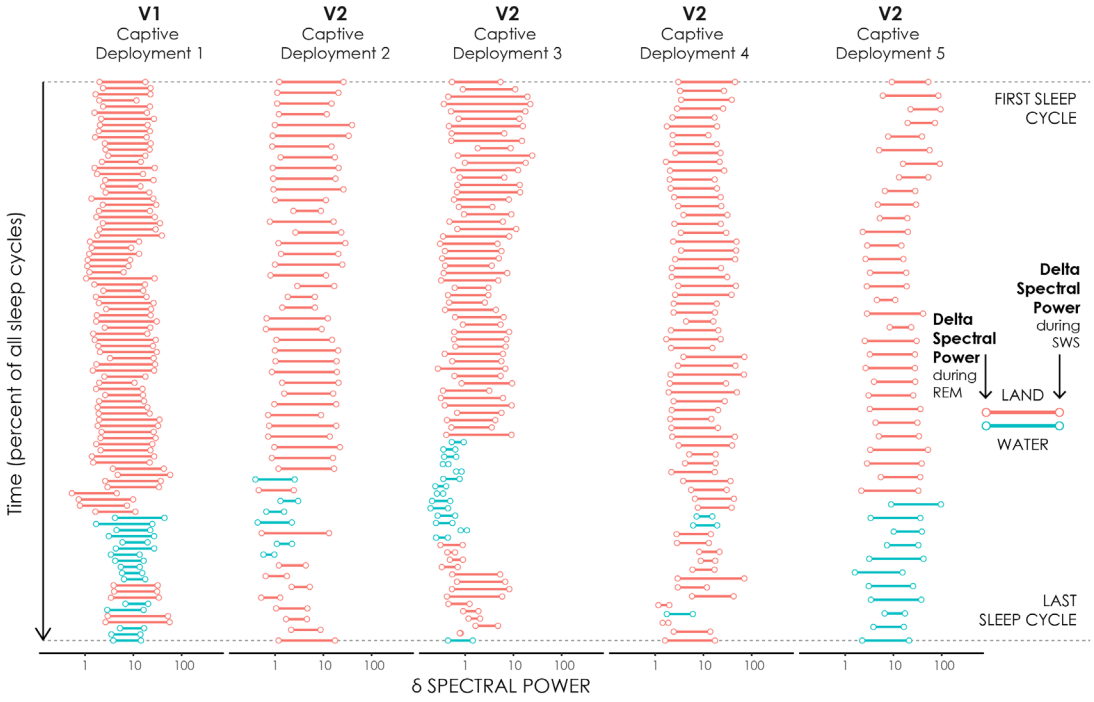

Figure 1.12. Effect of water submersion on signal quality. Lollipop plots showing delta spectral power of slow-wave sleep (SWS) connected to subsequent delta during REM, colored according to recording location (land in red and water in blue). Plots are aligned such that the first and last sleep cycles of each recording are aligned. Smaller lines after initial water submersion show the resulting decrease in signal quality, which is minimized in later iterations of the tag.

1.5 DISCUSSION

In Phase 1 of our study, we found the electrode type and configuration that performed best in our experiments: a differential montage of Genuine Grass goldcup electrodes attached with a conductive paste. The differential montage outperformed the single reference electrode because it allowed us to obtain reliable signals despite the occasional loss of individual channels. We then created and tested a robust, portable system in Phase 2. Our logger housing design enabled the use of up to 21 independent electrical signals (separate wires) and the detection of pressure, illumination, LED, and Bluetooth signals from the exterior of the housing. We found that small acrylic windows allowed adequate signal transmission despite the housing's thick aluminum wall. Ultimately, we designed a system using electrically shielded and reinforced wires combining polyurethane and silicone potting materials to minimize water intrusion, expedite patch removal, and facilitate patch renewal and reattachment.

We reliably identified SWS on land and in water. Still, signals were smaller in water than on land. The effects of age and tissue thickness were difficult to tease apart statistically due in part to our iterative design process. Despite typically smaller amplitude slow waves in water and in older animals, we were always able to distinguish between SWS and REM in older animals using our final design iteration, even during rest behavior in our most challenging recording environment (drifting through seawater in the wild). This leads us to believe that careful waterproofing and attachment could allow recordings with free-ranging adult animals. Based on pilot

studies at TMMC, we also expect to obtain reliable EEG signals (potentially including seizure detection) from surface-mounted sensors with California sea lions (*Zalophus californianus*). It is difficult to predict the success of surface-mounted sensors for continuous EEG recordings for animals with smooth skin and thicker blubber layers such as cetaceans. However, improvements in suction cups, sensor technology, and signal processing have allowed short-term EEG recordings, in-water auditory evoked potential recordings, and artifact removal in bottlenose dolphins (41,53). If suction cups can adequately exclude water and minimize lateral movement, longer-term surface EEG recordings of cetacean sleep may be possible (41).

We successfully removed heart artifacts with ICA and identified an IC that best expressed brain activity. This IC was most reliable for sleep scoring and maintained the spectral properties of sleep states. A primary concern in signal processing is whether the methods remove essential features of the signal of interest along with contaminating artifacts. In our case, it was critical to examine the spectral features of the IC that we identified as maximally expressing brain activity to ensure that this IC was sufficient for identifying sleep stages. When we compared the power spectrum of the raw EEG, pruned EEG, and the maximal brain IC, we observed that the power density spectrum of the IC during SWS (bottom-most bold line; Figure 1.13A) closely resembled the power density spectrum of raw signals during SWS in the absence of any heart rate artifacts (bottom lines; Figure 1.13B). This suggests that the maximal brain IC preserves the spectral features of SWS. Likewise, the power density spectrum of the raw EEG signal in

the presence of artifacts (top-most line; Figure 1.13A) closely resembles the raw electrocardiogram signal (top-most line; Figure 1.13B), suggesting that the contaminating signals removed via pruning with ICA are primarily generated by the heart.

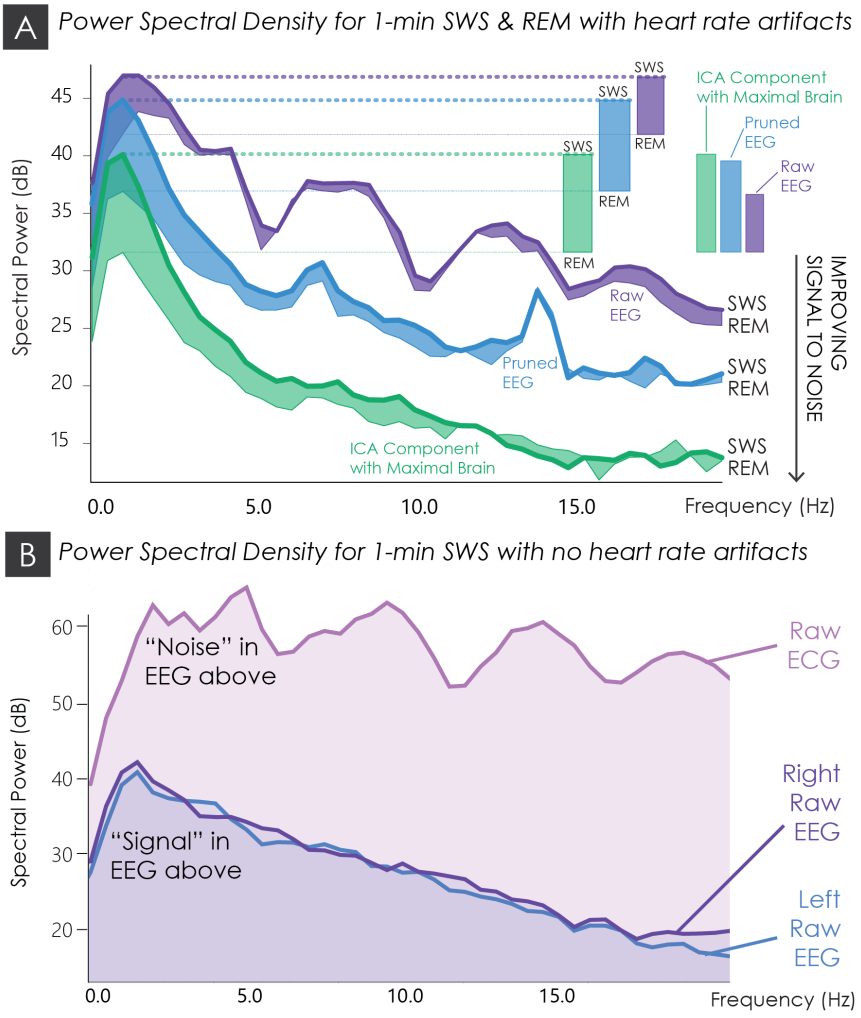

Figure 1.13. Power spectral density plots pre- and post-ICA. (A) Power spectral density plot for one minute of slow-wave sleep (SWS) and one minute of rapid-eye-movement sleep (REM)

(see Figure 11 for raw waveforms) with significant heart rate artifacts in the electroencephalogram (EEG). The plot compares spectral power over frequency for raw EEG (violet), EEG pruned with ICA (blue), and the IC that maximally expressed brain activity (green) for both SWS (bold upper line) and REM (thin lower line). This demonstrates the greater discriminatory power between SWS and REM in the delta frequency range in EEG signals processed with ICA (shaded areas). (B) Power spectral density (PSD) plot for 1 minute of SWS where there was no significant heart rate artifact in the EEG, demonstrating the spectral features of the raw electrocardiogram (ECG) signal, apparent in the raw EEG signal in 13A. In addition, left and right raw EEG signals show that the spectral features of SWS are primarily preserved in the maximal brain IC, shown in 13A. Note the different horizontal and vertical scales of A & B.

We reliably recorded heart rate on land and in water during motion and at rest but recorded the highest quality signals with shielded wires that were reinforced with heat shrink. Although we could detect larger-scale eye blink detections in the electrooculogram (EOG), we could not reliably detect smaller amplitude eye deflections during REM sleep that are readily picked up from electrodes implanted into the eye orbit (42). Similarly, our surface-mounted electromyography (EMG) electrodes only occasionally demonstrated a difference in muscle tone between SWS and REM sleep, suggesting a lower sensitivity than previous studies using invasive EMG to distinguish REM sleep in elephant seals (27,28). However, we could reliably identify REM using low-frequency heart rate variability, as in previous sleep apnea studies in walruses (13).

There were additional considerations when pairing the sleep-recording device with typical animal tracking tags. The typical transmission frequency for a VHF animal tracking tag is less than two seconds, not long enough for the electrophysiological signals to return to baseline after an interruption of high-frequency noise collapsed into the 500Hz recording frequency of the logger. We ordered a custom VHF tag duty cycled so that the transmitter would remain off for five days after being activated, and then

would ping at a frequency of only once per minute, allowing us to record reliable electrophysiological signals between each ping. In addition, because we had to place the sleep recording device on the top of the head, we had to place the Argos transmitter further back on the body, where it seldom exited the water to provide location coordinates. Future research can focus on creating a smaller, integrated, potted unit mounted on the head to maximize high quality location data.

Future studies can reduce the size and impact of the datalogger housing by potting the device in epoxy. Our design prioritized SD-card recovery and datalogger adjustment at this early prototyping stage. Future research could include creating a smaller, streamlined version of this device that focuses on recording only EEG and heart rate, both necessary for discrimination between SWS and REM based on our results. This refinement would reduce the headcap's footprint by prioritizing EEG over less critical EOG sensors. For sleep studies of bilaterally sleeping phocids, a single reliable EEG and ECG pair (and additional ground electrode) could be adequate for sleep characterization. However, we recommend recording at least four independent channels to increase the likelihood of continuous sleep state characterization. In addition, the number of independent components available for signal processing is proportional to the number of channels. A higher number of channels facilitates isolating contaminating artifacts from signals of interest. For unihemispheric sleeping cetaceans, sirenians, and fur seals, additional EEG channels are required to characterize independent changes in each hemisphere.

Due to the large size and limited availability of underwater connectors with more than 21 pins, we were limited to recording 10 differential electrophysiological signals (we chose to record 9 with 3 redundant ground electrodes). However, if a differential montage or underwater connector is not required, it would be possible to record up to 32 independent signals using the same Neurologger3 to improve spatial coverage. While this number is still far below the quantity recommended for source estimation in humans (minimum of 128 channels recommended) (54), higher density arrays (even <32 channels) could provide helpful information in the assessment of auditory evoked potentials in free-moving cetaceans or epilepsy in California sea lions (41,55).

Our study builds on advances in animal biotelemetry and technological miniaturization to allow the first recordings of marine mammal sleep in the wild, the context in which it evolved. EEG recordings are necessary to distinguish between behavioral sleep, SWS, and REM sleep, each of which provides distinct restorative functions to the brain and body. Our EEG device enabled sleep state categorization for wild northern elephant seals across their sleeping habitats. Future studies can use these methods to examine sleep patterns across individuals, ontogeny, and habitats to establish activity budgets and total sleep time for a large, highly mobile mesopredator. Total sleep time can be used to investigate the ties between sleep, ecology, cognition, and body size, furthering our understanding of wild animal resting behavior and the function and evolution of mammalian sleep (56,57).

The phenology of sleep and stress is changing in the face of increasing anthropogenic stressors (79). Ecophysiological studies of sleep and heart rate shed light on the evolution and physiological underpinnings of natural behavior and the effect of anthropogenic disturbance (2,7,8,11,12). By further developing these methods, we can more accurately assess the natural physiology and behavior of wild animals and quantify its alteration due to anthropogenic disturbance.

1.6 CONCLUSION

Our study provided a new, non-invasive electrophysiological method to record sleep in wild marine mammals. We built a custom headcap that minimized water intrusion to allow successful EEG discrimination between SWS and REM sleep with captive and wild animals, on land and in water, stationary and drifting through seawater. Over subsequent design iterations, we were able to minimize water intrusion and the resulting signal quality loss (δ power SWS/δ power REM), such that most sleep cycles remained above a quantitative threshold (SWS 2-fold higher than REM) throughout multi-day recordings. Our ECG signals provided reliable heart rate measurements whether animals were moving or calm and captured largescale low-frequency heart rate variability that distinguished REM from quiet waking. We discuss signal quality challenges and solutions, including ICA to facilitate visual and quantitative sleep scoring. Our study builds on technological advances and provides detailed recommendations to guide scientists in creating new tools to investigate sleep and heart rate in wild animals.

1.7 REFERENCES

1. Andrews RD, Jones DR, Williams JD, Thorson PH, Oliver GW, Costa DP, et al. Heart rates of northern elephant seals diving at sea and resting on the beach. J Exp Biol. 1997;200:2083–95.
2. Goldbogen JA, Cade DE, Calambokidis J, Czapanskiy MF, Fahlbusch J, Friedlaender AS, et al. Extreme bradycardia and tachycardia in the world's largest animal. Proc Natl Acad Sci USA. 2019 Dec 10;116(50):25329–32.
3. Kooyman GL, Campbell WB. Heart rates in freely diving Weddell seals, *Leptonychotes weddellii*. Comp Biochem Physiol A Comp Physiol. 1972 Sep 1;43(1):31–6.
4. Rattenborg NC, Voirin B, Vyssotski AL, Kays RW, Spoelstra K, Kuemmeth F, et al. Sleeping outside the box: Electroencephalographic measures of sleep in sloths inhabiting a rainforest. *Biol Lett.* 2008 Aug 23;4(4):402-5.
5. Rattenborg NC, De La Iglesia HO, Kempenaers B, Lesku JA, Meerlo P, Scriba MF. Sleep research goes wild: New methods and approaches to investigate the ecology, evolution and functions of sleep. *Philos Trans R Soc Lond B Biol Sci.* 2017 Nov 19;372(1734):20160251.
6. Thompson D, Fedak MA. Thompson D, Fedak MA. Cardiac responses of grey seals during diving at sea. *J Exp Biol.* 1993 Jan;174:139-54.
7. Williams TM, Blackwell SB, Richter B, Sinding MHS, Heide-Jørgensen MP. Paradoxical escape responses by narwhals (*Monodon monoceros*). *Science.* 2017;358(6368):1328–31.
8. McDonald BI, Elmegaard SL, Johnson M, Wisniewska DM, Rojano-Doñate L, Galatius A, et al. High heart rates in hunting harbour porpoises. Proc Biol Sci. 2021 Nov 10;288(1962):20211596.
9. Malungo IB, Gravett N, Bhagwandin A, Davimes JG, Manger PR. Sleep in two free-roaming blue wildebeest (*Connochaetes taurinus*), with observations on the agreement of polysomnographic and actigraphic techniques. IBRO Neurosci Rep. 2021 Jun 1;10:142–52.
10. Rattenborg NC, Voirin B, Cruz SM, Tisdale R, Dell'Omo G, Lipp HP, et al. Evidence that birds sleep in mid-flight. Nat Commun. 2016;7:1–9.
11. Voirin B, Scriba MF, Martinez-Gonzalez D, Vyssotski AL, Wikelski M, Rattenborg NC. Ecology and Neurophysiology of Sleep in Two Wild Sloth Species. Sleep. 2014 Apr 1;37(4):753–61.
12. Lesku JA, Rattenborg NC, Valcu M, Vyssotski AL, Kuhn S, Kuemmeth F, et al.

Adaptive sleep loss in polygynous pectoral sandpipers. Science. 2012;337(6102):1654–8.

13. Gergely A, Kiss O, Reicher V, Iotchev I, Kovács E, Gombos F, et al. Reliability of Family Dogs' Sleep Structure Scoring Based on Manual and Automated Sleep Stage Identification. Animals (Basel). 2020 Jun;10(6):927.

14. Siegel JM. Clues to the functions of mammalian sleep. Nature. 2005 Oct 27;437(7063):1264-71. doi: 10.1038/nature04285.

15. Tobler I. Evolution of the sleep process: A phylogenetic approach. Sleep Mechanisms Exp Brain Res Suppl. 1984;8:207–26.

16. Tobler I. Phylogeny of sleep regulation in: Principles and practice of sleep medicine. Kryger MH, Roth T, Dement WC, editors. Elsevier Saunders, Philadelphia; 2005. 77–90 p.

17. Siegel JM. The REM sleep-memory consolidation hypothesis. Science. 2001;294(5544):1058–63.

18. Lyamin OI, Manger PR, Ridgway SH, Mukhametov LM, Siegel JM. Cetacean sleep : An unusual form of mammalian sleep. Neurosci Biobehav Rev. 2008;32:1451–84.

19. Lyamin OI, Kosenko PO, Korneva SM, Vyssotski AL, Mukhametov LM, Siegel JM. Fur Seals Suppress REM Sleep for Very Long Periods without Subsequent Rebound. Curr Biol. 2018;28(12):2000-2005.e2.

20. de Camp NV, Dietze S, Klaßen M, Bergeler J. Noninvasive EEG recordings from freely moving piglets. J Vis Exp.. 2018;2018(137):1–5.

21. Lyamin OI, Kosenko PO, Vyssotski AL, Lapierre JL, Siegel JM, Mukhametov LM. Study of Sleep in a Walrus. Dokl Biol Sci. 2012;444(4):188–91.

22. Scriba MF, Harmening WM, Mettke-Hofmann C, Vyssotski AL, Roulin A, Wagner H, et al. Evaluation of two minimally invasive techniques for electroencephalogram recording in wild or freely behaving animals. J Comp Physiol A Neuroethol Sens Neural Behav Physiol. 2013;199(3):183–9.

23. Ternman E, Hänninen L, Pastell M, Agenäs S, Nielsen PP. Sleep in dairy cows recorded with a non-invasive EEG technique. Appl Anim Behav Sci. 2012;140(1–2):25–32.

24. Cousillas H, Oger M, Rochais C, Pettoello C, Ménoret M, Henry S, et al. An Ambulatory Electroencephalography System for Freely Moving Horses: An Innovating Approach. Front Vet Sci. 2017 May 2;4:57.

25. Paulson C, Chien D, Lin F, Seidlits S, Cai Y, Sargolzaei S, et al. A Novel Modular Headmount Design for non-invasive Scalp EEG Recordings in Awake Animal Models. Annu Int Conf IEEE Eng Med Biol Soc. 2018 Jul;2018:5422-5425. doi:

10.1109/EMBC.2018.8513686.

26. Lyamin OI, Chetyrbok IS. Unilateral EEG activation during sleep in the Cape fur seal, *Arctocephalus pusillus*. Neurosci Lett. 1992 Aug 31;143(1-2):263-6.

27. Lyamin OI. Sleep in the harp seal (*Pagophilus groenlandica*). Comparison of sleep on land and in water. J Sleep Res. 1993 Sep;2(3):170-174.

28. Lyamin OI, Mukhametov LM, Chetyrbok IS, Vassiliev AV. Sleep and wakefulness in the southern sea lion. Behav Brain Res. 2002 Jan 22;128(2):129-38.

29. Lyamin OI, Siegel JM. Sleep in Aquatic Mammals. In: Handb Behav Neurosci. 2019;30:375-393. doi: 10.1016/b978-0-12-813743-7.00025-6. Epub 2019 Jun 21.

30. Mukhametov LM, Lyamin OI, Polyakova IG. Interhemispheric asynchrony of the sleep EEG in northern fur seals. Experientia. 1985 Aug 15;41(8):1034-5.

31. Ridgway SH. Asymmetry and symmetry in brain waves from dolphin left and right hemispheres: Some observations after anesthesia, during quiescent hanging behavior, and during visual obstruction. Brain Behav Evol. 2002;60(5):265-74.

32. Ridgway SH, Harrison RJ, Joyce PL. Sleep and Cardiac Rhythm in the Gray Seal. Science. 1975 Feb 14;187(4176):553-5.

33. Castellini MA, Milsom WK, Berger RJ, Costa DP, Jones DR, Castellini JM, et al. Patterns of respiration and heart rate during wakefulness and sleep in elephant seal pups. Am J Physiol. 1994 Mar;266(3 Pt 2):R863-9. doi: 10.1152/ajpregu.1994.266.3.R863.

34. Milsom W, Castellini M, Harris M, Castellini J, Jones D, Berger R, et al. Effects of hypoxia and hypercapnia on patterns of sleep-associated apnea in elephant seal pups. Am J Physiol. 1996 Oct;271(4 Pt 2):R1017-24. doi: 10.1152/ajpregu.1996.271.4.R1017.

35. Serafetidines EA, Shurley JT, Brooks RE. Electroencephalogram of the pilot whale, *Globicephala scammoni*, in wakefulness and sleep: lateralization aspects. Int J Psychobiol. 1972;2:129–135.

36. Buzsáki G, Anastassiou CA, Koch C. The origin of extracellular fields and currents-EEG, ECoG, LFP and spikes. Nat Rev Neurosci. 2012 May 18;13(6):407-20.

37. Wendel K, Väisänen J, Seemann G, Hyttinen J, Malmivuo J. The influence of age and skull conductivity on surface and subdermal bipolar EEG leads. Comput Intell Neurosci. 2010;2010:397272.

38. Romero S, Mañanas MA, Clos S, Gimenez S, Barbanoj MJ. Reduction of EEG Artifacts by ICA in Different Sleep Stages. Proc. EEE Eng. Med. Biol. Soc., Sep. 2003, pp. 2675–2678.

39. Onton J, Makeig S. Chapter 7 Information-based modeling of event-related brain dynamics. Prog Brain Res. 2006;159:99-120. doi: 10.1016/S0079-6123(06)59007-7

40. Ventouras EM, Ktonas PY, Tsekou H, Paparrigopoulos T, Kalatzis I, Soldatos CR. Independent Component Analysis for Source Localization of EEG Sleep Spindle Components. Comput Intell Neurosci. 2010;2010:329436.

41. Schalles MD, Houser DS, Finneran JJ, Tyack P, Shinn-Cunningham B, Mulsow J. Measuring auditory cortical responses in *Tursiops truncatus*. J Comp Physiol A Neuroethol Sens Neural Behav Physiol. 2021 Sep;207(5):629-640.

42. Lyamin OI, Mukhametov LM, Siegel JM, Nazarenko EA. Unihemispheric slow wave sleep and the state of the eyes in a white whale. Behav Brain Res. 2002 Feb 1;129(1-2):125-9.

43. Lyamin OI, Lapierre JL, Kosenko PO, Mukhametov LM, Siegel JM. Electroencephalogram asymmetry and spectral power during sleep in the northern fur seal. J Sleep Res. 2008 Jun;17(2):154-65.

44. Fedak MA, Pullen MR, Kanwisher J. Circulatory responses of seals to periodic breathing: heart rate and breathing during exercise and diving in the laboratory and open sea. Can J Zool. 1988 Jan 1;66(1):53–60.

45. Kendall-Bar JM, Vyssotski AL, Mukhametov LM, Siegel JM, Lyamin OI. Eye state asymmetry during aquatic unihemispheric slow wave sleep in northern fur seals (*Callorhinus ursinus*). PLoS ONE. 2019;14(5):1–13.

46. Mitani Y, Andrews RD, Sato K, Kato A, Naito Y, Costa DP. Three-dimensional resting behaviour of northern elephant seals: drifting like a falling leaf. Biol Lett. 2010 Apr 23;6(2):163-6.

47. Oliver GW, Morris PA, Thorson PH, Boeuf BJ le. Homing Behavior of Juvenile Northern Elephant Seals. Mar Mammal Sci. 1998;14(2):245–56.

48. Viola FC, Thorne J, Edmonds B, Schneider T, Eichele T, Debener S. Semi-automatic identification of independent components representing EEG artifact. Clin. Neurophysiol. Pract. 2009;120(5):868-877.

49. Cade DE, Gough WT, Czapanskiy MF, Fahlbusch JA, Kahane-Rapport SR, Linsky JMJ, et al. Tools for integrating inertial sensor data with video bio-loggers, including estimation of animal orientation, motion, and position. Anim Biotelemetry. 2021 Dec;9(1):34.

50. Berry RB, Brooks R, Gamaldo CE, Harding SM, Lloyd RM, Marcus CL and Vaughn BV for the American Academy of Sleep Medicine. The AASM Manual for the Scoring of Sleep and Associated Events: Rules, Terminology and Technical Specifications, Version 2.2. www.aasmnet.org. Darien, Illinois: American Academy of Sleep

Medicine, 2015.

51. JMP®. Cary, NC: SAS Institute Inc.; 1989.

52. Kendall-Bar J. Eavesdropping on the Brain at Sea - Github Repository. GitHub. 2021. https://github.com/jmkendallbar/Eavesdropping-on-the-Brain-at-Sea. Accessed 10 Dec 2021.

53. Yu Y, Li N, Li Y, Liu W. A Portable Waterproof EEG Acquisition Device for Dolphins. Sensors (Basel). 2021 May 11;21(10):3336.

54. Song J, Davey C, Poulsen C, Luu P, Turovets S, Anderson E, et al. EEG source localization: Sensor density and head surface coverage. J Neurosci Methods. 2015 Dec 30;256:9-21.

55. Michel CM, Brunet D. EEG Source Imaging: A Practical Review of the Analysis Steps. Front Neurol. 2019 Apr 4;10:325.

56. Zepelin H, Siegel JM, Tobler I. Chapter 8 Mammalian Sleep. Princ Pract Sleep Med Fourth Ed, MHKRC Dement Ed WB, Saunders Phila, 2005, pp. 91–100.

57. Capellini I, Barton RA, McNamara P, Preston BT, Nunn CL. Phylogenetic Analysis of the Ecology and Evolution of Mammalian Sleep. Evolution. 2008;62(7):1764–76.

58. Lyamin OI, Mukhametov LM, Siegel JM. Relationship between sleep and eye state in cetaceans and pinnipeds. Arch Ital Biol. 2004 Jul;142(4):557-68.

59. Mukhametov LM, Supin AY, Polyakova IG. Interhemispheric asymmetry of the electroencephalographic sleep patterns in dolphins. Brain Res. 1977 Oct 14;134(3):581-4. doi: 10.1016/0006-8993(77)90835-6.

60. Mukhametov LM. Unihemispheric slow-wave sleep in the Amazonian dolphin, *Inia geoffrensis*. Neurosci Lett. 1987 Aug 18;79(1-2):128-32. doi: 10.1016/0304-3940(87)90684-7.

61. Mukhametov LM, Lyamin OI, Chetyrbok IS, Vassilyev AA, Diaz RP. Sleep in an Amazonian manatee, *Trichechus inunguis*. Experientia. 1992 Apr 15;48(4):417-9. doi: 10.1007/BF01923447.

62. Lyamin OI, Chetyrbok IS. Unilateral EEG activation during sleep in the Cape fur seal, *Arctocehalus pusillus*. Neurosci Lett. 1992 Aug 31;143(1-2):263-6. doi: 10.1016/0304-3940(92)90279-g.

63. Lyamin OI, Lapierre JL, Kosenko PO, Kodama T, Bhagwandin A, Korneva SM, et al. Monoamine Release during Unihemispheric Sleep and Unihemispheric Waking in the Fur Seal. Sleep. 2016 Mar 1;39(3):625-36.

64. Lapierre JL, Kosenko PO, Lyamin OI, Kodama T, Mukhametov LM, Siegel JM. Cortical Acetylcholine Release Is Lateralized during Asymmetrical Slow-Wave

Sleep in Northern Fur Seals. J Neurosci. 2007 Oct 31;27(44):11999-2006.

65. Lyamin OI, Kosenko PO, Lapierre JL, Mukhametov LM, Siegel JM. Fur Seals Display a Strong Drive for Bilateral Slow-Wave Sleep While on Land. J Neurosci. 2008 Nov 26;28(48):12614-21.

66. Lyamin OI, Oleksenko AI, Polyakova IG. Sleep in the harp seal (*Pagophilus groenlandica*). Peculiarities of sleep in pups during the first month of their lives. J Sleep Res. 1993 Sep;2(3):163-169. doi: 10.1111/j.1365-2869.1993.tb00081.x.

67. Mulsow J, Reichmuth C. Electrophysiological Assessment of Temporal Resolution in Pinnipeds. Aquat Mamm. 2007 Jan 1;33(1):122–31.

68. Houser DS, Crocker DE, Reichmuth C, Mulsow J, Finneran JJ. Auditory Evoked Potentials in Northern Elephant Seals (*Mirounga angustirostris*). Aquat Mamm. 2007 Jan 1;33(1):110–21.

69. Kerem D, Elsner R. Cerebral tolerance to asphyxial hypoxia in the harbor seal. Respir Physiol. 1973 Nov;19(2):188-200. doi: 10.1016/0034-5687(73)90077-7.

70. Murayama T, Aoki I, Ishii T. Measurement of the electroencephalogram of the bottlenose dolphin under different light conditions. Aquat Mamm. 1993; 19.3:171–182

71. Hashio F, Tamura S, Okada Y, Morimoto S, Ohta M, Uchida N. Frequency analysis of electroencephalogram recorded from a bottlenose dolphin (*Tursiops truncatus*) with a novel method during transportation by truck. J Physiol Sci. 2010 Jul;60(4):235–44.

72. McDonald BI, Ponganis PJ. Deep-diving sea lions exhibit extreme bradycardia in long-duration dives. J Exp Biol. 2014 May 1;217(Pt 9):1525–34.

73. Williams TM, Fuiman LA, Kendall T, Berry P, Richter B, Noren SR, et al. Exercise at depth alters bradycardia and incidence of cardiac anomalies in deep-diving marine mammals. Nat Commun. 2015 May;6(1):6055.

74. Ponganis PJ, Kooyman GL, Winter LM, Starke LN. Heart rate and plasma lactate responses during submerged swimming and trained diving in California sea lions, *Zalophus californianus*. J Comp Physiol B. 1997 Jan;167(1):9-16.

75. Cruz-Aguilar MA, Hernández-Arteaga E, Hernández-González M, Ramírez-Salado I, Guevara MA. Principal component analysis of electroencephalographic activity during sleep and wakefulness in the spider monkey (*Ateles geoffroyi*). Am J Primatol. 2020 Aug;82(8).

76. Cruz-Aguilar MA, Ramírez-Salado I, Arenas-Rosas RV, Santillán-Doherty AM, Muñoz-Delgado JI. Sleep characterization of a one-month-old freely moving stumptail macaque (*Macaca arctoides*): a pilot study. J Med Primatol. 2009

Oct;38(5):371-6.

77. Lesku JA, Meyer LCR, Fuller A, Maloney SK, Dell'Omo G, Vyssotski AL, et al. Ostriches Sleep like Platypuses. Balaban E, editor. PLoS ONE. 2011 Aug 24;6(8):e23203.

78. Massot B, Rattenborg NC, Hedenstrom A, Akesson S, Libourel P-A. An Implantable, Low-Power Instrumentation for the Long Term Monitoring of the Sleep of Animals under Natural Conditions. Annu Int Conf IEEE Eng Med Biol Soc. 2019 Jul;2019:4368-4371. doi: 10.1109/EMBC.2019.8856359.

79. Szymczak JT. Seasonal changes of daily sleep pattern in the starling, Sturnus vulgaris. Journal of Interdisciplinary Cycle Research. 1986 Sep;17(3):189–96.

80. van Hasselt SJ, Rusche M, Vyssotski AL, Verhulst S, Rattenborg NC, Meerlo P. Sleep Time in the European Starling Is Strongly Affected by Night Length and Moon Phase. Curr Biol. 2020 May 4;30(9):1664-1671.e2. doi: 10.1016/j.cub.2020.02.052. Epub 2020 Mar 19. PMID: 32197088.

81. van Hasselt SJ, Rusche M, Vyssotski AL, Verhulst S, Rattenborg NC, Meerlo P. The European starling (Sturnus vulgaris) shows signs of NREM sleep homeostasis but has very little REM sleep and no REM sleep homeostasis. Sleep. 2020 Jun 15;43(6):zsz311.

82. Nordt A, Klenke R. Sleepless in Town – Drivers of the Temporal Shift in Dawn Song in Urban European Blackbirds. PLOS ONE. 2013 Aug 7;8(8):e71476

Author Contributions

J.K.B. (candidate): conceptualization, funding acquisition, methodology, validation, visualization, project administration, software, data curation, formal analysis, resources, investigation, writing- original draft, writing- review and editing. R.M., J.N., C.L., D.A.L.: data curation, visualization, formal analysis, investigation, writing- review and editing. J.K.P. & M.D.S.: methodology, investigation, data analysis supervision, writing- review and editing. R.R.H., R.S.B., C.L.F., & S.P.J.: investigation, project administration, formal analysis, writing- review and editing. A.L.V.: methodology, software, resources. T.M.W. &

D.P.C.: conceptualization, funding acquisition, resources, project supervision, project administration, writing- review and editing. All authors read and approved the final manuscript and approved its use in the dissertation.

Ethics Approval

All animal procedures were approved at the federal and institutional levels under National Marine Fisheries Permits #19108, #23188, and #18786 (TMMC), and by the Institutional Animal Care and Use Committee (IACUC) of University of California Santa Cruz (Costd1709 and Costd2009-2) and The Marine Mammal Center (TMMC #2019-2).

Acknowledgments

We acknowledge the students, volunteers, and researchers who have all contributed to the long-term Año Nuevo elephant seal research program. We thank Año Nuevo State Park and the Año Nuevo UC Natural Reserve for their ongoing support. We especially thank field researchers P. Robinson, A. Favilla, T. Keates, J. Mulsow, G. McDonald, D. Crocker, L. Hückstädt, R. Jones, M. Krieg, R. Cuthbertson, A. Manriquez, A. Gutierrez, A. Lankow, L. Solis, L. Keehan, L. Carswell, E. Nazario, I. Shukla, and L. Pallin. We thank TMMC veterinarians E. Whitmer, S. Whoriskey, E. Trumbull, D. Whittaker, F. Gulland, and S. Pattison. We also thank Long Marine Lab staff and volunteers for facilitating lab-based studies, especially D. Casper, R. Skrovan, N. Moore, C. Reichmuth of the Pinniped Lab, and T. Kendall of the Marine Mammal Physiology Project. We would like to thank P.

Guerrero, E. Slattery, J. Bielke, colleagues at Ocean Innovations, Scripps Institution of Oceanography, and the Shorter lab at University of Michigan for engineering support and mentorship.

Table 1-3. Supplementary Table. A history of electrophysiological recordings, including marine mammal sleep studies, non-invasive and wild recordings in other mammals and birds, and electrophysiological recordings of wild marine mammals (ECG only) to highlight the shifts in recording methodologies over time and across vertebrate systems as well as emphasize the need for non-invasive recordings of freely moving wild marine mammals, in their natural environment. For each paper, we display the citation number (for referencing icons in Figure 1), citation, family, species, number of animals (N), recording duration (N/A indicates evoked potential studies involving averaged responses over multiple stimulus presentations [no baseline synchronous data collected]), recording location (including restraint technique within land or water environments), animal mobility (physical restraint [P], chemical restraint [C], trained restraint [T], tethered (attached to a stationary recording device via cables), or no restraint), captive (C) versus wild (W), electrode invasiveness (non-invasive [NI]: does not pierce the skin, minimally invasive [MI]: needle electrodes, or invasive [I]: implanted in the skull [epidural] or brain [subdural]).

		Citation #	Citation	Family	Species	N	Recording duration	Recording location	Animal mobility	Captive v Wild	Invasiveness	Electrode invasiveness
MARINE MAMMALS												
MARINE MAMMALS	SLEEP STUDIES	1	Lyamin et al., 2002 (42)	Monodontidae	*Delphinapterus leucas*	1	2 days	harness	Restraint - P	C	**I**	subdural
		2	Lyamin et al., 2004 (58)	Monodontidae	*Delphinapterus leucas*	1	2 days	sling	Restraint - P	C	**I**	epidural
		3	Lyamin et al., 2004 (58)	Delphinidae	*Tursiops truncatus*	1	2 days	sling	Restraint - P	C	**I**	epidural
		4	Serafetinides, 1972 (35)	Delphinidae	*Globicephala scammoni*	1	<12h	sling	Restraint - P	C	**M I**	sub-Q
		5	Mukhametov et al. 1977 (59)	Delphinidae	*Tursiops truncatus*	9	3 x 72h	pool	Tethered	C	**I**	epidural
		6	Mukhametov, 1987 (60)	Platanistidae	*Inia geoffrensis*	2	several days	pool	Tethered	C	**I**	subdural
		7	Mukhametov et al., 1992 (61)	Trichechidae	*Trichechus inunguis*	1	5 days	pool	Tethered	C	**I**	epidural
		8	Lyamin et al., 1992 (62)	Otariidae	*Arctocephalus pusillus*	1	2 x 24h	enclosure	Tethered	C	**I**	epidural
		9	Lyamin et al., 2002 (28)	Otariidae	*Otaria flavescens*	3	3-4 days	enclosure	Tethered	C	**I**	epidural
		10	Lyamin et al., 2016 (63)	Otariidae	*Callorhinus ursinus*	8	4-6h daily	enclosure	Tethered	C	**I**	epidural
		11	Lapierre et al., 2007 (64)	Otariidae	*Callorhinus ursinus*	4	4-6h daily	enclosure	Tethered	C	**I**	epidural

12	Lyamin et al., 2008 (2X) (43,65)	Otariidae	*Callorhinus ursinus*	4	several days	enclosure	Tethered	C	**I**	epidural
13	Lyamin, 1993 (66)	Phocidae	*Pagophilus groenlandicus*	4	24h	enclosure	Tethered	C	**I**	epidural
14	Lyamin, 1993 (27)	Phocidae	*Pagophilus groenlandicus*	4	2 x 24h	pool	Tethered	C	**I**	epidural
15	Lyamin et al., 2012 (21)	Odobenidae	*Odobenus rosmarus*	1	5 days	enclosure	Tethered	C	**I**	epidural
16	Lyamin et al., 2012 (21)	Odobenidae	*Odobenus rosmarus*	1	3 days	pool	No Restraint	C	**I**	epidural
17	Lyamin et al., 2004 (58)	Otariidae	*Callorhinus ursinus*	2	several days	enclosure	No Restraint	C	**I**	epidural
18	Ridgway 2002 (31)	Delphinidae	*Tursiops truncatus*	1	7h	pool	No Restraint	C	**I**	epidural
19	Ridgway et al., 1975 (32)	Phocidae	*Halichoerus grypus*	4	12 x 14h	enclosure	No Restraint	C	**I**	epidural
19	Ridgway et al., 1975 (32)	Phocidae	*Halichoerus grypus*	4	12 x 14h	pool	No Restraint	C	**I**	epidural
20	Lyamin et al., 2018 (19)	Otariidae	*Callorhinus ursinus*	4	2 days	enclosure	No Restraint	C	**I**	epidural
21	Lyamin et al., 2018 (19) ; Kendall-Bar et al., 2019 (45)	Otariidae	*Callorhinus ursinus*	4	10-14 days	pool	No Restraint	C	**I**	epidural
22	Castellini et al., 1994 (33); Milsom et al., 1996 (34)	Phocidae	*Mirounga angustirostris*	12	10h	enclosure	Tethered	C	**MI**	sub-Q
22	Castellini et al., 1994 (33); Milsom et al., 1996 (34)	Phocidae	*Mirounga angustirostris*	12	4.5 h*	pool	Tethered	C	**MI**	sub-Q

NON-SLEEP EEG	23	Mulsow et al., 2007 (AEP) (67)	Otariidae	*Zalophus californianus*	5	N/A	enclosure	Restraint - C	C	**MI**	sub-Q
	24	Mulsow et al., 2007 (AEP) (67)	Phocidae	*Phoca vitulina*	1	N/A	enclosure	Restraint - T	C	**MI**	sub-Q
	25	Mulsow et al., 2007 (AEP) (67)	Phocidae	*Mirounga angustirostris*	1	N/A	enclosure	Restraint - C & P	C	**MI**	sub-Q
	26	Houser et al., 2007 (AEP) (68)	Phocidae	*Mirounga angustirostris*	9	N/A	beach	Restraint - C	C	**MI**	sub-Q
	27	Houser et al., 2007 (AEP) (68)	Phocidae	*Mirounga angustirostris*	1	N/A	board	Restraint - P	C	**MI**	sub-Q
	28	Kerem et al., 1973 (69)	Phocidae	*Phoca vitulina*	1	N/A	board	Restraint - P	C	**MI**	sub-Q
	29	Murayama, 1993 (70)	Delphinidae	*Tursiops truncatus*	2	9 minutes	mattress	Restraint - P	C	**NI**	surface
	30	Hashio et al. 2010 (71)	Delphinidae	*Tursiops truncatus*	1	<15 min sessions	sling	Restraint - P	C	**NI**	surface
	31	Yu et al., 2021 (53)	Delphinidae	*Tursiops truncatus*	2	short session	mattress	No Restraint	C	**NI**	surface
	31	Yu et al., 2021 (53)	Delphinidae	*Tursiops truncatus*	2	short session	pool	No Restraint	C	**NI**	surface
ONLY ECG	32	Kooyman & Campbell, 1972 (3)	Phocidae	*Leptonychotes weddellii*	5	not stated	ocean	Tethered	W	**MI**	sub-Q
	33	McDonald et al., 2014 (72)	Otariidae	*Zalophus californianus*	5	10-17h	ocean	No Restraint	W	**MI**	sub-Q
	34	Thompson & Fedak, 1993 (6)	Phocidae	*Halichoerus grypus*	3	> 5h	ocean	No Restraint	W	**NI**	surface
	35	Fedak et al., 1988 (44)	Phocidae	*Phoca vitulina*	2	20 days	sea	No Restraint	W	**NI**	surface
	36	Andrews et al., 1997 (1)	Phocidae	*Mirounga angustirostris*	7	several days	ocean	No Restraint	W	**NI**	surface
	37	Williams et al., 2015 (73)	Phocidae	*Leptonychotes weddellii*	3	5-21 days	ocean	No Restraint	W	**NI**	surface
	38	Ponganis et al., 1997 (74)	Otariidae	*Zalophus californianus*	4	36 h	ocean	No Restraint	W	**NI**	surface
	39	Goldbogen et al., 2019 (2)	Balaenopteridae	*Balaenoptera musculus*	1	8.5 h	ocean	No Restraint	W	**NI**	surface

NON-MARINE MAMMALS

Non-marine mammals	SLEEP STUDIES	40	Malungo et al., 2021 (9)	Wildebeest *(Connochaetes taurinus)*	2	72h	enclosure	No Restraint	C	**I**	epidural
		41	Scriba et al., 2013 (22)	Barn owls *(Tyto alba)*	8	24h	flight room	No Restraint	C	**NI**	surface
		42	Ternman et al., 2012 (23)	Cows *(Bos taurus)*	8	6h	pen	No Restraint	C	**NI**	surface
		43	Gergely et al., 2020 (13)	Family dogs *(Canis familiaris)*	10	3h	home	No Restraint	C	**NI**	surface
		44	Cruz-Aguilar et al., 2020 (75)	Spider monkey *(Ateles geoffroyi)*	6	24h	enclosure	No Restraint	C	**NI**	surface
		45	Cruz-Aguilar et al., 2009 (76)	Stumptail macaque *(Macaca arctoides)*	1	14h	enclosure	No Restraint	C	**NI**	surface
		46	Lesku et al., 2011 (77)	Ostrich *(Struthio camelus)*	6	1-18 days	reserve	No Restraint	W	**I**	epidural
		47	Lesku et al., 2012 (12)	Sandpipers *(Calidris melanotos)*	>10	87 - 226h	free	No Restraint	W	**I**	epidural
		48	Rattenborg et al., 2016 (10)	Great frigatebird *(Fregata minor)*	15	10 days	free	No Restraint	W	**I**	epidural
		49	Rattenborg et al., 2008 (4)	Sloths *(Bradypus variegatus)*	3	5 days	free	No Restraint	W	**MI**	sub-Q
		50	Voirin et al., 2014 (11)	Sloths *(Bradypus variegatus & pygmaeus)*	9. 6	212 - 241h	free	No Restraint	W	**MI**	sub-Q
		51	Massot et al., 2019 (78)	Swifts *(Apus apus)*	>1	>48h	free	No Restraint	W	**MI**	sub-Q
		52	Szymczak, 1986 (79)	European Starling (*Sturnus vulgaris*)	10	Several days	enclosure	No Restraint	C	**I**	epidural
		53	van Hasselt et al., 2020 (Curr. Biol.) (80)	European Starling (*Sturnus vulgaris*)	12	3 days	Semi-natural enclosure	No Restraint	C	**I**	epidural
		54	van Hasselt et al., 2020 (SLEEP) (81)	European Starling (*Sturnus vulgaris*)	12	3 days	cage	No Restraint	C	**I**	epidural

Chapter 2. **Extreme breath holds allow wild seals to sleep while diving**

Jessica M. Kendall-Bar[1]*, Terrie M. Williams[1], Ritika Mukherji[2], Daniel A. Lozano[1], Julie K. Pitman[3], Rachel R. Holser[1], Theresa Keates[1], Roxanne S. Beltran[1], Patrick Robinson[1], Daniel Crocker[4], Taiki Adachi[1], Oleg I. Lyamin[5], Alexei L. Vyssotski[6], Daniel P. Costa[1]

Affiliations:

1: Ecology and Evolutionary Biology, University of California Santa Cruz, CA
2: Miranda House, University of Delhi, India
3: Sleep Health MD, Santa Cruz, CA
4: Sonoma State University, Rohnert Park, CA
5: University of California Los Angeles, Los Angeles, CA
6: Institute of Neuroinformatics, University of Zurich and Swiss Federal Institute of Technology (ETH), Zurich, Switzerland

*This research represents partial requirements for the dissertation of J. Kendall-Bar.

2.1 ABSTRACT

While it is widely recognized that sleep is critical for mammalian survival, marine mammals are constantly on the move- often traveling thousands of kilometers in search of food. We developed a novel system to measure sleep in deep-diving northern elephant seals (*Mirounga angustirostris*; N=13). Their breath-holding capacity liberates a niche where they can safely sleep at depth, during short (< 20 min) naps up to 377 m below the surface (N= 104 sleeping dives). We apply these results to identify rest in time-depth records for 323 seals. Seals travelled thousands of kilometers, sleeping ~2 h per day for several months, an endurance sprint to gather sustenance at sea.

2.2 INTRODUCTION

Across the animal kingdom, sleep plays a critical role in energy conservation, immune function, memory, and learning (1). In humans, disruptions to sleep negatively impact health with severe consequences. Humans suffer from obstructive sleep apnea, where intermittent breathing disrupts sleep, lowers sleep quality, and causes widespread pathology (2). Shift work in humans disrupts endogenous cycles and impacts immune function (3). For wild animals, diverse sleep patterns reflect adaptation to conflicting demands to feed, maximize fitness, and escape predation. Daily circadian rhythms confer adaptive advantages (4). Sandpipers that sacrifice sleep sire more offspring (5). While sleeping, cows chew, horses stand, ostriches stare, frigatebirds fly, and dolphins swim (6–10). Our understanding of sleep's function and pathology is augmented by studying its most extreme forms in the wild (1).

Marine mammals must feed, maintain vigilance for predators, regulate body temperature, and surface to breathe. Activity budgets of mammals at sea balance these tradeoffs and push them towards physiological extremes. Adult female northern elephant seals (Mirounga angustirostris) travel more than 10,000 km during seven-month foraging trips, spending only 2 min at the surface between 10 to 30 min dives (11, 12). On dives, seals routinely experience hypoxemia and near-complete blood oxygen depletion (13). Round-the-clock foraging (1000 to 2000 times a day) is critical to support their large body mass given relatively small prey (14). While functioning at

these physiological extremes, an open question remains: how do these marine mammals survive and sleep at sea?

2.3 METHODS

2.3.1 *A new tool to detect brain activity at sea*

We developed a novel submersible electroencephalogram (EEG) system (Figure 2.1; Kendall-Bar *et al*. 2022; in press) to non-invasively detect the brain activity of free-moving juvenile female northern elephant seals (N=13 seals). We recorded sleep in a controlled lab environment (N=5 seals) and in the wild (N=8 seals) among 4 locations: (a) on the beach, (b) in shallow water, (c) on the continental shelf (< 250 m), and (d) in the open ocean (> 250 m). We used these EEG records to identify sleep signatures within dive records, which allowed us to estimate sleep in dive records of 323 adult female northern elephant seals at sea over several months.

2.4 RESULTS

We recorded electrophysiological sleep during 104 dives at sea, where seals either slept on the ocean floor (64-249 m) or drifted through the water column (82-377 m) (Figure 2.1). Sleep in marine mammals is unique given that inactivity matching the definition of behavioral sleep can be absent entirely (8). As a result, electrophysiological recordings are essential to assess total sleep time. EEG recordings also discriminate rapid eye movement (REM) from non-REM slow-wave sleep (SWS), each with unique physiological and behavioral implications. Most notably for an animal sleeping at sea, REM sleep often results in sleep paralysis.

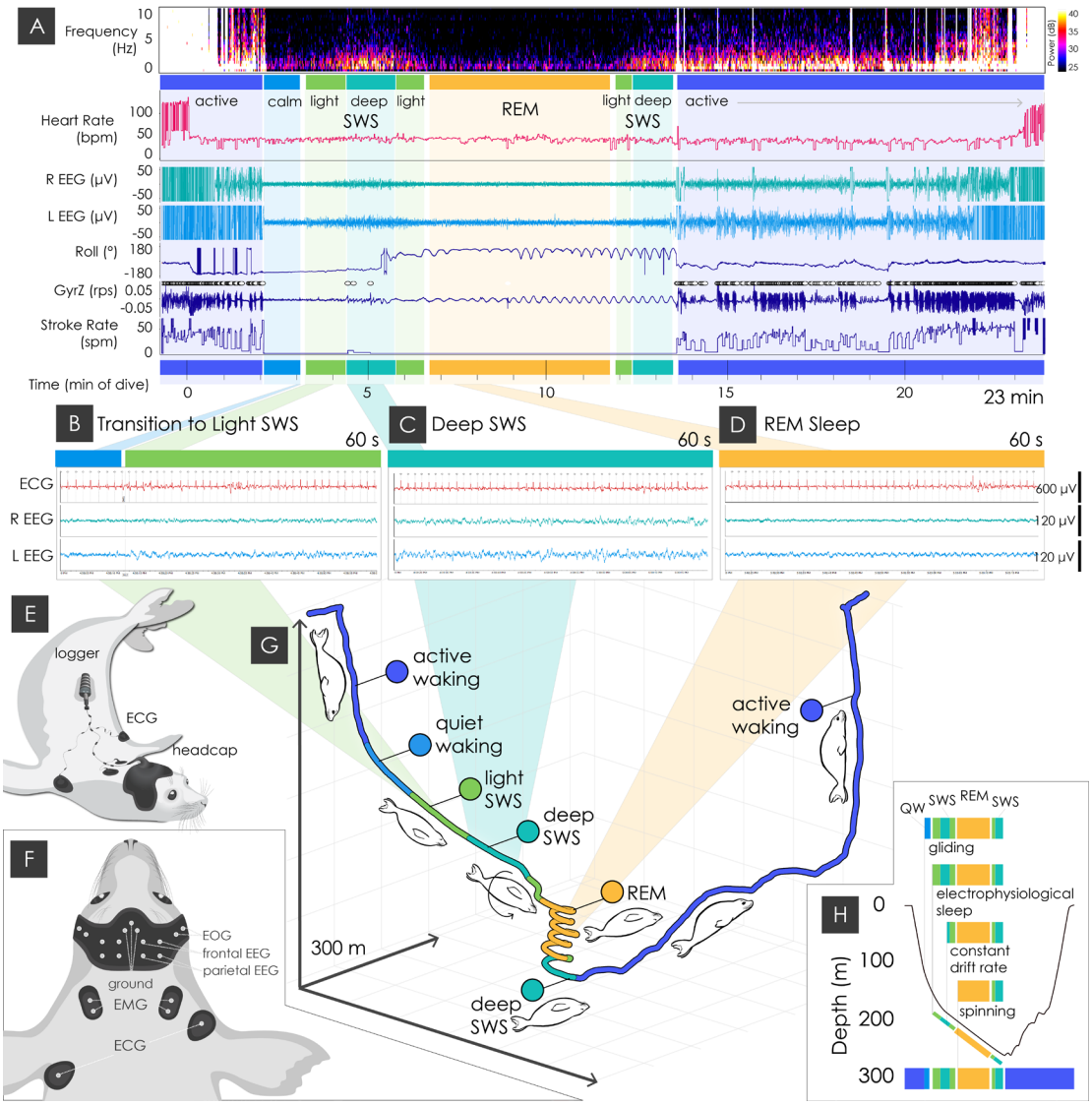

Figure 2.1. Three-dimensional drift dive sleep patterns. (A) Timeseries data for a 23-minute drift dive showing L EEG spectrogram (Power (dB) for Frequency (Hz) over time), Heart rate (beats per minute [bpm]), R and L EEG (µV), Roll (degrees [°]), z-axis Gyroscope (rotations per seconds [rps]), Strsoke rate (strokes per minute [spm]), and Time (minute of dive). (B, C, & D) Raw EEG and ECG signals demonstrate differences between waking (left of B), light sleep with K-

complexes and sleep spindles (right of B), deep slow-wave sleep (C) with large amplitude slow waves, and rapid-eye-movement sleep (D) with low voltage, high-frequency EEG activity, and high low-frequency heart rate variability. (E) EEG logger attachment configuration demonstrating headcap and logger placement. (F) Schematic demonstrating placement of EOG, EEG, EMG, ECG, and ground electrodes. (G) Three-dimensional dive profile color-coded by sleep state (Active Waking [AW] in dark blue; Quiet Waking [QW] in light blue; Light SWS [SWS1] in light green, Deep SWS [SWS2] in teal; REM in yellow-orange). (H) Depth over time shows nested durations of gliding, electrophysiological sleep, constant drift rate, and spinning.

As a result of this sleep paralysis, animals are particularly vulnerable to predation (1). This might suggest that seals at sea, evading killer whales and white sharks (15, 16), would limit REM in preference to SWS. Cetaceans studied in captivity have no signs of REM sleep, presumably because this cessation of activity would prevent them from surfacing to breathe (8). However, even in seals at sea, we found that elephant seals exhibit a relatively large proportion of REM sleep (26.5% ± 5.0% of total sleep time across all animals and 29.1 ± 4.3% at sea; compared to 3%, 4%, and 1% in captive harp seals, walruses, and fur seals (19-21).

The seals' three-dimensional behavior in the open ocean confirmed that they always lost postural control, were upside down, and near horizontal during REM sleep (|roll| = 2.8 ± 0.12 radians; pitch = -0.024 ± 0.26 radians) (Figure 2.1). This long-lasting combination of high roll and low pitch resulted in a slow spiraling behavior (~1 min per spiral). These patterns, not present during waking, provide a biomechanical signature of sleep. However, sleeping seals in SWS could maintain postural control while gliding upright for several minutes. These results challenge earlier hypotheses that sleep begins once animals are upside down and underscore the importance of EEG to assess sleep state (15).

Daily sleep estimates are central to comparative sleep studies investigating sleep's function and evolution. We observed marked changes in total sleep time across land and sea, where opportunities for social learning are replaced by foraging opportunities and, in turn, the risk of being eaten (Figure 2.2). Seals slept up to 14.1 h on the beach but as little as 0 h a day at sea (10.6 ± 3.4 h on land; 1.7 ± 0.7 h in the open ocean). When they returned to land, seals exhibited characteristic sleep rebound consisting of a long, consolidated period of high-voltage slow-wave sleep followed by shorter, lower-voltage sleep cycles.

We built a custom rest identification model (92% accuracy; see Supplementary material) based on the biomechanical signatures of SWS and REM from EEG-based sleep recordings (Figure 2.3). We applied this model to estimate sleep quotas over several months at sea, using a 20-year dataset with high-resolution diving data from 323 seals (N=183 short trips [79.9 ± 18.0 days] and N=140 long trips [221.7 ± 19.2 days]).

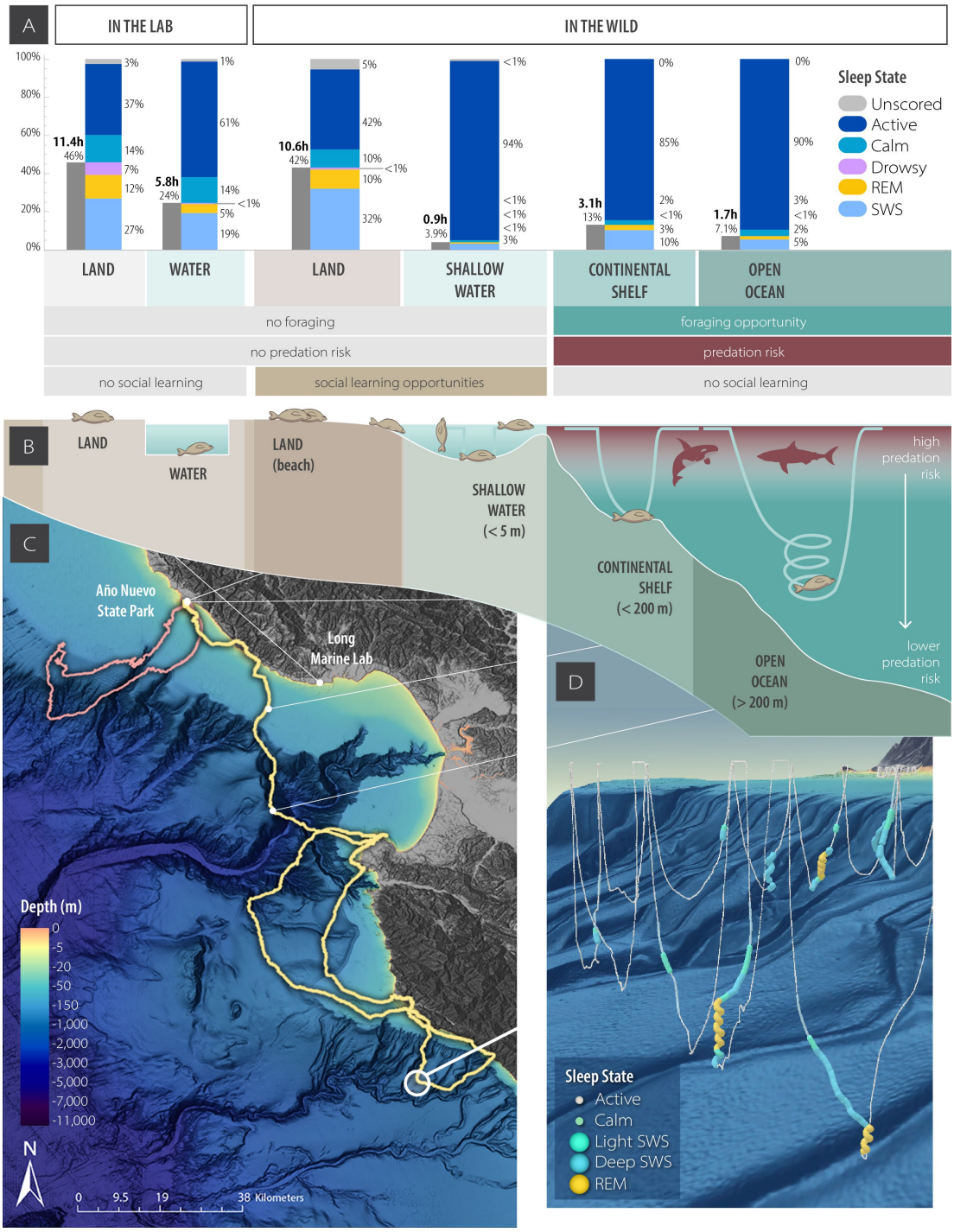
A
IN THE LAB
IN THE WILD
100%
80%
60%
40%
20%
0%
11.4h
46%
3%
37%
14%
7%
12%
27%
5.8h
24%
1%
61%
14%
<1%
5%
19%
10.6h
42%
5%
42%
10%
<1%
10%
32%
0.9h
3.9%
<1%
94%
<1%
<1%
<1%
3%
3.1h
13%
0%
85%
2%
<1%
3%
10%
1.7h
7.1%
0%
90%
3%
<1%
2%
5%
Sleep State
Unscored
Active
Calm
Drowsy
REM
SWS
LAND
WATER
LAND
SHALLOW WATER
CONTINENTAL SHELF
OPEN OCEAN
no foraging
foraging opportunity
no predation risk
predation risk
no social learning
social learning opportunities
no social learning
B
LAND
WATER
LAND (beach)
SHALLOW WATER (< 5 m)
CONTINENTAL SHELF (< 200 m)
OPEN OCEAN (> 200 m)
high predation risk
lower predation risk
C
Año Nuevo State Park
Long Marine Lab
Depth (m)
0
-5
-20
-50
-150
-1,000
-2,000
-3,000
-5,000
-7,000
-11,000
N
0
9.5
19
38 Kilometers
D
Sleep State
Active
Calm
Light SWS
Deep SWS
REM

Figure 2.2. Sleep patterns from land to sea. (A) Daily sleep quotas for seals in the lab (on land and in shallow water) and in the wild (on land, in shallow water, on the continental shelf, and in the open ocean), including Active Waking (dark blue), Calm (lighter blue), Drowsiness (purple), Rapid-eye movement (REM) sleep (yellow), and Slow-wave Sleep (SWS in light blue). (B) Schematic showing resting postures of seals in each habitat, including seals resting on the ocean floor on the continental shelf and drifting in the open ocean. (C) 2D map with bathymetry shows georeferenced dead-reckoned tracks for two animals recorded at sea. (D) 3D map demonstrates drift dive sequence off the continental shelf including drift dive from Figure 1 (center of figure).

Daily sleep quotas were universally low (1.2 ± 1.2 h for short 80-day trips and 2.4 ± 1.6 h for >200-day trips) (Figure 2.4). Surprisingly, seals slept more on the continental shelf than in the open ocean (Figure 2.2), where predation risk from white sharks and killer whales is likely greater (15, 18, 19). Seals at sea slept in 'bouts' lasting from 5 (open ocean) to 36 (continental shelf) consecutive sleeping dives. At-sea deployments co-occurred with frequent orca predation events in Monterey Bay (20) and we recorded several dive inversions characteristic of a behavioral response to disturbance (21). One disturbance occurred upon ascent from the 5th of a 7-drift-dive bout (Fig. S9). However, the animal performed an additional sleeping dive after the disturbance, comprised mainly of REM sleep. This response suggests that sleeping at depth may not place the seal at elevated predation risk.

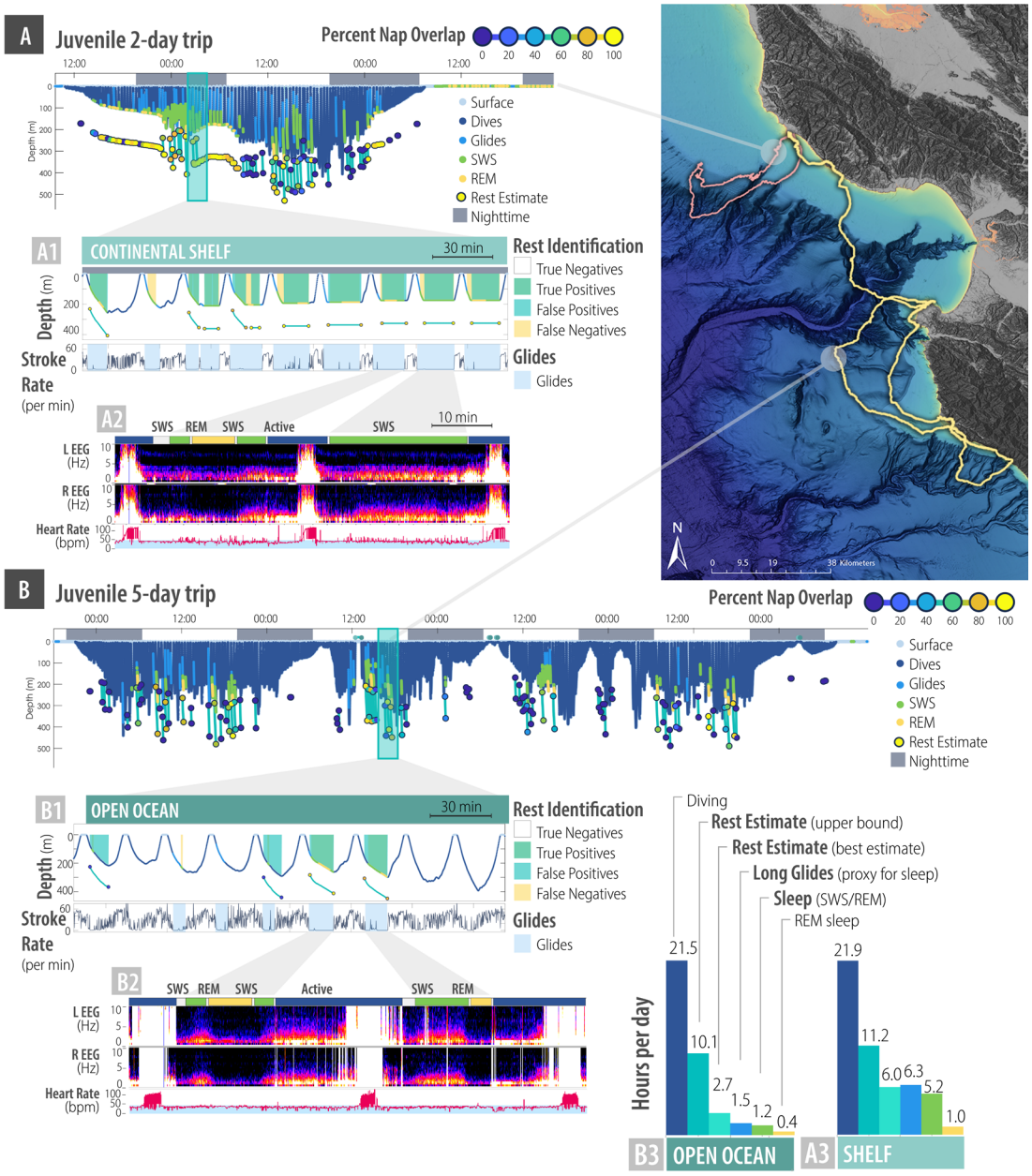

Figure 2.3. Sleep identification model to identify the biomechanics of sleep. Time-depth records for two juveniles (A & B) are colored to indicate surface intervals (light blue), dives (dark blue), glides (blue), SWS (green), and REM (yellow). Identified sleep segments are denoted below the dive profile, where outlined dots at the beginning and end of rest segments are colored from

yellow to dark blue according to their overlap with a nap ("Percent Nap Overlap" in A & B). Panels A1 & B1 demonstrate rest identification accuracy (false positives in blue, false negatives in yellow, and true positives in green) for periods of sleep on the continental shelf, in the open ocean, during negative buoyancy, and positive buoyancy. Panels A2 & B2 display EEG spectrograms and heart rate for two adjacent sleeping dives. Panels A3 & B3 quantify daily activity budgets (or provide estimates) in hours per day of diving, sleeping (upper bound - includes all long drifts and surface intervals exceeding 10 minutes; best estimate includes filtered long drifts and extended surface intervals), gliding (long glides more than 200 s), sleeping (both SWS & REM), and exhibiting REM sleep.

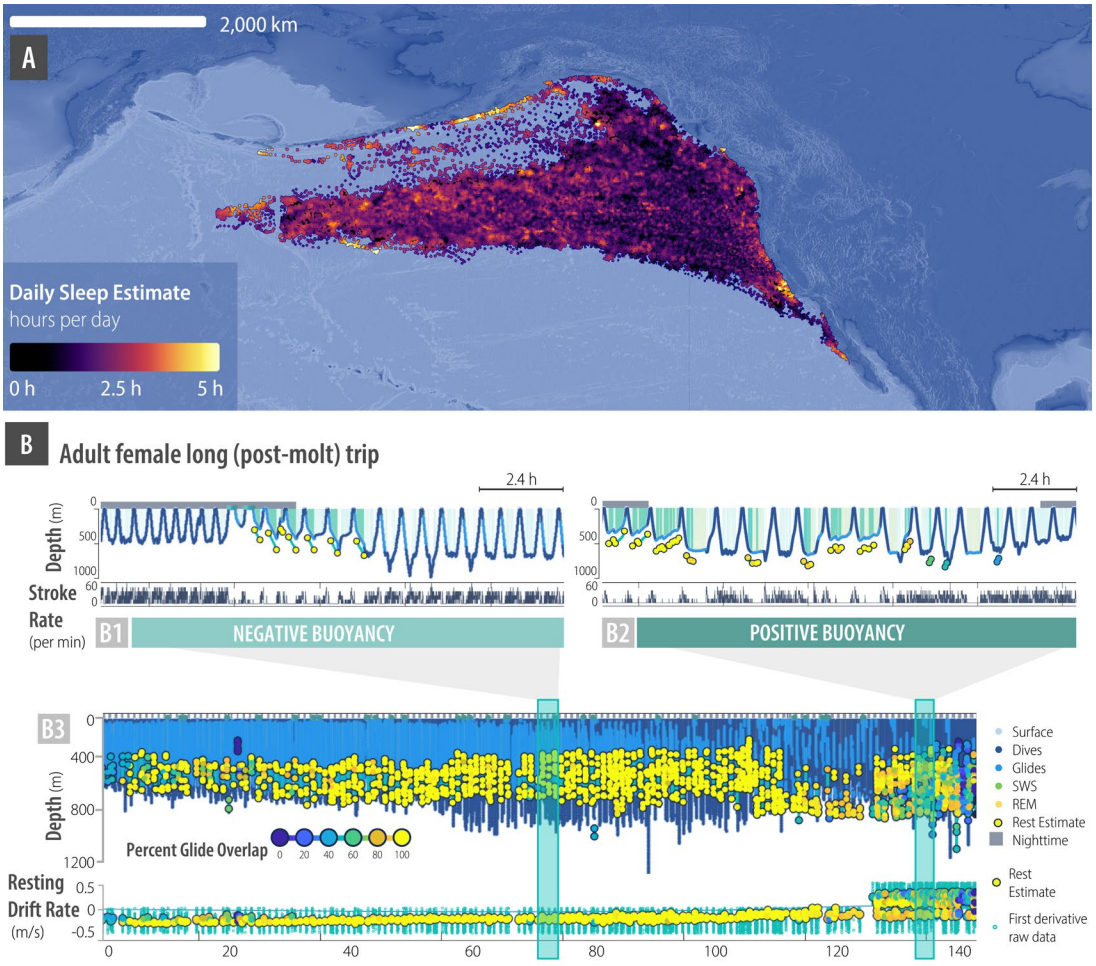

Figure 2.4. Estimating daily rest for 323 adult females. (A) Map with interpolated data for sleep time per day across 323 adult females demonstrates higher sleep time along the coast and foraging grounds. (B) Dive profiles for adult females are colored according to the same color scheme in Figure 2.3. Outlined dots are now colored from yellow to dark blue according to their overlap with a glide ("Percent Glide Overlap").

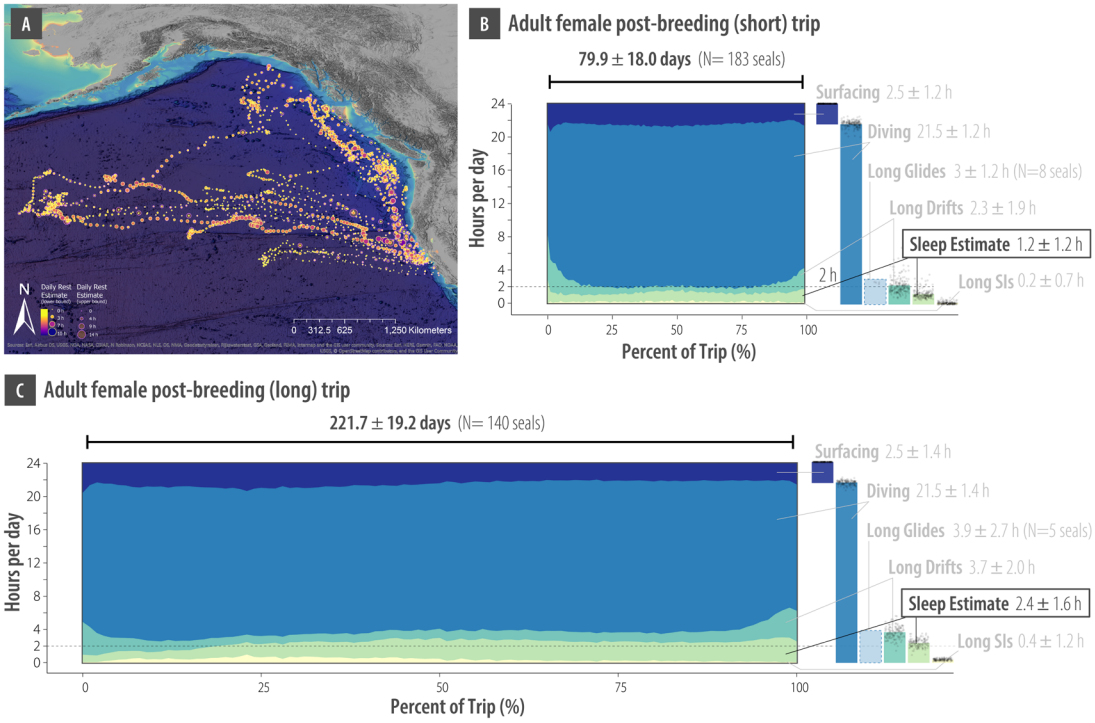

Figure 2.5. (A) Map showing estimated sleep per day across the North Pacific in the 13 seals instrumented with stroke rate loggers. Each circle represents one day. Larger circles with darker purple edges represent sleep upper bounds and smaller circles with bright yellow edges represent best estimates of sleep. There are more and larger circles (indicating more time spent and more sleep) near the coast and the seals' foraging grounds. **(B & C) Daily activity budgets for adult female foraging trips.** Daily activity budgets denote the hours per day spent during surface intervals, diving, long glides (when available for N=13 accelerometer-equipped seals), long drifts, sleeping (as estimated using our custom sleep identification model), and performing long (extended) surface intervals (SIs). Northern elephant seal females demonstrated consistently low sleep time throughout both trips, with lower sleep quotas during the shorter foraging trip. The area plots represent averages across seals for each percentage of the trip. The bar plots represent the mean across seals and trip percentages.

2.5 DISCUSSION

Our study spans multiple habitats and physiological demands to reveal the extreme requirements for sustained foraging and predator vigilance for a trans-Pacific shift worker. These recordings of brain activity at sea show a unique behavior that

allows seals to drift safely in and out of consciousness as they move through space. Previous studies speculated that floating patterns and cessation of feeding during drift dives might be associated with rest (17, 22, 23). We demonstrate conclusive evidence of electrophysiological sleep during and before corkscrew drifting patterns.

Among marine mammals, unihemispheric sleep (SWS in only one hemisphere) allows swimming and breathing during sleep in captive cetaceans and eared seals (8, 24). In the wild, this means that dolphins and eared seals might be free to sleep during transit or while maintaining vigilance for predators at the surface. True seals do not have this option– they sleep bilaterally like humans. True seals either lost or did not acquire unihemispheric sleep and developed an alternative solution: their superior breath-holding capacity, which presumably evolved to exploit deep ocean food resources, allowed them to sleep underwater (25).

Even while on land, the northern elephant seal exhibits bilateral sleep during long, ~20-min apneas (26, 27). During sleep at sea, prolonged apneas can cause blood oxygen depletion up to 81% Hb O_2 (13). High rates of oxygen depletion during sleeping dives (despite low activity) could be explained by the fact that seals may use this time to process food (22) and/or, at least partially, by the fact that brain blood flow is higher during REM than during waking or SWS (28). Further investigation into cerebral hemodynamics in deep-diving seals may allow us to elucidate the metabolic demands of the brain at sea.

Sleep in terrestrial mammals is well-documented compared to marine mammals. Sleep quotas range from as high as 20 h per day (African lion - (29)) to as low as 2 h per day (African elephant - (30)). Large terrestrial herbivores support their body size by diverting time from sleep toward continued foraging for low energy density prey, while large carnivores typically spend bursts of energy on energy-rich prey (31, 32). As large carnivores, elephant seals partition these two strategies over long timescales. In the absence of predators and prey while on land, seals slept like a lion, resting between high-energy-expenditure trips to sea. At sea, elephant seals resemble elephants, grazing continuously in dark depths. The adaptations that enable this predator to forage on deep-sea prey also allow it to sleep (albeit very little) in those depths, far from predators at the surface.

2.6 CONCLUSION

At the scale of a dive, elephant seals sacrifice oxygen to sleep far from predators. Across the Pacific, their large body mass facilitates this enhanced diving capacity at the cost of an increased energetic demand that requires elephant seals to sacrifice sleep to prioritize feeding for months on end. Strong evolutionary demands to avoid predation and starvation have sculpted this elite diver into a highly specialized sleeper that leverages its extreme physiology to circumvent the chronic and pervasive pathology of sleep apnea and sleep deprivation that plagues humans.

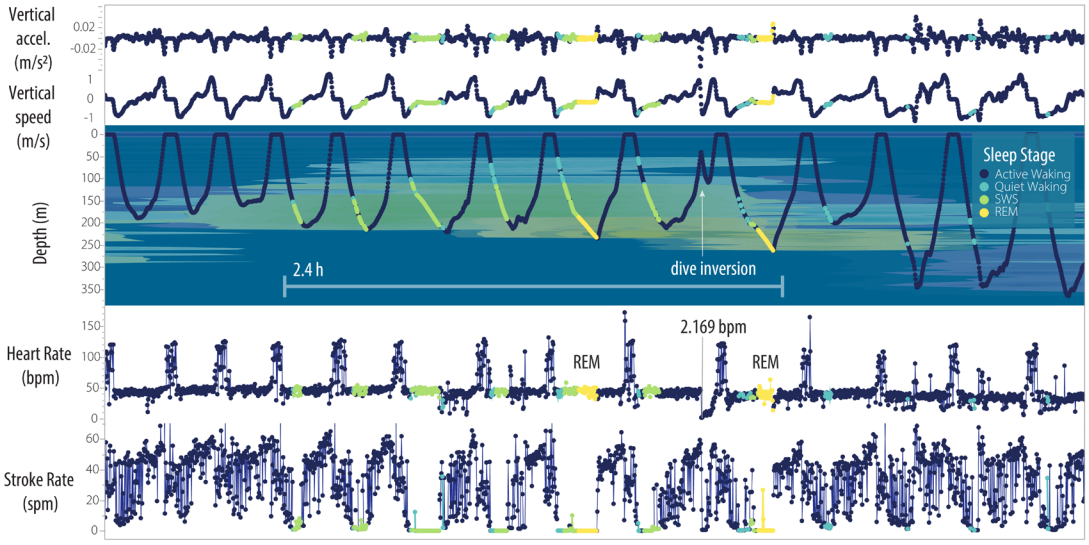

Figure 2.6. Sleeping amidst risk. An apparent disturbance (as evidenced by a dive inversion and reduction in heart rate [2.169 beats per minute] and stroke rate) occurs in the middle of a 7-dive sleeping bout and is followed by a (deeper) period of REM sleep.

2.7 REFERENCES

1. J. M. Siegel, Clues to the functions of mammalian sleep. Nature. 437, 1264–1271 (2005).
2. C. V. Senaratna, J. L. Perret, C. J. Lodge, A. J. Lowe, B. E. Campbell, M. C. Matheson, G. S. Hamilton, S. C. Dharmage, Prevalence of obstructive sleep apnea in the general population: A systematic review. Sleep Med. Rev. 34, 70–81 (2017).
3. C. M. O. de Almeida, A. Malheiro, Sleep, immunity and shift workers: A review. Sleep Sci. 9, 164–168 (2016).
4. C. A. Wyse, A. N. Coogan, C. Selman, D. G. Hazlerigg, J. R. Speakman, Association between mammalian lifespan and circadian free-running period: the circadian resonance hypothesis revisited. Biol. Lett. 6, 696–698 (2010).
5. J. A. Lesku, N. C. Rattenborg, M. Valcu, A. L. Vyssotski, S. Kuhn, F. Kuemmeth, W. Heidrich, B. Kempenaers, Adaptive Sleep Loss in Polygynous Pectoral Sandpipers. Science. 337, 1654–1658 (2012).

6. E. Ternman, L. Hänninen, M. Pastell, S. Agenäs, P. P. Nielsen, Sleep in dairy cows recorded with a non-invasive EEG technique. Appl. Anim. Behav. Sci. 140, 25–32 (2012).

7. T. Belling, in Equine Practice (1990), vol. 12, pp. 2–26.

8. O. I. Lyamin, P. R. Manger, S. H. Ridgway, L. M. Mukhametov, J. M. Siegel, Cetacean sleep : An unusual form of mammalian sleep. 32, 1451–1484 (2008).

9. N. C. Rattenborg, B. Voirin, S. M. Cruz, R. Tisdale, G. Dell'Omo, H.-P. Lipp, M. Wikelski, A. L. Vyssotski, Evidence that birds sleep in mid-flight. Nat. Commun. 7, 12468 (2016).

10. J. A. Lesku, L. C. R. Meyer, A. Fuller, S. K. Maloney, G. Dell'Omo, A. L. Vyssotski, N. C. Rattenborg, Ostriches Sleep like Platypuses. PLoS ONE. 6, e23203 (2011).

11. B. J. Le Boeuf, D. P. Costa, A. C. Huntley, S. D. Feldkamp, Continuous, deep diving in female northern elephant seals, *Mirounga angustirostris*. Can. J. Zool. 66, 446–458 (1988).

12. P. W. Robinson, D. P. Costa, D. E. Crocker, J. P. Gallo-Reynoso, C. D. Champagne, M. A. Fowler, C. Goetsch, K. T. Goetz, J. L. Hassrick, L. A. Hückstädt, C. E. Kuhn, J. L. Maresh, S. M. Maxwell, B. I. McDonald, S. H. Peterson, S. E. Simmons, N. M. Teutschel, S. Villegas-Amtmann, K. Yoda, Foraging behavior and success of a mesopelagic predator in the northeast Pacific Ocean: insights from a data-rich species, the northern elephant seal. PloS One. 7 (2012), doi:10.1371/journal.pone.0036728.

13. S. J. Jorgensen, S. Anderson, F. Ferretti, J. R. Tietz, T. Chapple, P. Kanive, R. W. Bradley, J. H. Moxley, B. A. Block, Killer whales redistribute white shark foraging pressure on seals. Sci. Rep. 9, 6153 (2019).

14. N. Hammerschlag, R. A. Martin, C. Fallows, Effects of environmental conditions on predator–prey interactions between white sharks (*Carcharodon carcharias*) and Cape fur seals (*Arctocephalus pusillus*) at Seal Island, South Africa. Environ. Biol. Fishes. 76, 341–350 (2006).

15. T. Adachi, A. Takahashi, D. P. Costa, P. W. Robinson, L. A. Hückstädt, S. H. Peterson, R. R. Holser, R. S. Beltran, T. R. Keates, Y. Naito, Forced into an ecological corner: Round-the-clock deep foraging on small prey by elephant seals. Sci. Adv. (2021), doi:10.1126/sciadv.abg3628.

16. J. U. Meir, C. D. Champagne, D. P. Costa, C. L. Williams, P. J. Ponganis, Extreme hypoxemic tolerance and blood oxygen depletion in diving elephant seals. Am. J. Physiol.-Regul. Integr. Comp. Physiol. 297, R927–R939 (2009).

17. Y. Mitani, R. D. Andrews, K. Sato, A. Kato, Y. Naito, D. P. Costa, Three-dimensional resting behaviour of northern elephant seals: drifting like a falling leaf. Biol. Lett. 6, 163–166 (2009).

18. R. S. Beltran, J. M. Kendall-Bar, E. Pirotta, T. Adachi, Y. Naito, A. Takahashi, J. Cremers, P. W. Robinson, D. E. Crocker, D. P. Costa, Lightscapes of fear: How mesopredators balance starvation and predation in the open ocean. Sci. Adv. 7, eabd9818 (2021).

19. O. I. Lyamin, Sleep in the harp seal (*Pagophilus groenlandica*). Comparison of sleep on land and in water. J. Sleep Res. 2, 170–174 (1993).

20. O. I. Lyamin, P. O. Kosenko, J. L. Lapierre, L. M. Mukhametov, J. M. Siegel, Fur Seals Display a Strong Drive for Bilateral Slow-Wave Sleep While on Land. J. Neurosci. 28, 12614–12621 (2008).

21. O. I. Lyamin, P. O. Kosenko, A. L. Vyssotski, J. L. Lapierre, J. M. Siegel, L. M. Mukhametov, Study of Sleep in a Walrus. 444, 188–191 (2012).

22. B. J. Le Boeuf, D. E. Crocker, D. P. Costa, S. B. Blackwell, P. M. Webb, D. S. Houser, Foraging Ecology of Northern Elephant Seals. Ecol. Monogr. 70, 353–382 (2000).

23. N. Nasby-Lucas, H. Dewar, C. H. Lam, K. J. Goldman, M. L. Domeier, White Shark Offshore Habitat: A Behavioral and Environmental Characterization of the Eastern Pacific Shared Offshore Foraging Area. PLOS ONE. 4, e8163 (2009).

24. S. Fregosi, H. Klinck, M. Horning, D. P. Costa, D. Mann, K. Sexton, L. A. Hückstädt, D. K. Mellinger, B. L. Southall, An animal-borne active acoustic tag for minimally invasive behavioral response studies on marine mammals. Anim. Biotelemetry. 4 (2016), doi:10.1186/s40317-016-0101-z.

25. D. E. Crocker, B. J. L. Boeuf, D. P. Costa, Drift diving in female northern elephant seals: implications for food processing. Can. J. Zool. 75, 27–39 (2008).

26. Y. Naito, D. P. Costa, T. Adachi, P. W. Robinson, M. Fowler, A. Takahashi, Unravelling the mysteries of a mesopelagic diet: A large apex predator specializes on small prey. Funct. Ecol. 27, 710–717 (2013).

27. J. M. Kendall-Bar, A. L. Vyssotski, L. M. Mukhametov, J. M. Siegel, O. I. Lyamin, Eye state asymmetry during aquatic unihemispheric slow wave sleep in northern fur seals (*Callorhinus ursinus*). PloS One. 14, e0217025 (2019).

28. O. I. Lyamin, L. M. Mukhametov, J. M. Siegel, E. A. Nazarenko, I. G. Polyakova, O. V. Shpak, Unihemispheric slow wave sleep and the state of the eyes in a white whale. Behav. Brain Res. 129, 125–129 (2002).

29. N. C. Rattenborg, C. J. Amlaner, S. L. Lima, Behavioral, neurophysiological and evolutionary perspectives on unihemispheric sleep. Neurosci. Biobehav. Rev. 24, 817–842 (2000).
30. W. Milsom, M. Castellini, M. Harris, J. Castellini, D. Jones, R. Berger, S. Bahrma, L. Rea, D. Costa, Effects of hypoxia and hypercapnia on patterns of sleep-associated apnea in elephant seal pups. Am. J. Physiol. 271, R1017–R1024 (1996).
31. M. A. Castellini, W. K. Milsom, R. J. Berger, D. P. Costa, D. R. Jones, J. M. Castellini, L. D. Rea, S. Bharma, M. Harris, Patterns of respiration and heart rate during wakefulness and sleep in elephant seal pups. Am. J. Physiol.-Regul. Integr. Comp. Physiol. 266, R863–R869 (1994).
32. J. U. Meir, P. W. Robinson, L. I. Vilchis, G. L. Kooyman, D. P. Costa, P. J. Ponganis, Blood Oxygen Depletion Is Independent of Dive Function in a Deep Diving Vertebrate, the Northern Elephant Seal. PLOS ONE. 8, e83248 (2013).
33. T. V. Santiago, E. Guerra, J. A. Neubauer, N. H. Edelman, Correlation between ventilation and brain blood flow during sleep. J. Clin. Invest. 73, 497–506 (1984).
34. G. B. Schaller, The Serengeti Lion: A Study of Predator-Prey Relations (University of Chicago Press, Chicago, IL, 1976; https://press.uchicago.edu/ucp/books/book/chicago/S/bo42069173.html), Wildlife Behavior and Ecology series.
35. N. Gravett, A. Bhagwandin, R. Sutcliffe, K. Landen, M. J. Chase, O. I. Lyamin, J. M. Siegel, P. R. Manger, Inactivity/sleep in two wild free-roaming African elephant matriarchs – Does large body size make elephants the shortest mammalian sleepers? PLOS ONE. 12, e0171903 (2017).
36. T. Allison, Comparative and evolutionary aspects of sleep. In: Perspectives in the brain sciences: the sleeping brain. (Brain Information Service, Los Angeles, 1972).
37. I. Capellini, R. A. Barton, P. McNamara, B. T. Preston, C. L. Nunn, Phylogenetic Analysis of the Ecology and Evolution of Mammalian Sleep. Evolution. 62, 1764–1776 (2008).

Author Contributions

J.K.B. (candidate): conceptualization, funding acquisition, methodology, validation, visualization, project administration, software, data curation, formal analysis, resources,

investigation, writing- original draft, writing- review and editing. T.M.W. & D.P.C.: conceptualization, funding acquisition, resources, project supervision, project administration, writing- review and editing. R.M., J.N., C.L., D.A.L.: data curation, visualization, formal analysis, investigation, writing- review and editing. J.K.P.: methodology, investigation, data analysis supervision, writing- review and editing. R.R.H., T.K., R.S.B., P.R., D.C., O.I.L., & T.A.: investigation, project administration, formal analysis, writing- review and editing. A.L.V.: methodology, software, resources. All authors read and approved the final manuscript and approved its use in the dissertation.

2.8 **SUPPLEMENTARY MATERIALS**

2.8.1 ***Animals and Instrumentation***

2.8.1a *Sleep (EEG) Recordings*

We recorded electroencephalogram (EEG), electrocardiogram (ECG), electrooculogram (EOG), electromyogram (EMG), depth, environmental temperature, illumination, and three-dimensional inertial motion sensing (accelerometry, magnetometry, and gyroscope) in 13 juvenile female northern elephant seals using a custom, non-invasive EEG headcap and ruggedized housing (Kendall-Bar et al., 2022, in press; Table 2-1). The custom headcap attached with AquaSeal™ adhesive (GEAR AID ®) was designed to minimize water intrusion to surface-mounted Genuine grass goldcup electrodes measuring the front-parietal derivations of the left and right

hemisphere (4 EEG, 2 EOG signals). Patches attached near the pectoral flippers and neck measured ECG and EMG. The custom, ruggedized, and waterproofed (>2000 m) housing contained a Neurologger3 (© 2016 Evolocus LLC) for data storage at 500Hz (electrophysiological signals) and ~36Hz (250/7 ≈ 35.7143Hz; environmental and motion sensors) on a 200 GB microSD card. We down-sampled inertial motion sensors to 8 s^{-1} intervals for the training and validation of the sleep-identification model of a larger dataset, including records with 8 s^{-1} sampling frequency.

(1A) Sleep in the lab. First, we recorded sleep in 5 juveniles (2 8-month-olds and 3 20-month-olds) temporarily housed at Long Marine Lab at UC Santa Cruz in Santa Cruz, CA on land (310.4 h total – 12.6 days) and in a shallow pool (4.9 m x 3.0 m x 1.4 m; 153.5 h total – 6.3 days) (Table 2-1). **(1B) Sleep in the wild.** Next, we instrumented seals (3 2-month-olds and 3 juveniles [14 or 24 months old]) on the beach that stayed on land (375.9 h total – 14.3 days) and in shallow lagoons (205.5 h total – 8.3 days) at Año Nuevo State Park, CA. One of these seals also carried an animal-borne camera. **(1C) Sleep at sea.** We recorded sleep at sea from 3 seals (194.4 h total – 8.1 days). One was instrumented on the beach and spent 43.9 h at sea before returning to the beach. The other two seals were translocated ~60 kilometers south of Año Nuevo State Park and released at Asilomar Beach in Monterey, CA. For all seals, instruments were recovered 2.5-5 days after attachment (total of 51.6 recording days). Recordings of EEG at sea (8.1 days total) were used as a to determine quantitative thresholds to interpret and identify behavioral sleep in the following categories: time-depth and stroke-rate recordings.

2.8.1b *Time-depth Recorder (TDR) Recordings*

Between 2004 and 2019, we instrumented 323 adult female northern elephant seals with time-depth recorders and satellite transmitters (Wildlife Computers, Redmond, WA, USA or Sea Mammal Research Unit, St Andrews, UK) for their post-molt or post-breeding foraging trips according to established protocols (1–3) (Table 2-1). Data was collected at 4 or 8 second intervals. We down-sampled data to 8 s^{-1}.

2.8.1c *Stroke-Rate (SR) Recordings – Validation Subset*

A subset of these TDR seals was instrumented with accelerometers (N=13). Accelerometers allowed detection of individual swimming strokes (using back- or flipper-attached accelerometers) and foraging attempts (from jaw-attached accelerometers). We used these recordings to calculate the false positive rate for our sleep identification model (see 'Sleep Identification Validation' below). Original data was collected at 50Hz using customized "kami kami" dataloggers (4). We processed stroke counts and foraging attempts from accelerometer data into 5-second bins, later down-sampled to 10 s^{-1}, and subsequently paired to the KNN-nearest-neighbor 8 s^{-1} sample to maintain consistency across the larger dataset (sampled at 8 s^{-1}). We defined glides as consecutive segments where stroke rate was less than 15 strokes per minute.

Table 2-1. Animal metadata table providing details on the animals' ages, sex, morphometrics, recording location (Long Marine Lab [LML], Año Nuevo State Park [ANO], Translocation [XLOC]), recording type (lab, wild, or translocation), recording duration (in days; Land [LD], Shallow Water [SW], Continental Shelf [CS], Open Ocean [OO]), total sleep time (hours per day), and type of data collected (electroencephalogram [EEG], electrocardiogram [ECG], webcam, animal-borne camera, kami-kami [jaw-mounted accelerometer], 3D motion, stroke rate [back or flipper mounted accelerometer], DSLR video, and time-depth recorder).

Sleep Data	Animal Information			Morphometrics						Recording duration (days)					Total Sleep Time (h/day)							Data Collected								
TOPPID	Age Class	Sex	Age (mo.)	Length (cm)	Girth (cm)	Mass (kg)	Phase	Location	Recording Type	Land (LD)	Shallow Water (SW)	Continental Shelf (CS)	Open Ocean (OO)	Total Duration (days)	LD - TST	SW - TST	CS - TST	OO - TST	Total Sleep Time (h/day)	Max sleep (in 24h)	Min sleep (in 24h)	EEG	ECG	Continuous Webcam	Animal-borne camera	Kami kami	3D Motion	Stroke Rate	High-resolution Video	TDR
2019058	**Yearling**	**F**	**~8**	152	132	118	1	LML	Lab	2.1	1.2	0.0	0.0	3.3	8.9	4.9	-	-	7.4	9.0	5.9				-	-				
2020045	**Weanling**	**F**	**2**	165	143	200	2	ANO	Wild	0.7	1.8	0.0	0.0	2.6	10.5	2.6	-	-	4.8	5.7	3.6			-		-				
2020046	**Juvenile**	**F**	**26**	187	102	~120	2	ANO	Wild	1.8	1.1	0.0	0.0	2.9	5.3	1.3	-	-	3.7	3.5	3.1			-	-	-				
2020047	**Juvenile**	**F**	**20**	188	124	141	1	LML	Lab	2.8	1.8	0.0	0.0	4.6	9.7	4.8	-	-	7.8	11.6	4.5				-	-				
2020048	**Juvenile**	**F**	**20**	206	147	196	1	LML	Lab	3.1	1.7	0.0	0.0	4.8	9.9	5.7	-	-	8.4	9.3	6.3				-	-				
2020049	**Juvenile**	**F**	**20**	206	129	177	1	LML	Lab	2.7	0.2	0.0	0.0	2.9	8.0	7.2	-	-	7.9	7.0	6.9				-	-				
2020050	**Yearling**	**F**	**~8**	165	139	148	1	LML	Lab	1.9	1.4	0.0	0.0	3.3	12.6	7.6	-	-	**10.5**	**14.1**	6.8				-	-				
2021041	**Weanling**	**F**	**2**	157	130	116	2	ANO	Wild	3.0	2.1	0.0	0.0	5.0	10.7	0.1	-	-	6.4	9.3	4.0			-	-	-				
2021042	**Weanling**	**F**	**~2**	151	129	118	2	ANO	Wild	2.1	0.2	1.1	0.7	4.1	13.0	0.0	7.5	2.6	9.1	13.9	5.3			-	-	-				
2021043	**Juvenile**	**F**	**~26**	177	134	154	2	ANO	Wild	2.5	2.5	0.0	0.0	5.0	14.0	0.6	-	-	7.3	8.1	6.4			-	-	-				
2021044	**Juvenile**	**F**	**~26**	177	140	163	3	XLOC	XLOC	0.3	0.2	1.8	2.5	4.8	0.6	0.0	0.0	1.4	**0.8**	1.3	0.6			-	-	-				
2021045	**Juvenile**	**F**	**~14**	170	140	157	2	ANO	Wild	4.2	0.6	0.0	0.0	4.8	11.1	0.0	-	-	9.8	12.6	6.5			-	-	-				
2022033	**Juvenile**	**F**	**~26**	199	160	211	3	XLOC	XLOC	1.0	0.5	1.4	0.6	3.5	9.6	0.0	0.0	1.0	2.9	8.7	**0.0**			-	-	-				
	EEG Dataset							*N*	*Type*					*total dur. (d)*	x̄ ± SD	x̄ ± SD	x̄ ± SD	x̄ ± SD												
								5	**Lab**	12.6	6.3	0.0	0.0	18.9	9.8 ± 1.7	6.0 ± 1.3	- ± -	- ± -	8.4 ± 1.1	14.1	4.5									
								6	**Wild**	14.3	8.3	1.1	0.7	24.4	10.8 ± 3.0	0.8 ± 1.0	- ± -	- ± -	6.9 ± 2.2	13.9	6.5									
								2	**XLOC**	1.3	0.6	3.2	3.1	8.3	5.1 ± 6.3	0.0 ± 0.0	0.0 0.0	1.2 ± 0.3	1.9 ± 1.1	8.7	0.0									
								13	**Total**	28.2	15.2	4.3	3.9	51.6	9.5 ± 3.4	2.7 ± 2.8	2.5 ± 3.5	1.7 ± 0.7	6.7 ± 2.7	14.1	0.0					**Kami kami**	**3D Motion**	**Stroke Rate**	**Video**	**TDR**
TDR Data	***TDR Dataset***							*N*	***Season***					***mean dur. (d)***					*TST*			***Data Collected***								
	Adult	**F**						183	**PB**					79.9 ± 18.0					1.2 ± 1.2											
	Adult	**F**						140	**PM**					221.7 ± 19.2					2.4 ± 1.6											
Stroke Rat	***Validation Dataset***							*N*	***Season***													***Data Collected***								
	Adult	**F**						8	**PB**																					
	Adult	**F**						5	**PM**																					
								323	ALL																					

2.8.2 *Procedures & Ethics*

All animal procedures were approved at the federal and institutional levels under National Marine Fisheries Permits 496, 836, 786–1463, 87-1743, 19108, 14636, and 23188, and by the Institutional Animal Care and Use Committee (IACUC) of University of California Santa Cruz (Costd1709 and Costd2009-2). All animals were sedated for tag placement following standard protocols (5–10). Briefly, an induction injection of intramuscular Telazol® [tiletamine and zolazepam] (1 mg/kg) was maintained with doses of Telazol/ketamine/valium as needed. With the exception of the EEG headcap and patches which were attached with flexible, skin-compliant AquaSeal™ (GEAR AID ®), all other tags were attached via flexible nylon mesh epoxied to the animal's fur, consistent with established practices for external attachment of animal telemetry tags (11). At each handling, most animals were weighed in a canvas sling from a hanging scale with precision ±1 kg.

2.8.3 *EEG Animal Observations*

In addition to the datalogger's inertial motion sensors, we recorded behavior using video cameras whenever possible. Continuous low-resolution webcam footage (Wyze Cam Outdoor 1080p HD Webcam; Wyze Labs, Inc.) and intermittent high-resolution DSLR footage (Nikon® D7200) was used to document fine-scale eye, nostril, and vibrissae movement for seals at Long Marine Lab and while animals were on the beach at Año Nuevo State Park. One weanling elephant seal was instrumented with a small animal-borne camera to observe conspecific interactions while sleeping. Video

data were visually scored at 1 Hz, where we recorded the animal's activity level (galumphing [active forward movement on land], swimming, quiet waking, visibly breathing, or not visibly breathing), posture (prone, supine, left, right, vertical up, or vertical down), social interactions (alone, not alone [conspecifics within 5 m], or social [actively interacting with other animals]), location (land, wet [in water shallower than body height], at surface, or underwater) (Figure 2.7; Table 2-2). With high-resolution video, we recorded eye state (open, closed, eye movements), muscle twitches, whisker twitches, and vocalizations.

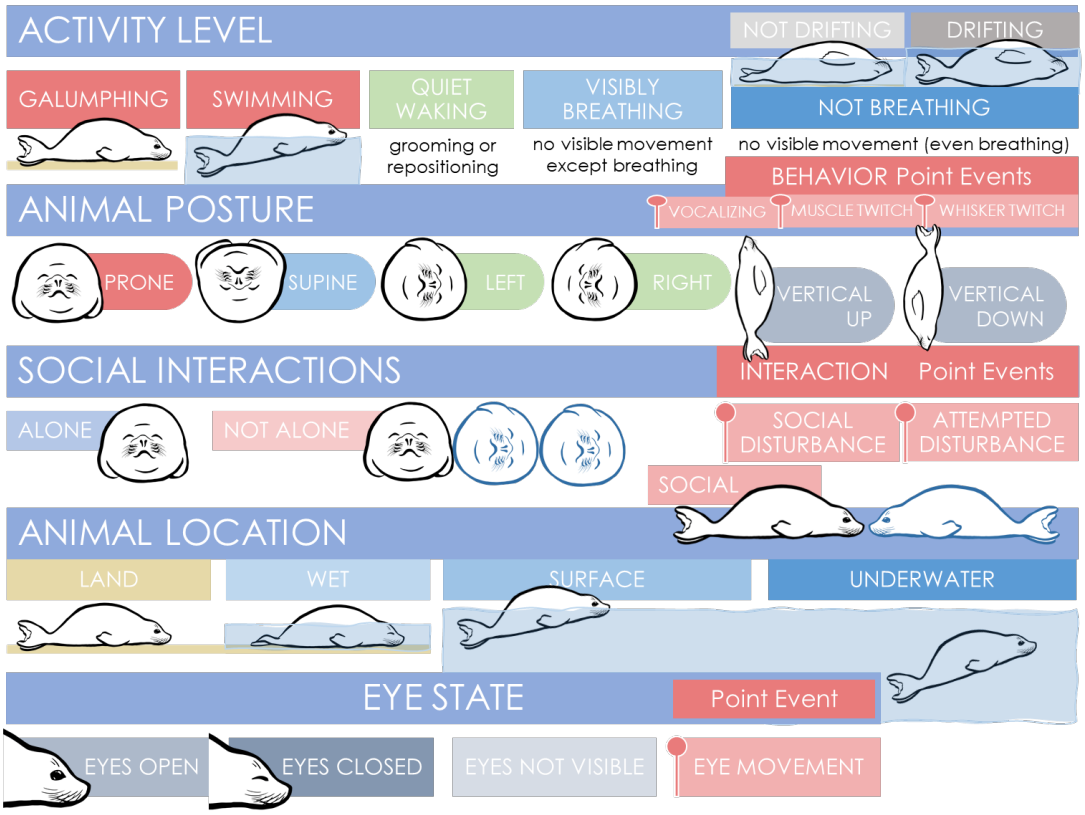

Figure 2.7. Illustrations of behaviors coded during video scoring.

2.8.4 *EEG Data Processing*

Binary 500Hz electrophysiological data were converted into EDF (European Data Format) using a custom MATLAB (MathWorks, Inc.) application (Neurologger Converter & Visualizer © Evolocus LLC). Raw electrophysiological data were processed using Independent Components Analysis (ICA) in the MATLAB toolbox EEGLAB (v2020.0) to identify and remove heart signals from EEG, EOG, and EMG, as discussed in previous studies (12, 13). Raw signals were always maintained for cross-comparison.

Table 2-2. Verbal descriptions of behaviors coded during video scoring.

	Behavior code	***Description***
Animal Behavior	Not visible	Animal is not in the field of view of the camera
	Galumphing	Actively moving forward using fore flippers and abdomen.
	Swimming	Actively swimming with fore or hind flippers.
	Quiet waking	Animal is obviously awake (grooming, yawning, or repositioning).
	Visibly breathing	Animal is stationary, but visibly breathing.
	Not breathing	Animal is completely stationary and not visibly breathing.
	Muscle twitch	Muscle jerk (often happens during REM sleep)
	Whisker twitch	Whisker twitch where whiskers flinch, only score when stationary.
	Vocalizing	Animal vocalizing while jerking head up and down.
Body Position	Prone (on belly)	Animal laying on belly
	Supine (on back)	Animal laying on back.
	Left side	Animal laying on its left side
	Right side	Animal laying on its right side
	Vertical up	Animal with nose pointed up
	Vertical down	Animal with nose pointed down
Animal Location	Land	on Land
	Surface	Surface of Water
	Underwater	Underwater
	Wet	in water shallower than body height
Interactions	Alone	No animals visible nearby (or within 20 feet)
	Not alone	With other animals, but not actively interacting with other animals (for example, sleeping side-by-side, calm or active within 20 feet of other animals).
	Social	Focal animal actively engaging with other animals socially (by touching them, climbing over them, or swimming with each other).
	Disturbance	Conspecific activity causes a visible disturbance to the animal.
	Attempted disturbance	Conspecific activity fails to cause a visible disturbance to the animal

2.8.5 *EEG Qualitative Analysis: Sleep Scoring*

Guidelines for visual sleep scoring followed parameters established for lab-based sleep studies of northern elephant seals and other marine mammals (6, 7, 14–16). Sleep scoring criteria is as follows, with additional qualitative and quantitative criteria in Kendall-Bar et al. (24):

1. Quiet Waking (QW; Figure 2.8**D)** – low voltage, high-frequency background EEG activity (>50% of 30 s epoch) and accelerometer demonstrating only subtle breathing or motion (i.e. rolling, grooming, or repositioning). **2. Active Waking (AW; Figure** 2.8**E)** – low voltage, high-frequency background EEG with motion artifacts or accelerometer demonstrating more than subtle breathing or motion (>50% epoch). **3. Slow-wave sleep (SWS; Figure** 2.8**D)** – high voltage, low-frequency (0.5 - 4 Hz) EEG (>50% epoch). We further subdivided SWS into SWS2 (maximal amplitude SWS) and SWS1 (transitional state, voltage >1.5X QW with sleep spindles and K-complexes). **4. Rapid-eye-movement (REM; Figure** 2.8**E)** – low-voltage, high-frequency EEG with an increase or change in heart rate variability (HRV) compared to SWS or QW. We conservatively subdivided REM into putative REM (REM1) or certain REM (REM2) based on the extent of HRV. We based our scoring of REM using HRV on previous studies of bilateral aquatic sleep in marine mammals (14) and further quantify the extent of low-frequency HRV by calculating the very low frequency (0-0.005Hz) power of heart rate. We scored certain REM2 wherever this quantitative measure of HRV exceeded ~1 (with some variability across animals), outside of a tachycardic eupneic

episode and its adjacent transition periods (Fig. S2 & Fig. S3). During both REM1 and REM2, video footage demonstrated behavior consistent with REM, where we observed closed eyes, no intentional movement, occasional whisker and muscle twitches, and whole-body jerks. We provide sleep scoring results with and without putative REM for comparison Table 2-3.

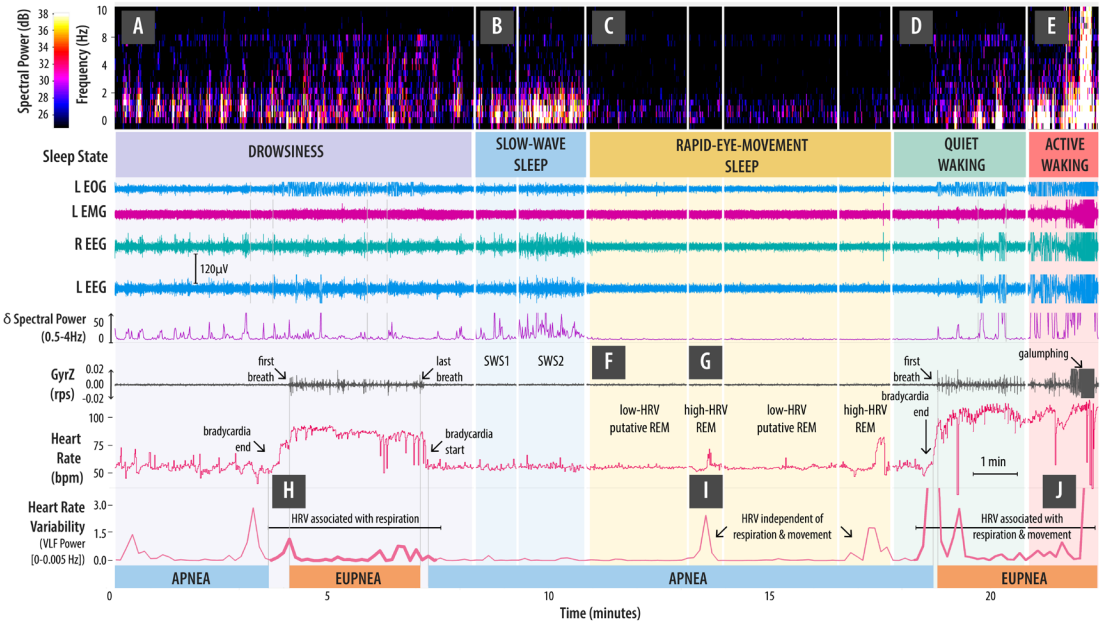

Figure 2.8. Sleep scoring methods. Sleep stages were distinguished from distinct characteristics of the EEG spectrogram, z-axis gyroscope (for breath detection), and heart rate. Spectral power varied across stages from (A) Drowsiness (DW) with slow (10 s) oscillations between slow waves and waking, (B) Slow-Wave Sleep (SWS1: low-amplitude SWS & SWS2: high-amplitude SWS) high amplitude low-frequency activity, (C) REM Sleep with lowest amplitude high-frequency activity and highest heart rate variability (HRV) (putative REM: low HRV & certain REM (high HRV)), and (D) Quiet Waking (QW) low amplitude high-frequency activity, and (E) Active Waking (AW) motion artifacts >50% of the epoch. We used the combination of low delta spectral power, apnea, and high heart rate variability (not associated with changes in respiratory state - apnea [not breathing] & eupnea [breathing consistently]) to categorize REM sleep. During active waking, motion artifacts could be caused by large breaths or active forward movement ('galumphing' on land or swimming in water).

Table 2-3. Sleep scoring summary table. Total recording time (hours) spent in each sleep stage per recording. Total sleep time (TST) is then calculated as percentage of total scored recording time and normalized to h per 24 h day. Metadata match Table S1. Sleep stages include active waking, quiet waking, putative rapid-eye-movement (REM) sleep, certain REM sleep, low-voltage (LV) slow-wave sleep, high-voltage (HV) slow-wave sleep, and drowsiness. Average unscored daily hours are provided for reference. We compare TST and the proportion of REM/TST (REM % TST) with and without segments scored as putative REM (less pronounced heart-rate variability) for comparison.

	Animal Information				*Sleep time summary (h / day)*																
TOPPID	**Age Class**	**Sex**	**Age (mo.)**	**Recording Type**	Active Waking	Quiet Waking	Putative REM Sleep	Certain REM Sleep	LV Slow Wave Sleep	HV Slow Wave Sleep	Drowsiness	Unscorable	Total Scored	**Total hours of sleep**	Total hours not scored	**Total sleep time (per 24)**	**TST Certain REM Only**	**REM % TST (Certain only)**	**REM % TST (Certain & Putative)**
2019058	**Yearling**	**F**	**~8**	Lab	37.2	11.8	2.9	5.9	5.9	10.1	6.3	1.8	81.9	24.8	1.8	**8.1**	6.44	**23.8%**	**35.4%**
2020045	**Weanling**	**F**	**2**	Wild	46.0	3.1	0.6	1.9	3.4	6.5	0.0	12.3	73.8	12.4	12.3	**4.8**	3.83	**15.4%**	**20.2%**
2020046	**Juvenile**	**F**	**26**	Wild	52.6	6.4	0.5	1.8	3.3	5.2	0.5	4.7	75.2	10.9	4.7	**3.8**	3.32	**16.8%**	**21.8%**
2020047	**Juvenile**	**F**	**20**	Lab	53.4	14.2	1.9	7.5	10.4	16.4	7.3	5.9	116.9	36.2	5.9	**8.4**	7.05	**20.9%**	**26.0%**
2020048	**Juvenile**	**F**	**20**	Lab	51.6	16.5	1.6	9.5	10.3	18.4	6.6	1.3	115.9	39.9	1.3	**8.9**	7.93	**23.9%**	**28.0%**
2020049	**Juvenile**	**F**	**20**	Lab	29.6	16.2	1.8	6.3	4.1	10.8	0.8	0.1	69.6	22.9	0.1	**8.0**	7.29	**27.4%**	**35.2%**
2020050	**Yearling**	**F**	**~8**	Lab	36.8	6.8	1.9	6.2	8.1	18.3	0.6	1.0	79.7	34.5	1.0	**10.6**	9.81	**18.1%**	**23.6%**
2021041	**Weanling**	**F**	**2**	Wild	83.1	5.7	1.3	6.9	7.2	16.7	0.1	0.0	120.9	32.1	0.0	**6.4**	6.11	**21.4%**	**25.6%**
2021042	**Weanling**	**F**	**~2**	Wild	53.3	6.4	0.6	7.5	12.4	17.0	1.6	0.0	98.8	37.5	0.0	**9.3**	8.98	**20.1%**	**21.6%**
2021043	**Juvenile**	**F**	**~26**	Wild	73.7	9.0	1.0	9.1	9.2	17.0	0.0	1.1	120.0	36.3	1.1	**7.3**	7.06	**25.2%**	**27.8%**
2021044	**Juvenile**	**F**	**~26**	XLOC	109.2	1.4	0.2	1.0	0.7	1.8	0.0	0.0	114.4	3.8	0.0	**0.8**	0.75	**27.0%**	**33.3%**
2021045	**Juvenile**	**F**	**~14**	Wild	56.4	10.2	0.7	9.5	13.5	23.2	1.5	4.2	119.2	46.8	4.2	**9.9**	9.29	**20.2%**	**21.6%**
2022033	**Juvenile**	**F**	**~26**	XLOC	69.2	4.4	0.3	2.3	3.0	4.8	0.2	2.3	86.4	10.3	2.3	**2.9**	2.78	**22.0%**	**24.8%**
					x̄ ± SD	x̄ ± SD	x̄ ± SD	x̄ ± SD	x̄ ± SD	x̄ ± SD	x̄ ± SD	x̄	x̄	x̄	x̄	x̄ ± SD		x̄ ± SD	
				Lab	41.7 ± 9.2	13.1 ± 3.6	2.0 ± 0.4	7.1 ± 1.3	7.8 ± 2.5	14.8 ± 3.6	4.3 ± 3.0	2.0 ± 2.0	92.8	31.7	2.0	**8.8 ± 1.0**	7.7	**22.8% ± 3.1%**	**29.6% ± 4.8%**
				Wild	60.8 ± 13.1	6.8 ± 2.3	0.8 ± 0.3	6.1 ± 3.1	8.2 ± 4.0	14.3 ± 6.4	0.6 ± 0.7	3.7 ± 4.3	101.3	29.3	3.7	**6.9 ± 2.2**	6.4	**19.9% ± 3.2%**	**23.1% ± 2.7%**
				XLOC	89.2 ± 20.0	2.9 ± 1.5	0.3 ± 0.0	1.7 ± 0.6	1.9 ± 1.1	3.3 ± 1.5	0.1 ± 0.1	1.1 ± 1.1	100.4	7.1	1.1	**1.9 ± 1.1**	1.8	**24.5% 2.5%**	**29.1% 4.3%**
				Total	57.9 ± 20.7	8.6 ± 4.7	1.2 ± 0.8	5.8 ± 2.9	7.0 ± 3.8	12.8 ± 6.4	2.0 ± 2.7	2.7 ± 3.4	97.9	26.8	2.7	**6.9 ± 2.8**	6.2	**21.7% ± 3.6%**	**26.5% ± 5.0%**

2.8.6 *EEG Quantitative Analysis: Spectral Power*

We calculated delta spectral power (0.5-4Hz) for EEG channels over 30-second epochs. We calculated very low-frequency (VLF) heart rate (HR) power between 0-0.005 Hz in automated peak-detected heart rate traces (using the 'large dog' preset in LabChart®; ADInstruments; Colorado, USA). Spectral power analyses were performed with a Fast Fourier Transform (FFT) using a Hann (cosine-bell) data window with 50% overlap at 1K (EEG) or 8K (HRV) resolution. Quantitative analyses of variance of VLF HR Power (Figure 2.9) and EEG spectral power confirmed elevated HRV during visually scored REM and elevated delta EEG Power during SWS (Figure 2.10). We quantified

signal quality over time (using δ SWS / δ REM) and recorded at least two-fold greater amplitude SWS signals as compared to REM, despite signal reduction in water.

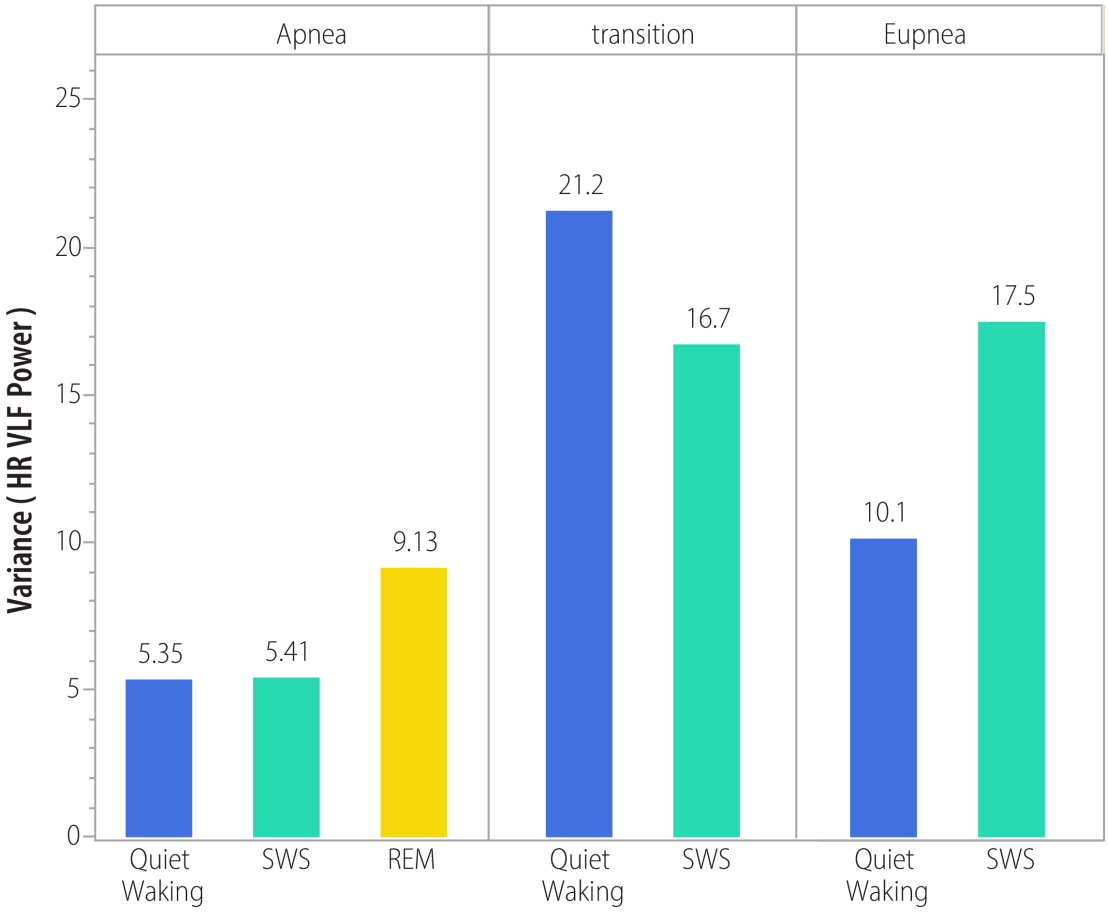

Figure 2.9. Heart Rate Variability (HRV) across sleep stage. Variance of very low frequency (VLF; 0-0.005 Hz) power for heart rate for animals at sea, sampled once per 8 seconds. REM has high low-frequency variability compared to SWS and QW during apnea and QW has elevated variability during eupnea and transitions to and from eupnea.

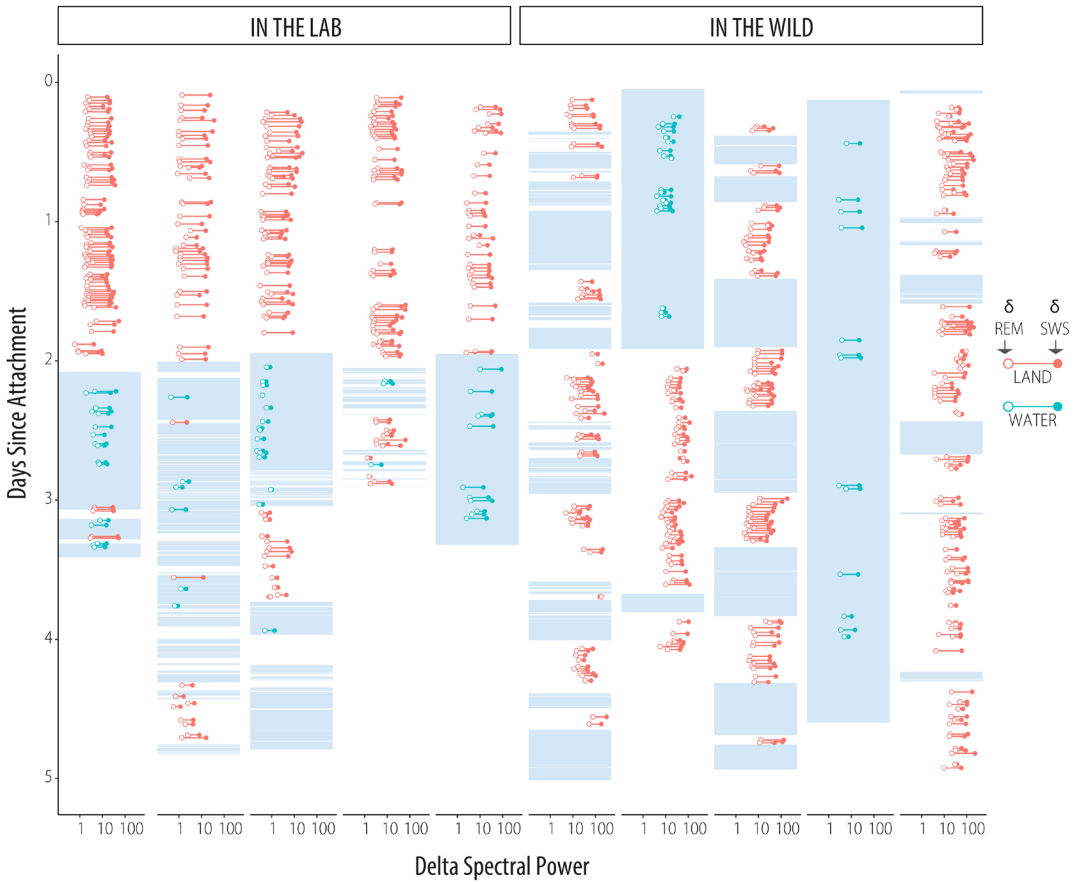

Figure 2.10. Signal quality (δ SWS / δ REM) for 5 recordings in the lab and in the wild. Detected signal amplitude during slow wave sleep was smaller during submersion in water, but remained at least 2-fold greater than that during REM.

2.8.7 *Motion & Environmental Sensor Processing*

For EEG studies, inertial motion sensing data was calibrated and processed using the Customized Animal Tracking Systems (CATS) toolbox (17). Speed was estimated using a custom MATLAB script based on stroke rate, pitch, and vertical speed using established thresholds for land and aquatic velocity from previous studies (8, 18). Processed inertial sensing data and speed estimates were paired with GPS coordinates

from Argos transmitters to create dead-reckoned tracks and reconstruct three-dimensional diving patterns. Three-dimensional tracks were then visualized in ArcGIS Pro (© 2019 ESRI) and Maya (© 2022 Autodesk) using the Visualizing Life in the Deep tools and scripts for visualizing underwater behavior (19, 20).

2.8.8 *Sleep Identification Model*

We estimated sleep in time-depth records using our EEG results and a hierarchical filtering algorithm to identify potential sleep. The sleep identification model incorporated elements of previously established hierarchical methods for identifying "drift dives," where the first derivative is constant for the majority of the dive (1, 21, 22). Existing methods often prioritized obtaining smooth estimates of these constant drift rates, used as a proxy for fat content and mass gain via buoyancy (21, 22). As such, these methods often rely on data abstraction that reduces complexity (via segmentation or the "broken-stick method") that may not allow for multiple independent drift segments in a single dive (21, 23). This model aimed to assess more sensitively the upper bound of time spent passively drifting through the water column.

Importantly, we refined our sleep identification algorithm to include dives that contained sleep, but that lack the sharp inflection points typically used to identify drift dives (12). These dives, though providing electrophysiological benefits of sleep, would not have been included in previous drift-dive identifications. In addition, current depth-based dive categorization does not differentiate between transiting or resting flat-

bottom dives. In our case, benthic sleep accounted for up to 5.2 h per day in an animal sleeping near shore. We incorporated the potential for benthic sleep in our model.

To identify *drifts*, we found consecutive segments satisfying broad preliminary vertical speed and acceleration criteria (compared to existing drift dive identification metrics) to minimize false negatives (Figure 2.12 & Figure 2.13). We then applied a minimum duration (>3 min) to identify *long drifts* and further filter these results (*filtered long drifts*) to obtain our *sleep estimate*. Our filter criteria were designed to maximize accuracy while minimizing false negatives and false positives based on our EEG data. Filter criteria were further adjusted to minimize false positives based on stroking data on long recordings where seals shifted to positive buoyancy. The *long drifts* were maintained as an *upper bound sleep estimate* to ensure sensitivity in the case of overly sensitive filter criteria. Filter criteria were designed to ensure accuracy and sensitivity across a broad range of challenging scenarios: (i) when animals are positively buoyant while shallow and negative while deep and (ii) when animals are close to neutrally buoyant and drift downwards and upwards in a single dive (Figure 2.11). Filter criteria minimized false positives (ensured specificity) during: (iii) transit dives (where animals' vertical speed is minimal, but they are actively swimming), and (iv) benthic dives that follow a bottom contour within the vertical speed and acceleration criteria (Figure 2.11).

We estimated sleep quotas for N=323 adult female northern elephant seals across foraging trips at sea (N=183 short post-breeding trips (79.9 ± 18.0 days); and long post-molt trips (221.7 ± 19.2 days); Table 2-1). A subset of 13 seals (8 post-breeding and 5 post-molt) were instrumented with accelerometers to assess the false positive rate of our model (propensity to falsely identify segments where the animal is swimming) (25).

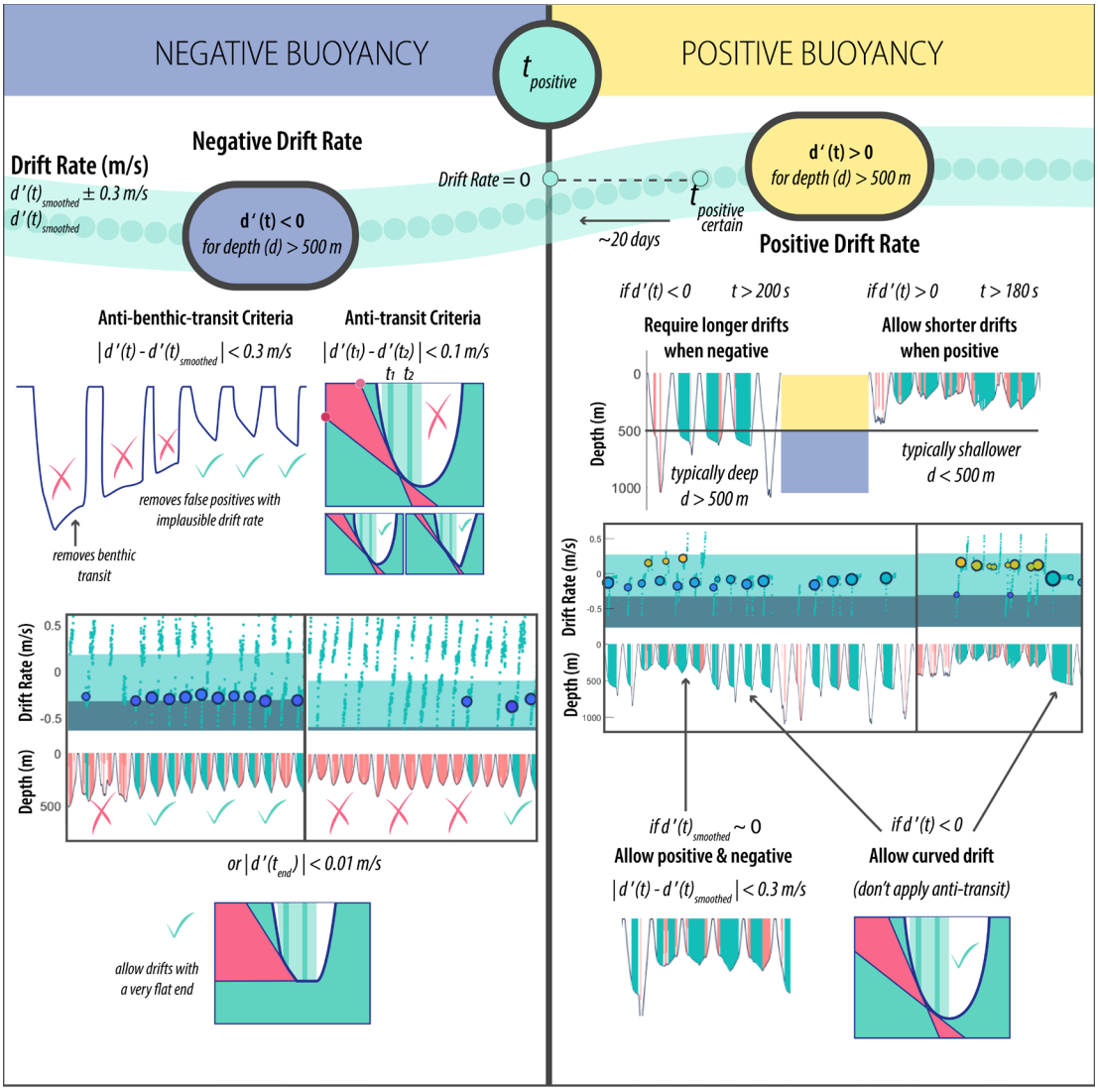

Figure 2.11. Schematic illustrating filter criteria for sleep identification output. Depth and first derivative of depth as a function of time are represented as d(t) and d'(t).

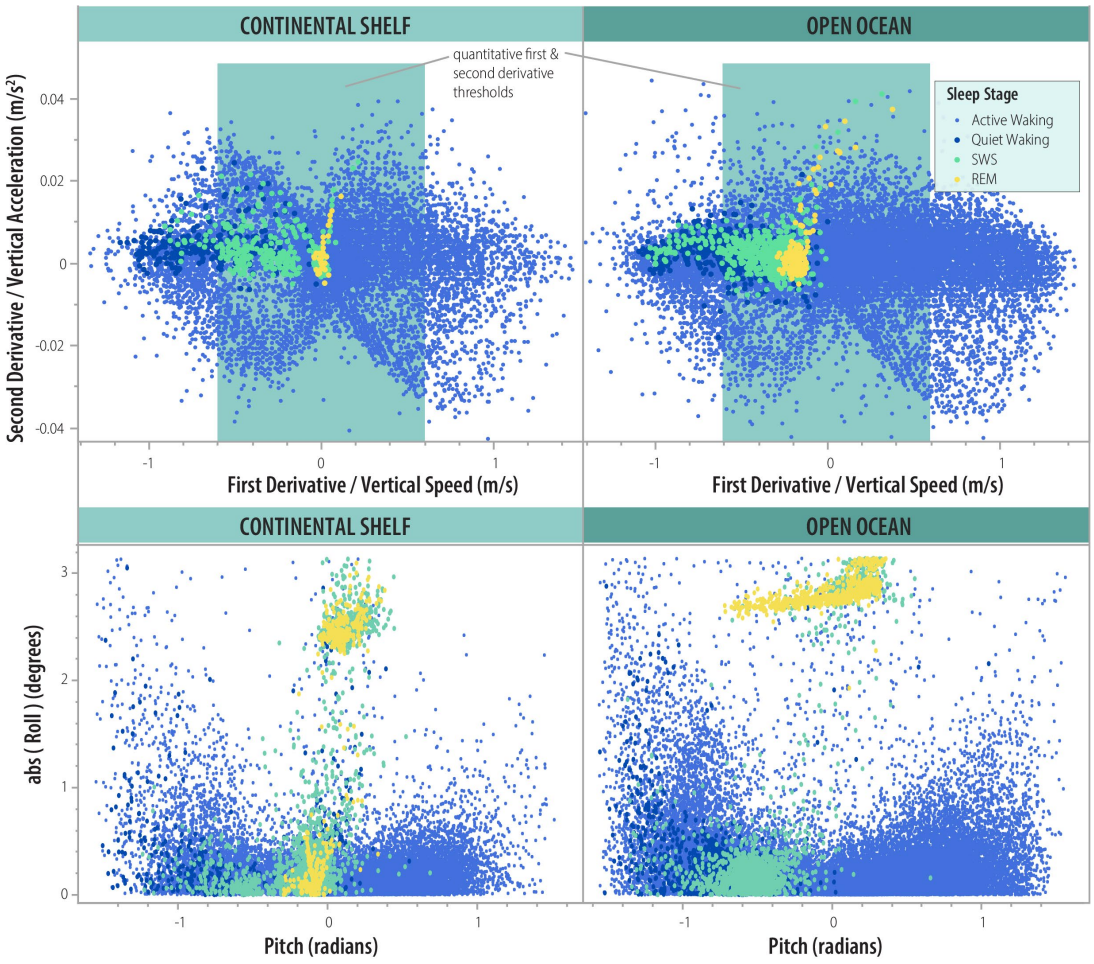

Figure 2.12. Quantitative parameters for raw data (at 10s^{-1}) by sleep stage (Active Waking [small light blue dots], Quiet Waking [large blue dots], SWS [large green dots], and REM [large yellow dots]). Teal rectangle demonstrates first and second derivative thresholds applied to dataset for sleep identification. Note that REM sleep only occurs while animals are rolled upside down, at which point the seals oscillate from pitch up to pitch down.

We analyzed diving behavior using a custom script in MATLAB that identifies consecutive segments that meet thresholds. Therefore, an important first processing step was to standardize the resolution and sensitivity of each time-depth record. We down-sampled data to 8 s^{-1} and applied a first pass Gaussian smoother (window size of

6) to remove noise in sensor data. For example, precise depth sensors like the EEG logger's Keller Druck 4LD sensor detected oscillations when the animal rolled back and forth on the seafloor. Smoothing dampens the amplitude of such oscillations. We then rounded the data to the nearest meter to reduce the probability of the first derivative to change sign (which would interrupt a consecutive drift segment). We then smoothed the data again (same window) to minimize spikes in vertical speed.

To apply an in-situ depth calibration, we applied a zero-offset correction to adjust surface intervals (and associated dives) to zero across the recording. A threshold of 2 meters differentiated surface intervals and dives. *Extended surface intervals* exceeding 10 minutes were labeled. A threshold of 10 strokes per minute differentiated periods of stroking and gliding. Glides exceeding 3 minutes (duration that minimized false positives) were labeled *long glides*.

An absolute first derivative ($d'(t)$ or vertical speed) threshold of 0.6 m/s differentiated descents and ascents from drifts. Drifts also had to meet a second derivative ($d''(t)$ or vertical acceleration) criterion of 0.05 m/s^2 (with $d(t)$ = depth as a function of time; $|d'(t)| < 0.60$ & $|d''(t)| < 0.05$). We labeled drifts exceeding 3 minutes *long drifts*.

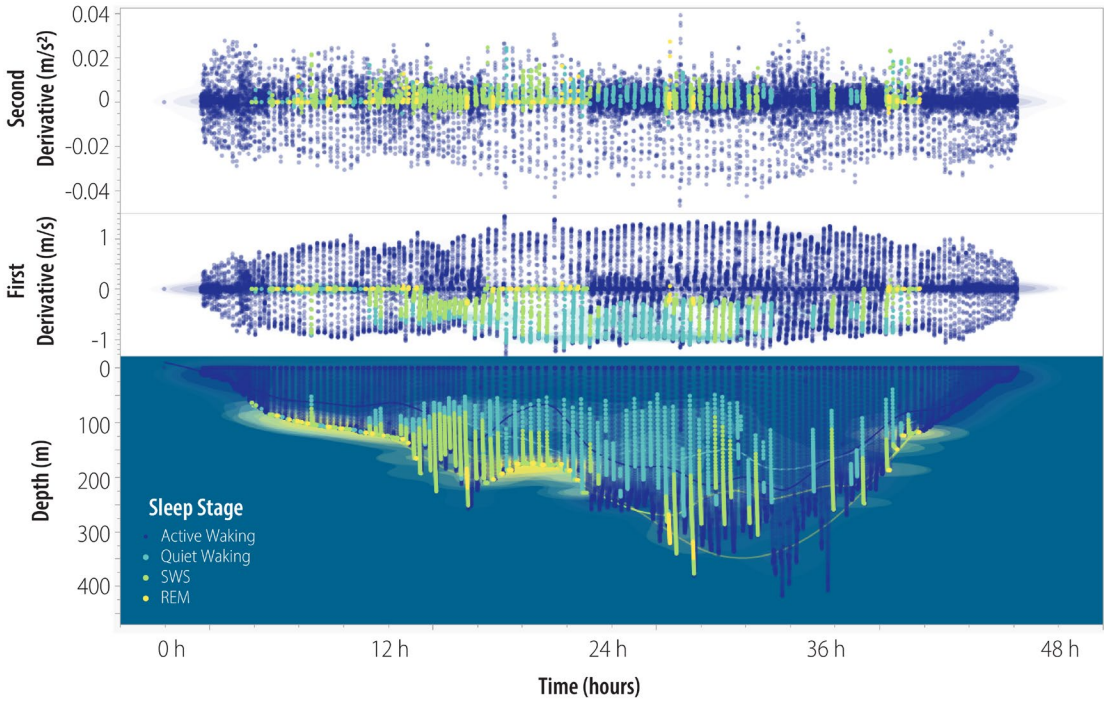

Figure 2.13. Quantitative derivative metrics for sleep. Vertical speed (first derivative (m/s)), Vertical acceleration (second derivative (m/s^2)), and Depth (m) over time, colored by sleep state (active waking, quiet waking, slow-wave sleep (SWS), or rapid-eye movement (REM) sleep) to show the quantitative patterns in the depth parameters associated with sleep.

Extended surface intervals exceeding 10 minutes were labeled and also included extended surface intervals in our sleep estimate, where animals could spend up to 8 hours at the surface without significant stroking activity. Although we do not have direct EEG observations at sea to confirm this, one animal in the lab spent several days sleeping vertically at the surface of the pool and bottling is a common sleep and sleep behavior for seals and walruses (14).

We also included *long flats* as a proxy for benthic sleep in our sleep estimate. *Long flats* included all *long drifts* ending in a flat segment (| mean ($d'(t_{end})$) | < 0.01 m/s where t_{end} is between 7/8 and 8/9 of the segment).

Filtering criteria for long drifts: To minimize false positives (where animals were stroking), we filtered *long drifts* according to several criteria. First, we eliminated long drifts that deviated from a smoothed drift rate throughout the trip to eliminate physiologically implausible drift rates. We calculated smoothed drift rates for shallow (< 500 m) *long drifts* using a Gaussian smoother (window size 1/20 of the trip duration). We preserved a broad threshold of drift rates surrounding this smoothed drift rate to minimize false negatives (| $d'(t) - d'(t)_{\text{smoothed}}$ | < 0.3 m/s) (Figure 2.11). Previous studies implemented similar filters, including spline regressions or Kalman filters (*21, 23, 24*).

Next, we applied additional filtering criteria depending on the buoyancy of the animal. Generally, the criteria for *positively buoyant* seals were broader than for *negatively buoyant* seals. *Positively buoyant* seals could drift upward and downward, while *negatively buoyant* seals only drifted downward. We considered the animal *positively buoyant* 20 days before this smoothed drift rate exceeded 0 m/s (t_{positive}). If an animal was positively buoyant near the beginning of the trip (within the first 20 days), we used the broader *positively buoyant* criteria for the entire trip.

Filter criteria aimed to minimize false positives by eliminating "benthic transit" (seals swimming along the continental shelf at a relatively constant ascent or descent

rate) and "transit" (U-shaped transit dives with low vertical speed) (Figure 2.11). *Anti-transit* criteria eliminated segments where the drift rate changed significantly between the beginning and the end of the drift ($| d'(t_1) - d'(t_2) | < 0.10$ m/s where t_1 is between 1/4 and 2/3 of the segment and t_2 is between 2/3 and 3/4 of the drift duration). *Anti-benthic-transit criteria* eliminated drifts with slopes lower than 0.08 m/s. For *negatively buoyant* seals, we only allowed negative long drifts that passed both *anti-transit* and *anti-benthic-transit* criteria. For *positively buoyant* seals, we used different criteria for positive and negative drifts. Positive drifts for positively buoyant seals ($d'(t) > 0$ & $t > t_{positive}$) were eliminated if they violated *anti-transit* criteria, but not *anti-benthic-transit* criteria (eliminating curved drifts but not low-slope drifts, because seals near neutral buoyancy could have drift rates near zero). We allowed curved downward drifts for *positively buoyant* seals, where the seal would be decelerating (Figure 2.11). For both positively and negatively buoyant seals, only *long* negative drifts for positively buoyant seals were kept (> 200s compared to 180s for often-fragmented positive drifts).

For the first and last 15 days from the calculation of smoothed drift rate, where false positives were more likely, we applied more restrictive filtering criteria (0.15 m/s around a drift rate calculated from only the shallow (< 500 m), non-flat long drifts at the beginning or end of the trip). We assumed a constant drift rate calculated based on filtered long drifts for the first and last 15 days. If seals were positively buoyant, we did not restrict drift rates.

The output of these filtering steps, *filtered long drifts,* were added to *long flats* (benthic sleep) and *extended surface intervals* (potential sleep at surface) to constitute our *sleep estimate*. *Unfiltered long drifts* (includes long flats), derived solely from first and second derivative criteria, were added to *extended surface intervals* to constitute our *upper bound sleep estimate*.

2.8.9 *Model Accuracy Assessment*

We validated our model by calculating its accuracy, sensitivity, and specificity compared to EEG-identified sleep. The sleep identification model yielded 93% accuracy (Figure 2.3 & Table 2-4). We also calculated an upper-bound sleep estimate (unfiltered *long drifts*) with high sensitivity (93.6%) to minimize false negatives (1.3% of classifications). Simply imposing a duration threshold increased accuracy of our sleep identifier from 46.3% to 77.1%. Filtering further improved the accuracy of our sleep identification model to 93% overall (Figure 2.14). While the sensitivity of the model decreased from 98.4% to 84.8% (from *drifts* to *filtered long drifts*/*sleep estimate*), the specificity increased from 42.0% to 94.1%. *Long glides* were fairly accurate (86.3%) and specific (89.9%) to estimate total sleep time, but not as accurate as our sleep identification model. Therefore, we used long glides as a proxy for sleep to identify false positive rates for the 13 adult females instrumented with stroke rate loggers.

Table 2-4. Performance of sleep identification model. We demonstrate the model's accuracy for identifying sleep using drifts (mathematical first and second derivative criteria alone), long drifts (derivative criteria and time threshold [>3 min]), and filtered long drift (long drifts filtered by criteria explained in text). # of categorized samples (8 s^{-1}) that were true negatives (TN – not sleep and not detected), false negatives (FN – sleep but not detected), false positives (FP – not sleep but detected), and true positives (TP – sleep and detected). We show the percentage of

total classifications for each category and provide measures of model accuracy (TN + TP / Total), sensitivity (TP / (TP + FN)), and specificity (TN / (TN + FP)).

Predicted Class	True Class	True Negatives	False Negatives	False Positives	True Positives	True Negatives (% of total)	False Negatives (% of total)	False Positives (% of total)	True Positives (% of total)	Accuracy (TN + TP / Total)	Sensitivity (TP/(TP+FN))	Specificity (TN/(TN+FP))
		7965	203	9044	4326	37.0%	0.9%	42.0%	20.1%	57.1%	95.5%	46.8%
		18565	7	28128	1621	38.4%	0.0%	58.2%	3.4%	41.8%	99.6%	39.8%
Drifts	Sleep	10533	0	16110	268	39.1%	0.0%	59.9%	1.0%	40.1%	100.0%	39.5%
		37063	**210**	**53282**	**6215**	**38.2%**	**0.3%**	**53.4%**	**8.1%**	**46.3%**	**98.4%**	**42.0%**
		13058	822	3951	3707	60.6%	3.8%	18.3%	17.2%	77.8%	81.9%	76.8%
		32470	18	14223	1610	67.2%	0.0%	29.4%	3.3%	70.5%	98.9%	69.5%
Long Drifts	Sleep	22081	0	4562	268	82.1%	0.0%	17.0%	1.0%	83.0%	100.0%	82.9%
		67609	**840**	**22736**	**5585**	**70.0%**	**1.3%**	**21.6%**	**7.2%**	**77.1%**	**93.6%**	**76.4%**
		15445	1049	1564	3480	71.7%	4.9%	7.3%	16.2%	87.9%	76.8%	90.8%
		44196	365	2497	1263	91.5%	0.8%	5.2%	2.6%	94.1%	77.6%	94.7%
Filtered Long Drifts	Sleep	25819	0	824	268	95.9%	0.0%	3.1%	1.0%	96.9%	100.0%	96.9%
		85460	**1414**	**4885**	**5011**	**86.4%**	**1.9%**	**5.2%**	**6.6%**	**93.0%**	**84.8%**	**94.1%**
		11144	53	5865	4476	51.7%	0.2%	27.2%	20.8%	72.5%	98.8%	65.5%
		37590	18	9103	1610	77.8%	0.0%	18.8%	3.3%	81.1%	98.9%	80.5%
Glides	Sleep	7089	0	19554	268	26.3%	0.0%	72.7%	1.0%	27.3%	100.0%	26.6%
		55823	**71**	**34522**	**6354**	**52.0%**	**0.1%**	**39.6%**	**8.4%**	**60.3%**	**99.2%**	**57.5%**
		15086	328	1923	4201	70.0%	1.5%	8.9%	19.5%	89.5%	92.8%	88.7%
		45794	374	899	1254	94.8%	0.8%	1.9%	2.6%	97.4%	77.0%	98.1%
Long Glides	Sleep	19069	0	7574	268	70.9%	0.0%	28.1%	1.0%	71.9%	100.0%	71.6%
		79949	**702**	**10396**	**5723**	**78.6%**	**0.8%**	**13.0%**	**7.7%**	**86.3%**	**89.9%**	**86.1%**

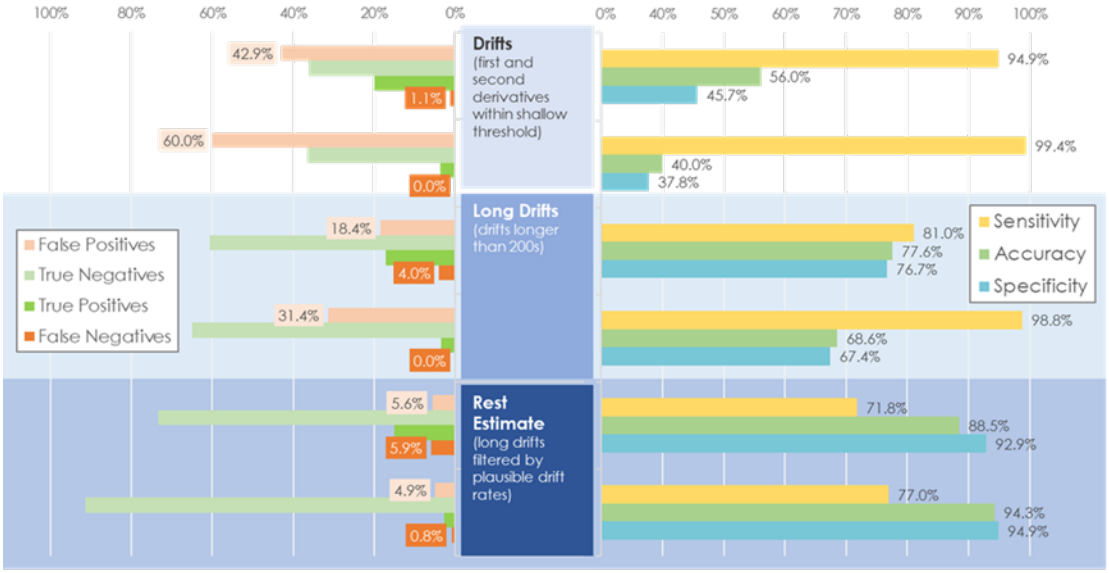

Figure 2.14. Accuracy of sleep identification model. Accuracy and specificity increase while the sensitivity and prevalence of false positives decrease from identified drifts to long drifts (longer than 200 s) and finally our filtered sleep estimate (long drifts filtered by plausible drift rate).

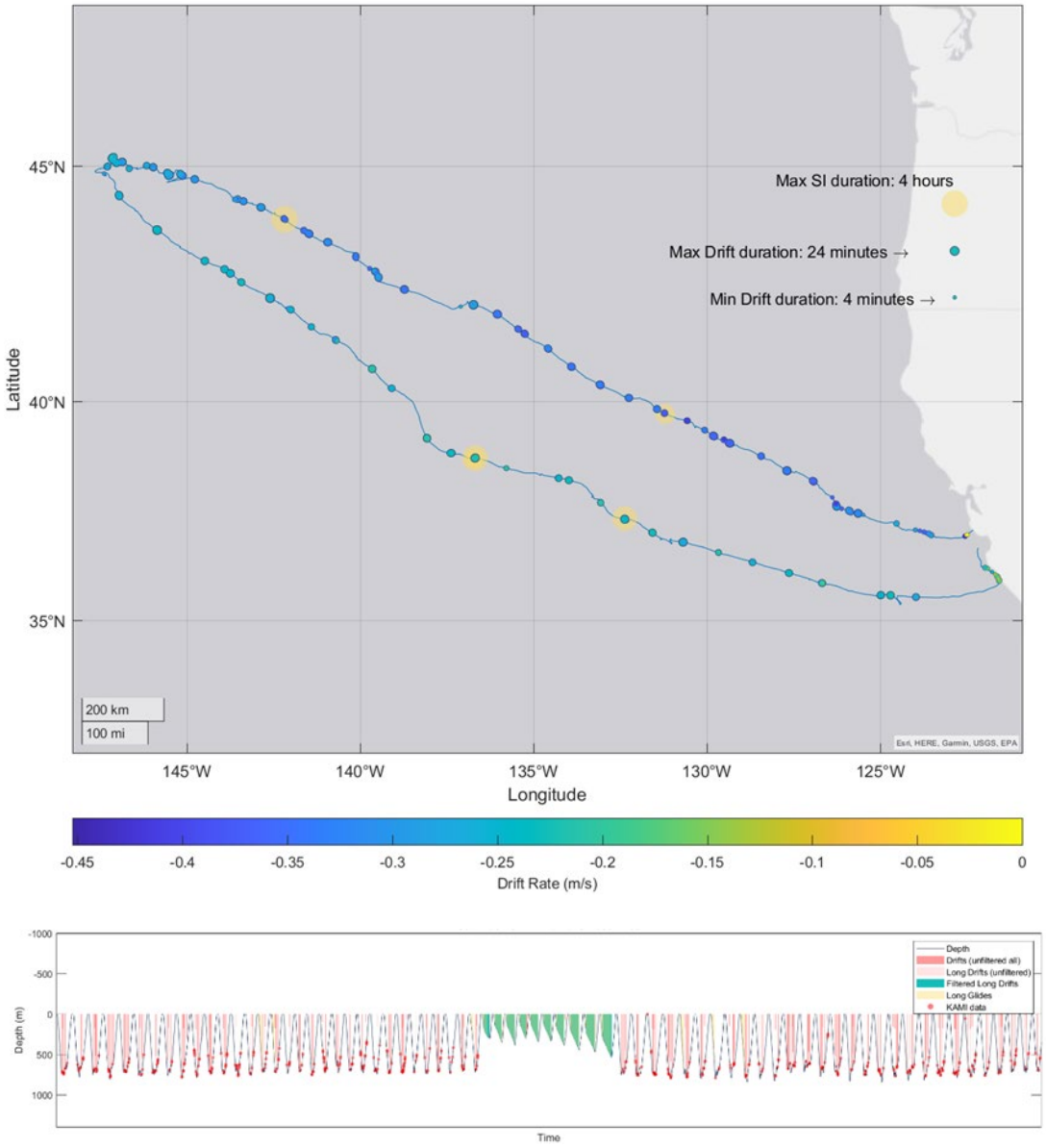

Figure 2.15. Sleep identification model output for pelagic animal. Nap map shows pelagic track and illustrates each identified sleep as a dot sized by its duration and colored by its drift rate. Large yellow dots are extended surface intervals (>10 min). Green indicates an identified sleep segment that coincides with a long glide (false negatives in yellow and false positives in blue). Red dots on the bottom figure indicate foraging attempts as recorded from kami kami logger. Light red indicates an eliminated short drift.

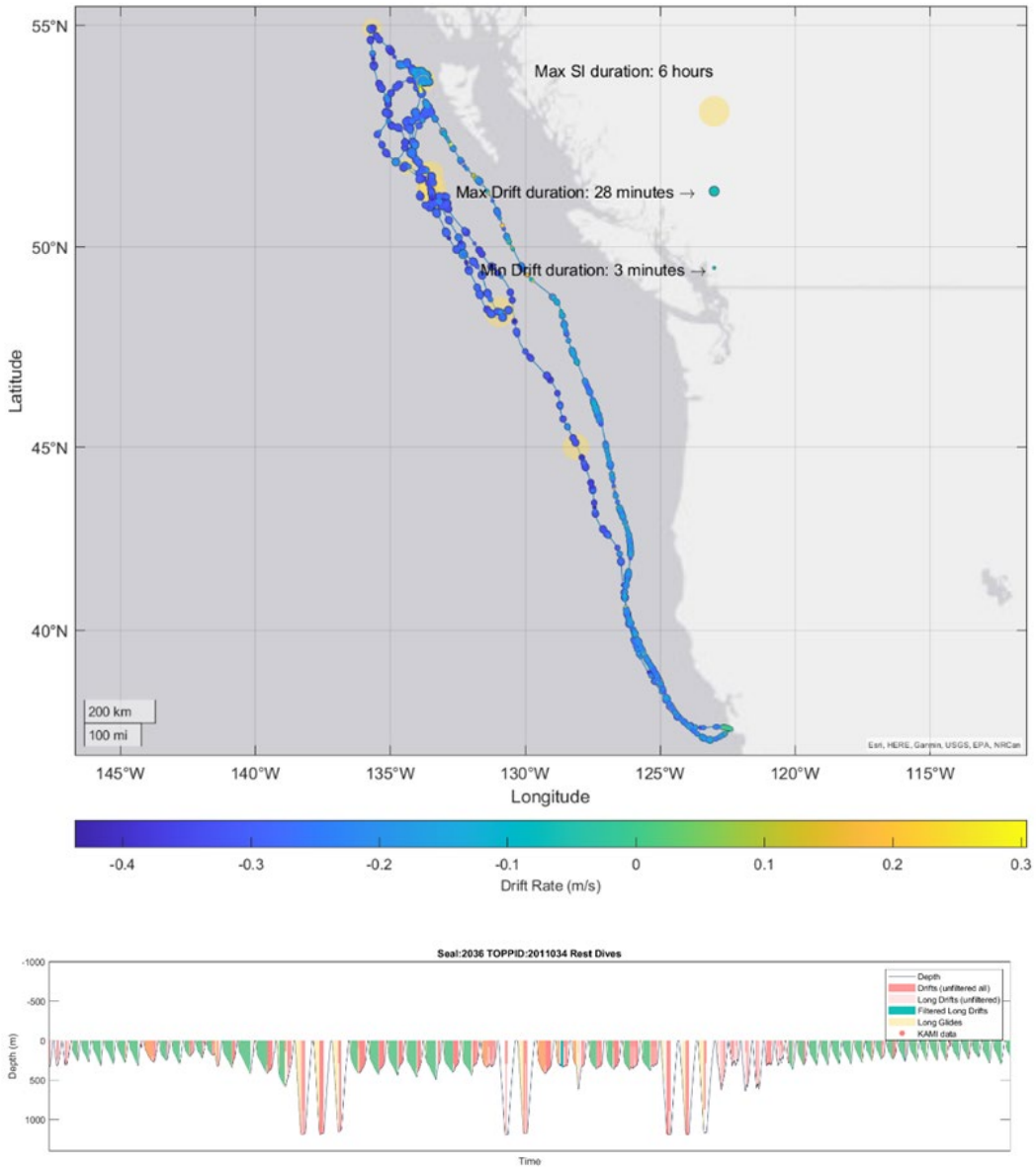

Figure 2.16. Sleep identification model output for coastal animal. Nap map shows pelagic track and illustrates each identified sleep as a dot sized by its duration and colored by its drift rate. Large yellow dots are extended surface intervals (>10 min). Green indicates an identified sleep segment that coincides with a long glide (false negatives in yellow and false positives in blue). Red dots on the bottom figure indicate foraging attempts as recorded from kami kami logger. Light red indicates an eliminated short drift.

1. P. W. Robinson, S. E. Simmons, D. E. Crocker, D. P. Costa, Measurements of foraging success in a highly pelagic marine predator, the northern elephant seal. Journal of Animal Ecology. 79, 1146–1156 (2010).
2. R. R. Holser, D. E. Crocker, P. W. Robinson, R. Condit, D. P. Costa, Density-dependent effects on reproductive output in a capital breeding carnivore, the northern elephant seal (Mirounga angustirostris). Proceedings of the Royal Society B: Biological Sciences. 288, 20211258 (2021).
3. S. S. Kienle, A. S. Friedlaender, D. E. Crocker, R. S. Mehta, D. P. Costa, Trade-offs between foraging reward and mortality risk drive sex-specific foraging strategies in sexually dimorphic northern elephant seals. Royal Society Open Science. 9, 210522 (2022).
4. T. Adachi, A. Takahashi, D. P. Costa, P. W. Robinson, L. A. Hückstädt, S. H. Peterson, R. R. Holser, R. S. Beltran, T. R. Keates, Y. Naito, Forced into an ecological corner: Round-the-clock deep foraging on small prey by elephant seals. Science Advances (2021), doi:10.1126/sciadv.abg3628.
5. R. D. Andrews, D. R. Jones, J. D. Williams, P. H. Thorson, G. W. Oliver, D. P. Costa, B. J. L. Boeuf, Heart rates of northern elephant seals diving at sea and resting on the beach. Journal of Experimental Biology. 200, 2083–2095 (1997).
6. M. A. Castellini, W. K. Milsom, R. J. Berger, D. P. Costa, D. R. Jones, J. M. Castellini, L. D. Rea, S. Bharma, M. Harris, Patterns of respiration and heart rate during wakefulness and sleep in elephant seal pups. American Physiological Society, R863–R869 (1994).
7. W. Milsom, M. Castellini, M. Harris, J. Castellini, D. Jones, R. Berger, S. Bahrma, L. Rea, D. Costa, Effects of hypoxia and hypercapnia on patterns of sleep-associated apnea in elephant seal pups. American Journal of Physiology-Regulatory, Integrative and Comparative Physiology. 271, R1017–R1024 (1996).
8. Y. Mitani, R. D. Andrews, K. Sato, A. Kato, Y. Naito, D. P. Costa, Three-dimensional resting behaviour of northern elephant seals: drifting like a falling leaf. Biology Letters. 6, 163–166 (2009).
9. G. W. Oliver, P. A. Morris, P. H. Thorson, B. J. le Boeuf, Homing Behavior of Juvenile Northern Elephant Seals. Marine Mammal Science. 14, 245–256 (1998).
10. P. W. Robinson, D. P. Costa, D. E. Crocker, J. P. Gallo-Reynoso, C. D. Champagne, M. A. Fowler, C. Goetsch, K. T. Goetz, J. L. Hassrick, L. A. Hückstädt, C. E. Kuhn, J. L. Maresh, S. M. Maxwell, B. I. McDonald, S. H. Peterson, S. E. Simmons, N. M. Teutschel, S. Villegas-Amtmann, K. Yoda, Foraging behavior and success of a mesopelagic predator in the northeast Pacific Ocean: insights from a data-rich

species, the northern elephant seal. PloS one. 7 (2012), doi:10.1371/journal.pone.0036728.

11. M. Horning, R. D. Andrews, A. M. Bishop, P. L. Boveng, D. P. Costa, D. E. Crocker, M. Haulena, M. Hindell, A. G. Hindle, R. R. Holser, S. K. Hooker, L. A. Hückstädt, S. Johnson, M.-A. Lea, B. I. McDonald, C. R. McMahon, P. W. Robinson, R. L. Sattler, C. R. Shuert, S. M. Steingass, D. Thompson, P. A. Tuomi, C. L. Williams, J. N. Womble, Best practice recommendations for the use of external telemetry devices on pinnipeds. Animal Biotelemetry. 7, 1–17 (2019).
12. M. D. Schalles, D. S. Houser, J. J. Finneran, P. Tyack, B. Shinn-Cunningham, J. Mulsow, Measuring auditory cortical responses in Tursiops truncatus. J Comp Physiol A (2021), doi:10.1007/s00359-021-01502-5.
13. S. Romero, M. A. Mañanas, S. Clos, S. Gimenez, M. J. Barbanoj, Reduction of EEG Artifacts by ICA in Different Sleep Stages. Annual International Conference of the IEEE Engineering in Medicine and Biology - Proceedings. 3, 2675–2678 (2003).
14. O. I. Lyamin, P. O. Kosenko, A. L. Vyssotski, J. L. Lapierre, J. M. Siegel, L. M. Mukhametov, Study of Sleep in a Walrus. 444, 188–191 (2012).
15. O. I. Lyamin, J. L. Lapierre, P. O. Kosenko, L. M. Mukhametov, J. M. Siegel, Electroencephalogram asymmetry and spectral power during sleep in the northern fur seal. Journal of Sleep Research. 17, 154–165 (2008).
16. J. M. Kendall-Bar, A. L. Vyssotski, L. M. Mukhametov, J. M. Siegel, O. I. Lyamin, Eye state asymmetry during aquatic unihemispheric slow wave sleep in northern fur seals (Callorhinus ursinus). PLoS ONE. 14, 1–13 (2019).
17. D. E. Cade, W. T. Gough, M. F. Czapanskiy, J. A. Fahlbusch, S. R. Kahane-Rapport, J. M. J. Linsky, R. C. Nichols, W. K. Oestreich, D. M. Wisniewska, A. S. Friedlaender, J. A. Goldbogen, Tools for integrating inertial sensor data with video bio-loggers, including estimation of animal orientation, motion, and position. Anim Biotelemetry. 9, 34 (2021).
18. D. E. Cade, K. R. Barr, J. Calambokidis, A. S. Friedlaender, J. A. Goldbogen, Journal of Experimental Biology, in press, doi:10.1242/jeb.170449.
19. J. Kendall-Bar, N. Kendall-Bar, A. G. Forbes, G. McDonald, P. J. Ponganis, C. Williams, M. Horning, A. Hindle, H. Klinck, R. S. Beltran, A. S. Friedlaender, D. Wiley, D. P. Costa, T. M. Williams, Visualizing Life in the Deep: A Creative Pipeline for Data-Driven Animations to Facilitate Marine Mammal Research, Outreach, and Conservation. IEEE VIS Arts Program. 2021, 10 (2021).
20. J. Kendall-Bar, Visualizing Life in the Deep: code repository for visualizing marine mammal tag data (2021; https://github.com/jmkendallbar/VisualizingLifeintheDeep).

21. S. A. Gordine, M. Fedak, L. Boehme, Fishing for drifts: Detecting buoyancy changes of a top marine predator using a step-wise filtering method. Journal of Experimental Biology. 218, 3816–3824 (2015).

22. D. E. Crocker, B. J. L. Boeuf, D. P. Costa, Drift diving in female northern elephant seals: implications for food processing. Canadian Journal of Zoology. 75, 27–39 (2008).

23. F. Arce, S. Bestley, M. A. Hindell, C. R. McMahon, S. Wotherspoon, A quantitative, hierarchical approach for detecting drift dives and tracking buoyancy changes in southern elephant seals. Sci Rep. 9, 8936 (2019).

24. T. Adachi, J. L. Maresh, P. W. Robinson, S. H. Peterson, D. P. Costa, Y. Naito, Y. Y. Watanabe, A. Takahashi, The foraging benefits of being fat in a highly migratory marine mammal. Proceedings of the Royal Society B: Biological Sciences. 281, 1–9 (2014).

25. Kendall-Bar, J.M., Mukherji, R., Nichols, J. et al. Eavesdropping on the brain at sea: development of a surface-mounted system to detect weak electrophysiological signals from wild animals. Anim Biotelemetry 10, 16 (2022). https://doi.org/10.1186/s40317-022-00287-x

Chapter 3. **Visualizing life in the deep: a creative pipeline for data-driven animations to facilitate marine mammal research, outreach, and conservation**

Jessica Kendall-Bar[1,2] Nicolas Kendall-Bar[2], Angus G. Forbes[3], Gitte McDonald[4], Paul J. Ponganis[5], Cassondra Williams[6], Markus Horning[7], Allyson Hindle[8], Holger Klinck[9,10], Roxanne S. Beltran[1], Ari S. Friedlaender[11], David Wiley[12], Daniel P. Costa[1], and Terrie M. Williams[1]

[1]Ecology & Evolutionary Biology, UC Santa Cruz, [2]Kendall-Bar Studios, [3]Computational Media, UC Santa Cruz, [4]Moss Landing Marine Laboratories, San Jose State University, [5]Scripps Institution of Oceanography, UC San Diego, [6]National Marine Mammal Foundation, [7]Wildlife Technology Frontiers, [8]School of Life Sciences, University of Nevada, Las Vegas, [9]Center for Conservation Bioacoustics, Cornell University, [10]Marine Mammal Institute, Oregon State University, [11]Institute of Marine Sciences, UC Santa Cruz, [12]Stellwagen Bank National Marine Sanctuary, National Oceanic and Atmospheric Administration

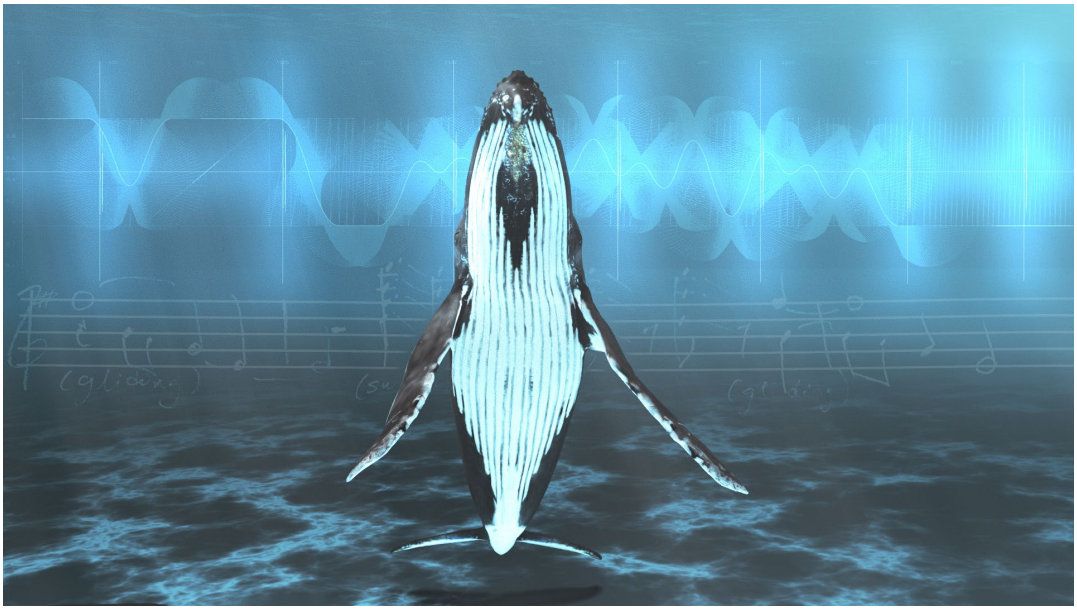

Figure 3.1. Illustration of an animated 3D humpback whale combined with a representation of several data streams used in our data-driven animation pipeline. The ribbons of data shown include: swimming and gliding data from an elephant seal, the waveform of a soundtrack generated from the beating heart of a narwhal, and notes of a custom musical score for one of our animations.

The text of this dissertation includes a reprint of the following published material:

Kendall-Bar, Jessica M., Nicolas Kendall-Bar, Angus G Forbes, Gitte McDonald, Paul J Ponganis, Cassondra Williams, Markus Horning, et al. 2021. *Visualizing Life in the Deep: A Creative Pipeline for Data-Driven Animations to Facilitate Marine Mammal Research, Outreach, and Conservation*. ***IEEE VIS Arts Program 2021.*** *DOI 10.1109/VISAP52981.2021.00007*.

3.1 ABSTRACT

In this paper, we introduce a creative pipeline to incorporate physiological and behavioral data from contemporary marine mammal research into data-driven animations, leveraging functionality from industry tools and custom scripts to promote scientific insights, public awareness, and conservation outcomes. Our framework can flexibly transform data describing animals' orientation, position, heart rate, and swimming stroke rate to control the position, rotation, and behavior of 3D models, to render animations, and to drive data sonification. Additionally, we explore the challenges of unifying disparate datasets gathered by an interdisciplinary team of researchers and outline our design process for creating meaningful data visualization tools and animations. As part of our pipeline, we clean and process raw acceleration and electrophysiological signals to expedite complex multi-stream data analysis and the identification of critical foraging and escape behaviors. We provide details about four animation projects illustrating marine mammal datasets. These animations, commissioned by scientists to achieve outreach and conservation outcomes, have successfully increased the reach and engagement of the scientific projects they describe. These impactful visualizations help scientists identify behavioral responses to disturbance, increase public awareness of human-caused disturbance, and help build momentum for targeted conservation efforts backed by scientific evidence.

3.2 INTRODUCTION

To mitigate disturbance and conserve marine mammal populations, it is critical to understand marine mammals' responses to disturbance [50]. Human-caused disturbances such as entanglement in fishing gear and exposure to underwater noise can negatively impact individuals with population-level consequences [39]. These responses lie at the confluence of physiology, kinematics, foraging behavior, and animal movement ecology. Tagging technology has allowed scientists to describe and quantify the three-dimensional responses of marine mammals below the surface, by simultaneously recording positional data such as accelerometry, magnetometry, gyroscope, depth, geolocation, video cameras, and additional sensors that provide physiological measurements such as electrocardiograms [4,32,55,58].

Behavioral and kinematic tagging data can also provide insight on physiological processes. Time depth recordings can provide information on the rate at which animals drift up or down in the water column, which is directly related to their buoyancy and thus their internal fat stores, a measure of body condition and health [4, 9, 18, 45]. Video footage of foraging can reveal total feeding attempts and prey availability, which has implications for animal health [2, 17]. Accelerometry informs 3D position, orientation, and the stroke rate of the fluke or flippers, which is related to the metabolic cost of transport [22,30,57].

In this paper, we explore the challenges of unifying disparate datasets with an interdisciplinary team and outline the design process for creating meaningful data visualization tools and animations (Figure 3.2). Our work involved close collaboration

between animators, computer scientists, and biologists to visualize and sonify the behavior and physiology of deep-diving marine mammals in extreme environments. Our framework directly incorporates behavioral and physiological data streams to depict stark shifts in swimming behavior (stroking and gliding), body condition (negatively buoyant to positively buoyant), and heart rate (extreme bradycardia and tachycardia). Our tools visualize changes across several orders of magnitude in space and time, from fine-scale body maneuvers to broad-scale trans-Pacific migratory patterns. We built custom tools including (1) scripts to visualize 3D position and orientation, (2) stroke and glide controllers to control organic swimming animations based on raw accelerometer data, and (3) a heartbeat sonifier to hear pronounced shifts in heart rate. In addition to developing new animation tools for data visualization and science communication, it is critical to provide accessible training to encourage broad use of these tools. Through a series of workshops titled “Animation for Science Communication” and several online tutorials and recordings, we taught a wide range of animation skills to over a hundred students, researchers, and faculty at the University of California, Santa Cruz throughout the 2020-21 academic year.

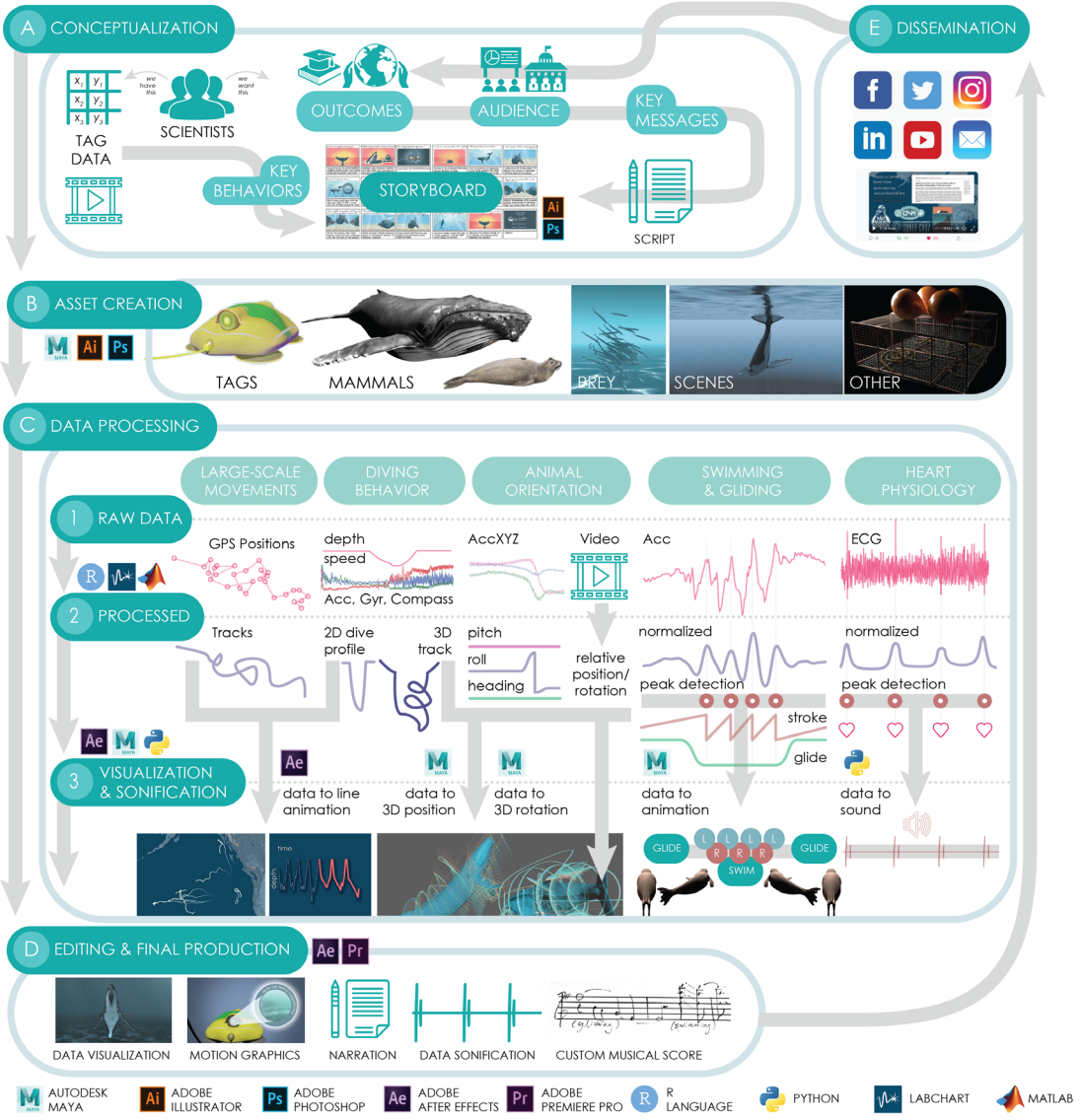

Figure 3.2. Conceptual diagram of the animation process from (A) conceptualization to (B) asset creation, (C) data processing, (D) editing and final production, and (E) dissemination. (A) Conceptualization. We demonstrate how we created a storyboard and script based on key features of the data as well as taking into account our desired outcomes (education and conservation) and audiences (government, NGOs, and academics). (B) Asset Creation. We demonstrate the range of customized assets we created in Autodesk Maya (3D models), Adobe Photoshop (digital paintings and 3D model textures), and Adobe Illustrator (vector graphics). (C)

Data Processing Pipeline. We show the process of data mapping from raw data to processed data to abstraction (data visualization or data sonification) for five major data types, including (1) large-scale movements (from GPS positions to line animations), (2) diving behavior (from inertial motion sensors to two- and three-dimensional dive tracks), (3) animal orientation (from inertial motion sensors to three-dimensional rotation), (4) swimming and gliding (from raw accelerometer data to animated swimming), and (5) heart physiology (from ECG data to sound). (D) Editing and Final Production. We combine data visualization, custom 2D illustrations and 3D assets, motion graphics, narration, data sonification, and custom musical scores in the final compositions to prepare them for (E) dissemination to reach our key audiences and achieve desired outcomes.

By reviewing existing approaches to animating ocean science data and meeting regularly with our interdisciplinary team of scientists and artists over the course of two years, we solidified the core goals for the development of our data-driven animations:

- **Research:** Collaborate with biologists to address the research tasks above and elucidate how marine mammals respond behaviorally and physiologically to different types of disturbance.
- **Clarity:** Ensure that each of those insights is communicated clearly via the visualization by combining 3D animation, narration, annotations, line animations, and visual effects.
- **Reach:** Increase the readership and comprehension of scientific papers by creating accessible and engaging animations.
- **Impact:** Work with scientists to develop a clear and succinct take-away that summarizes the consequences of disturbance and provides conservation recommendations.

3.2.1 *Related Work*

Researchers in the visualization and data art communities advocate for the incorporation of creative methodologies from interactive design and visual arts practice, particularly when working on collaborative projects that bridge multiple disciplines [14,15,48,51] and when translating scientific results to the public [20,42,43,52]. While data visualization research often focuses on the development of effective techniques and tools to facilitate exploration and analysis of data, data

storytelling approaches emphasize how visualization techniques can persuasively communicate scientific results through a compelling narrative and interpretation of a dataset [29,40,46]. To support scientific engagement and communication, researchers have recently promoted the use of "cinematic" data visualization, leveraging 3D modeling, motion graphics, and visual effects software tools used most often for animations and games [5,6,47]. Our data-driven animation pipeline draws from this work by creating cinematic depictions of contemporary marine mammal research that integrate physiological and behavioral datasets from a suite of animal-borne sensors (Figure 3.2).

3.2.1a *Visualization tools for tag data*

Visualization tools are critical for data exploration and interpretation for animal-borne tags. *TrackPlot*, a 3D visualization software created by biologists and data visualization experts, facilitated the first detailed description of benthic side-roll feeding by humpback whales and greatly advanced our understanding of complex biomechanics and kinematics [44,54–56]. Existing marine mammal tag visualization tools, such as *TrackPlot*, Sea Mammal Research Unit's *MAMVIS*, and Wildlife Computers' *Data Portal*, are primarily focused on geolocation or kinematic representations of dive behavior and rarely incorporate physiological measurements such as heart rate, which are often recorded using separate dataloggers [13,35,54]. Physiological instruments such as animal heart rate loggers by UFI Instruments and Star-Oddi currently do not support adjacent 3D track visualization. Our animations present behavior alongside

physiological data to unify and expedite data exploration and interpretation. In addition, our animations visualize fine-scale behaviors such as mouth openings, fluke and flipper swimming strokes, and fine-scale flipper maneuvers to improve realism and create an engaging experience.

3.2.1b *3D Modeling tools*

3D modeling of marine mammals is useful for assessing animal health, locomotion costs, and functional anatomy [1,21,53]. Beyond addressing scientific questions related to body mass and shape, certain anatomically accurate 3D models have been textured and rigged for use in animations [21]. However, high-quality rigged models with sophisticated animation controls often lack scientific rigor and accuracy. Although access to 3D photogrammetry and LIDAR 3D scanning has facilitated the creation of 3D models and even 3D reconstruction of an animal's environment, these tools are still challenging to implement in the field [21,31]. Behaviors of interest may not fit within the repertoire of a rigged model and custom controls and rigging may be required. By modifying existing rigged models and creating custom 3D models, we hope to increase the availability of realistic models for both scientists and animators.

3.2.1c *Marine Mammal Animations*

Marine mammals are commonplace in animations targeting younger students and children, including feature films, computer games, and educational videos [12, 28, 34]. Educational 3D animations accurately depict marine mammal anatomy and even simulations of dive physiology, but these animations do not usually incorporate tagging

data [11,36]. Our animations directly incorporate tagging data from current research projects to make it accessible to the scientific community, policymakers, and the public.

3.2.2 *Key tasks and data types*

Supporting our high-level goals, we worked closely with our collaborators to identify the key visualization tasks to facilitate effective scientific communication:

1. **Present and align behavioral and physiological data streams** collected from animal-borne tag sensors.
2. **Correlate data streams to generate hypotheses** about the responses of marine mammals to disturbance.
3. **Compare behaviors across time, ecosystems, and species** to generate overarching theories about the impact of disturbance across animal systems.
4. **Use this data to inform policy** related to marine mammal and ecosystem conservation.

We refer to these tasks below when describing details of the visualization pipeline (page 125). Achieving each of these tasks requires the use of a wide range of data types, including the following:

1. ***Position and rotation:*** We calculated pitch, roll, heading, and three-dimensional position from inertial sensors on tags from Customized Animal Tracking Solutions (Queensland, Australia; cats.is), UFI tags (Morro Bay, California; ufiservingscience.com), Wildlife Computers' Daily Diaries, and Mk10 tags (Redmond, WA; wildlifecomputers.com). Then, we visualized the position and rotation of 3D models of elephant seals, narwhals, and humpback whales to demonstrate underwater behaviors such as cooperative feeding and predator evasion.
2. ***Reconstructing social behaviors from video tags:*** We analyzed video footage from animal-borne CATS tags to reconstruct the 3D position, rotation, and swimming behavior of other humpback whales relative to the tagged whale. In addition, we

used timepoints from the video data to link the onset and duration of animated mouth openings and demonstrate feeding synchronicity.

3. ***Large scale animal movements:*** We linked the GPS position of a dozen elephant seals on their annual foraging trips from Beltran et al. [4] to line animations using Adobe After Effects.
4. ***Swimming speed (stroke rate):*** We analyzed accelerometer data for fluke and flipper strokes using normalized peak detection algorithms and paired the stroke rate (in fluke or flipper beats per minute) of the tagged animal to the rigged 3D model. Stroking and gliding have physiological implications for the animal's energy expenditure and oxygen utilization, which we visualize and sonify with the sound of a tail moving through water.
5. ***Heart rate:*** We analyzed electrocardiogram recordings of narwhals and elephant seals to extract heart rate data using cyclical peak detection algorithms [58]. We present this data visually as well as auditorily by linking instantaneous heart rate to the sound of a beating heart.
6. ***Body condition:*** From examining diving behavior and specific segments of dives where animals drift passively through the water column, we can identify shifts in the animal's buoyancy due to its changing fat stores throughout its migration [9,18]. We linked these shifts to line animations.

We established an interdisciplinary team with experts in illustration, animation, data visualization, visual effects, computer science, science communication, and marine mammal biology. We united experts in different animal systems to develop the 4 animations described below. These animations were designed to accompany the publication of scientific articles, some of which are in preparation and others published. Each animation was created following a fourstage approach: conceptualization (storyboarding and scriptwriting), asset creation (creating custom models and illustrations), animation of behavior and physiology (pairing data to 3D and 2D assets),

and final production (annotations, narration, and music) (Figure 3.2). Excerpts from these animations are included in the supplementary video that accompanies this article.

Our four animations incorporate the data described above to address our key tasks:

1. **Animation 1: Humpback Alliance.** Our 3D humpback whale animation visualizes the position and orientation of a group of whales foraging on the ocean floor to determine whether there is coordination or competition between individuals of the group. Our animation emphasizes the importance of minimizing the use of bottom-set fishing gear that could disturb and entangle bottom-feeding humpbacks.
2. **Animation 2: Lightscapes of Fear.** Our 2D elephant seal animation demonstrates state-dependent risk aversion by showing the shifting decision-making by a seal as it travels across the North Pacific [3,4]. The animation visualizes the geographic location, body condition, and rest timing of elephant seals on their 7-month-long foraging trip. This animation shows that as an animal shifts from inferior to superior body condition (negative buoyancy to positive buoyancy), the seals begin to prioritize resting during the safer, darker, and earlier hours of the day.
3. **Animation 3: Sounds of Fear.** Our 3D elephant seal animation visualizes the position, orientation, swimming behavior, and heart rate of a seal as it dives under two conditions: with and without disturbance caused by the vocalization of a killer whale predator produced from an animal-borne acoustic tag. We pair the animal's heart rate and stroke rate data to sound. This animation demonstrates the fear response of an elephant seal in the wild and helps us understand how these animals respond to stress in their natural environment.
4. **Animation 4: Paradox of Fear.** Our 3D narwhal animation visualizes the position, orientation, swimming behavior, and heart rate of a narwhal after release from net entanglement in East Greenland. We pair heart rate and stroke rate data to sound. The animation demonstrates the paradoxical fear response of a narwhal, where a very low heart rate co-occurs with rapid stroking [58]. This animation demonstrates the impact of an acute disturbance on a wild narwhal and elucidates potential paradoxical physiological responses which could contribute to marine mammal strandings.

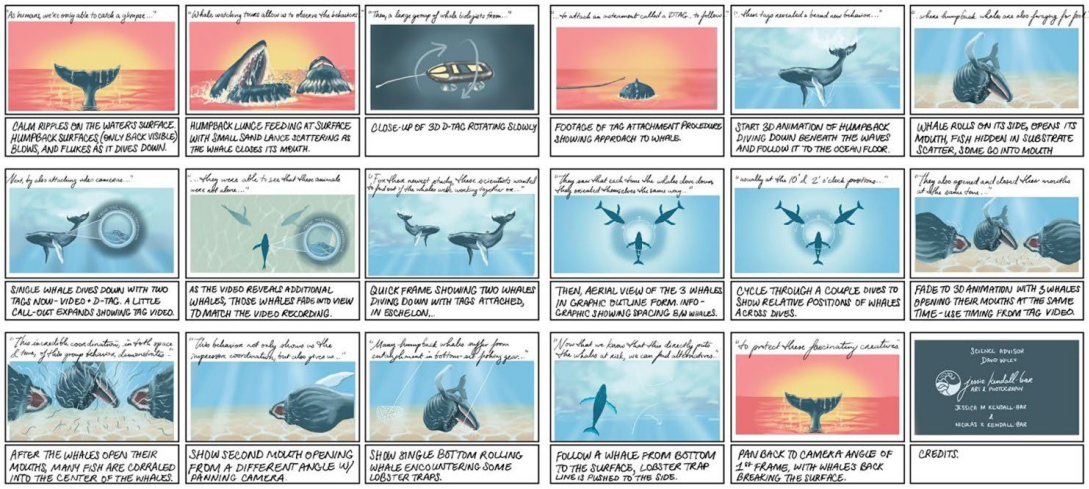

Figure 3.3. This figure shows an original illustrated storyboard for the Humpback Alliance animation. Shown here are 18 illustrations of the animation sequence, highlighting the action and camera angles for each shot. These storyboards were a valuable component of the creative pipeline, allowing us to begin discussing the necessary elements of the animations before devoting time to creating custom assets or data analysis tools.

3.3 VISUALIZATION PIPELINE

3.3.1 *Conceptualization*

A critical first step of each collaboration included an iterative process of storyboarding, data sharing, and scriptwriting. For each animation, we distilled the primary research findings, identified the target audience and the desired conservation or outreach outcome. For example, the storyboard shown in Figure 3.3 presents our vision for the *Humpback Alliance* animation. This storyboard helped us determine how to visualize social behaviors between humpbacks, especially the spatial orientation of the animals as they approach each other at the bottom of the ocean. In addition, this visual storyboard allowed us to identify critical data streams to integrate into the animation, such as the position and rotation of focal animals during feeding events, the

timing and duration of mouth openings, and the precise pectoral flipper movements used to regulate small adjustments in position. The conceptualization process also clarified our key message: the ocean floor presents an important foraging habitat for humpback whales and therefore, we must work to minimize the danger of whale entanglement from bottom-set fishing gear.

3.3.2 ***Asset Creation***

3.3.2a *References and existing assets*

When available, we assembled and incorporated existing assets either directly or as references for creating original assets, always ensuring explicit permission, proper attribution, and that we displayed relevant permit numbers. Helpful assets for this suite of animations included drone videos, reference photos, underwater videos, technical illustrations, biological illustrations, and photogrammetry models (including textures). For example, a detailed technical illustration by Alex Boersma of the CATS tag served as the basis of our 3D tag reconstruction [16]. Our 2D elephant seal animation incorporates illustrations by UC Santa Cruz undergraduate Danielle Dube who partnered with elephant seal biologists through the Art-Science residency at the Norris Center for Natural History.

3.3.2b *Creating customized 3D models*

We customized all our rigged 3D models to ensure that we could map behaviors of interest to these assets (Figure 3.4). We purchased and modified an existing rigged model for our humpback whale animation [33]. We added additional flipper joints and controls to enable fine-scale flipper maneuvers that allow the whales to navigate close quarters at the bottom of the ocean during cooperative feeding. We also created controls for opening the model's mouth to emulate realistic foraging behavior (up to 60-80 degrees). Finally, we created four separate controls to depict the expansion of ventral grooves during engulfment, which allowed flexible alteration of the forward, side, and back of the whale's buccal cavity. Our elephant seal model was similarly customized based on existing assets to augment anatomical accuracy [8]. We modified the mesh and dimensions of another rigged seal model to match those of juvenile elephant seals measured and photographed in the field. We painted a custom 3D texture using Substance Painter. Our 3D narwhal animation modifies an existing anatomical model to depict and emphasize physiological processes [10].

Figure 3.4. Custom assets for Humpback Alliance animation. We created (A, B & D) schooling Atlantic sand lance, (B) a buoyless lobster trap, (C) a 3D model of a CATS tag (used to collect the data analyzed), and (B & D) customized a rigged humpback whale to allow ventral groove expansion and flexible fin mobility.

In addition to creating 3D models of focal animals, we created unique or custom supplementary models that were critical to the narrative of our humpback whale animation. We created a 3D model based on technical drawings of CATS tags to describe the biologging technology and integrated sensors. We modified the buoy configuration of an existing lobster trap model and added a custom modeled rope to demonstrate the functionality of novel, buoyless fishing technology.

We created a school of 200 prey items, Atlantic sand lance, for the whales to feed on. We created a 3D mesh, custom texture, and rigged skeleton with 8 joints and 5 controllers to create a swim cycle for a single fish. Then, we rigged the single fish to a MASH flight network in Autodesk Maya, which creates a simulation of schooling or flocking patterns for dozens of individual nodes in three dimensions around an attractor. In our case, we generated an initial search path emanating from a central point below the sand's surface (where these bottom-dwelling fish reside) and customized their motion around an attractor path before disappearing into the sand again. We added the whales as collision nodes for scenes with humpback predators to create avoidance behaviors by schooling fish.

3.3.2c *Creating the ocean's surface and underwater lighting*

We created a photorealistic underwater environment for each of our 3D animations to depict the animal's natural environment and its turbidity, darkness, and depth (Figure 3.5). We generated surface waves with the Boss Spectral Wave Solver, a fluid simulation engine in Maya, with wind speed, wind fetch, water depth, and wave height parameters matching those in the open ocean. We rendered a single high-resolution ocean tile using these parameters and cached these results into a 120-frame animated sequence of wave motion. We then replicated this pattern for a larger ocean surface plane extending to the horizon. We imported the cached image sequence into

the displacement node of an Arnold surface shader with high specularity and transmission.

We placed our scene within an Arnold atmosphere volume with scattering and absorption coefficients matching those of water, where peak absorption fell within low wavelength red-orange hues. We used three-point lighting with a high-intensity key spotlight focused on the animal from the perspective of the camera, a low-intensity wide-angle overhead sunlight, and a spotlight for the dappled underwater caustics. To create dynamic underwater lighting ("caustics"), we generated an animated loop of fractal noise in Adobe After Effects that we used as a gobo filter over an Arnold spotlight.

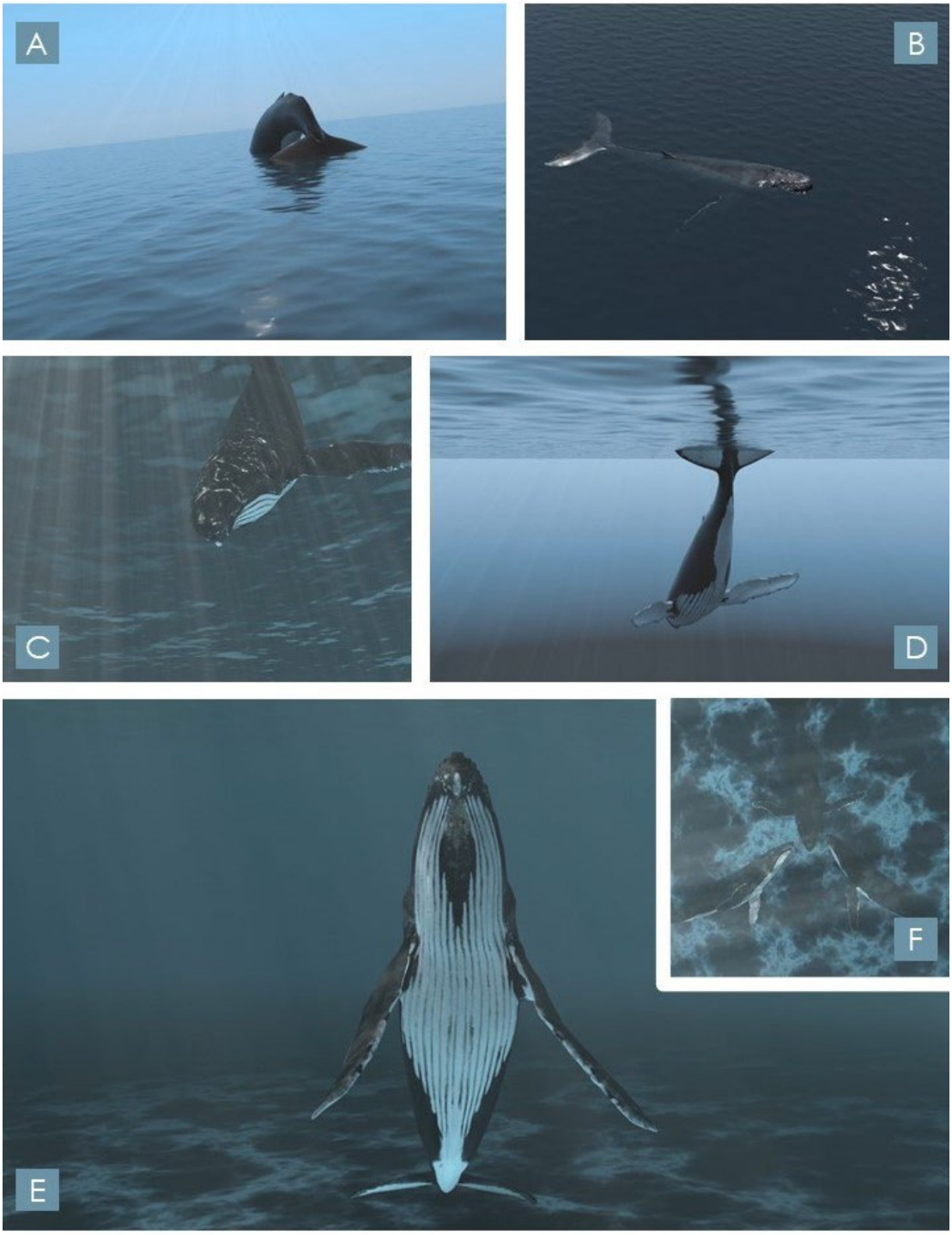
A
B
C
D
E
F

Figure 3.5. Underwater environment. Rendered results of our four-source lighting scheme (A & B) above water, (C & D) just below the surface, and (E & F) on the ocean floor (40m).

3.3.3 *Linking behavior to animation*

3.3.3a *Animating dive behavior*

We processed raw accelerometer data from inertial sensors on CATS tags, Wildlife Computers' Daily Diaries, and Mk10 tags to obtain the position (x, y, and depth) and rotation (pitch, roll, heading) of tagged animals. We used the following equations to estimate pitch (p) and roll (ˆ ˆr) from accelerometer data $A = [a_x\, a_y\, a_z]$ and then applied these and the magnetometer data to derive an estimate of heading (h) based on a gimbaled magnetometer in the horizontalˆ reference frame of the animal $M^h = [m_x\, m_y\, m_z]$ [23]:

$$p\hat{} = -asin(a_x/A)\ r\hat{} = atan(ay/az)$$

$$h\hat{} = atan(-m^h{}_y/m^h{}_x)$$

When possible given the collected data, we aligned tag axes with animal axes and made other corrections to improve estimation accuracy. In order to precisely calculate and incorporate three-dimensional position in the water column, it is necessary to estimate the animal's speed. For high-speed behaviors (>1ms^{-1}), estimates of speed can be performed based on the vibration of the tag, but these methods lose accuracy at lower speeds [7]. Therefore, our *Humpback Alliance* animation included three-dimensional rotation and position until the onset of low-speed benthic foraging events where we excluded shifts in horizontal position (Figure 3.6).

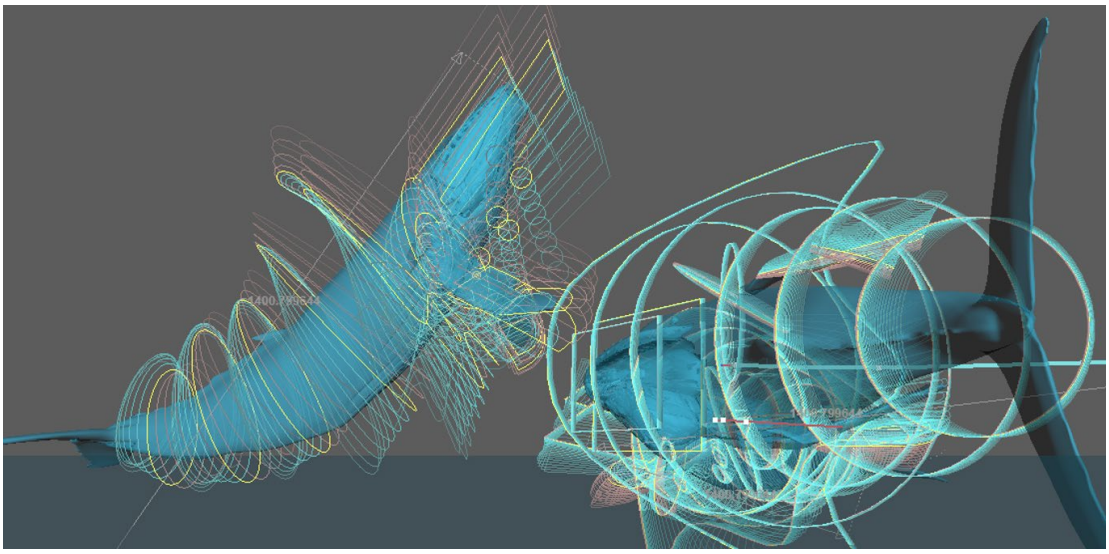

Figure 3.6. Integrating position and rotation data for 3D behavior of humpback whales. This image demonstrates the analytical advantages of loading and displaying data in Maya, where it is possible to enable motion paths for individual animals and enable ghosting to visualize and compare the speed and movement of animals over time.

Our elephant seal and narwhal animations (Animations 2, 3, and 4) visualize dive behavior on a single plane to simplify visualization of deep dives. We included measures of pitch and roll to demonstrate body position, translated the animal's vertical position with respect to depth, and approximated a speed of $1ms^{-1}$ for visualization. Data collected at high frequencies occasionally included artifacts that were smoothed using the "simplify curves" tool in Maya. Animation keyframes for position and rotation were set using a custom Python script and the .setKey() function in Maya's PyMEL core. Note that the default axis configuration in Maya is different from the default conventions for accelerometer data, with the z- and y- axes switched. Code, tutorials, and sample data are available on our GitHub code repository [27] and project webpage [24].

3.3.3b *Animating migratory behavior*

To reconstruct the migratory tracks of elephant seals for our *Lightscapes of Fear* elephant seal animation, we visualized animal position in two dimensions using time-referenced latitude and longitude positions from Wildlife Computers Spot and Mk10 tags [4]. We selected a subset of 12 seals that represented the vast geographic distance covered by these deep-diving marine mammals across the Northeast Pacific ocean [4]. We used a custom program in MATLAB to create Google Earth .kml files from matrices of time, latitude, and longitude [41]. We then assembled these .kml files and ingested them into the interactive Google "My Maps" app to display metadata, including animal age, total dives, number of drift dives, and trip duration [3]. We then converted this data into a scalable vector graphic (SVG) and animated the tracks using Adobe After Effects.

3.3.3c *Animating swimming behavior*

For our narwhal and elephant seal 3D animations, we created a method in which raw accelerometer data can be used to drive the animation of organic swim cycles, alternating between periods of swimming and gliding. We analyzed raw accelerometer data to obtain instantaneous flipper/fluke stroke rate. Beat detection for flipper and fluke strokes was performed in LabChart (ADInstruments™) with a sine-wave cyclic measurement using custom parameters for narwhals and elephant seals. For elephant seals, we analyzed the y-axis accelerometer data that captures the majority of back-and-forth swimming with the hind flippers. We chose 500-millisecond smoothing with a median window of 3 samples, high pass filtering at 0.3Hz, a detection threshold of

maxima above 0.5G, and excluded stroke cycles faster than 900ms. For narwhals, we analyzed z-axis accelerometry to reflect up-and-down fluke stroking. This allowed us to calculate instantaneous stroke rate as well as identify the onset of each stroke cycle.

We produced additional data streams to be used as inputs for the glide and stroke controllers. The glide controller was based on instantaneous stroke rate that maps stroke rates below 15 bpm to 1 (gliding) and above 15 bpm to 0 (stroking), with a triangular smoothing window of 15 seconds.

We animated a single swim cycle with each animal model (Figure 3.7).

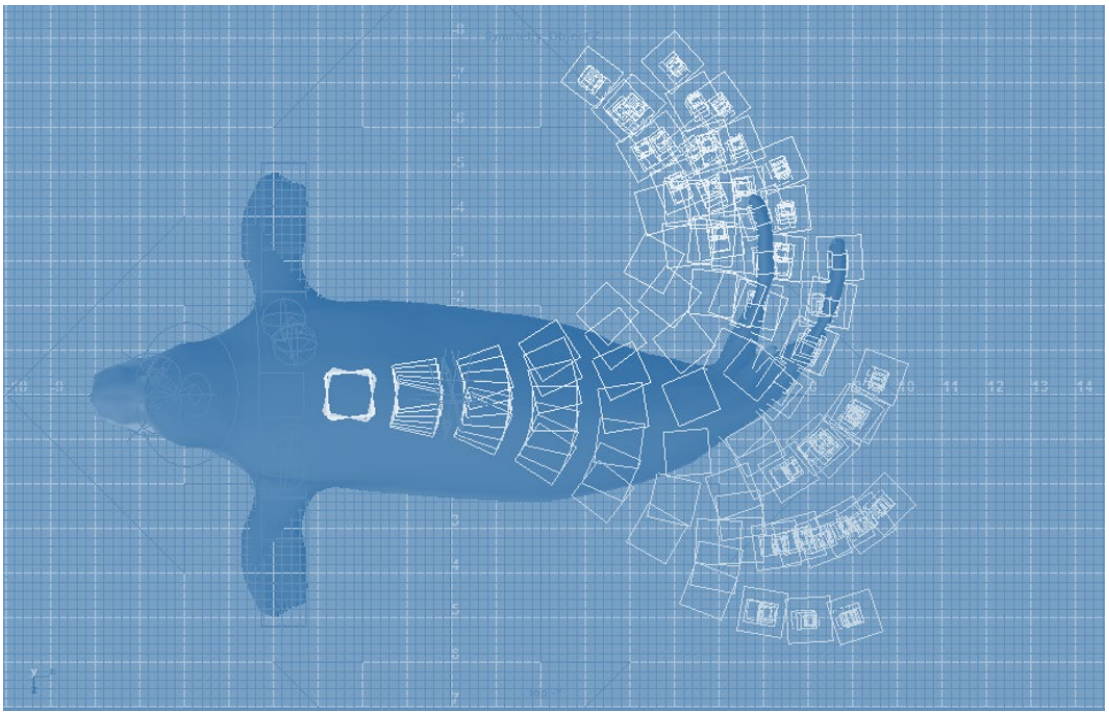

Figure 3.7. Elephant seal swim cycle. Snapshot of a frame from the offset swim cycle of a northern elephant seal with ghosting enabled to demonstrate future tail positions in pink and past tail positions in blue. This snapshot shows a central tail location to demonstrate that, with

an organic swimming animation, the central tail position includes posterior tail rotation which must be eliminated to bring the animal into a straight gliding position.

We offset the keyframes of successive joints to produce organic swimming movements from head to tail. Since this offset causes the tail to be curved when placed between right and left positions, we created two separate controllers: a swim controller and a glide controller. The swim controller controlled the back-and-forth movement of the tail, while the glide controller pulled the tail into a central gliding position.

We wrote a custom Python function in Maya that links the rotation of all joints in the skeleton to a set of expressions. The expressions set the animal's pose to a blended and interpolated output of both swim and glide controllers. A value of 0 for the swim controller sets the tail position to the first frame of the swim cycle (tail right) and 1 to the last frame of the swim cycle (return to tail right). A value of 0 for the glide controller does not inhibit the motion of the tail, while a value of 1 suppresses all tail rotation, bringing the tail to a central gliding position. After linking the rig's controls to the swim and glide controllers via these expressions, we set keyframes for the controllers based on the data (Figure 3.8).

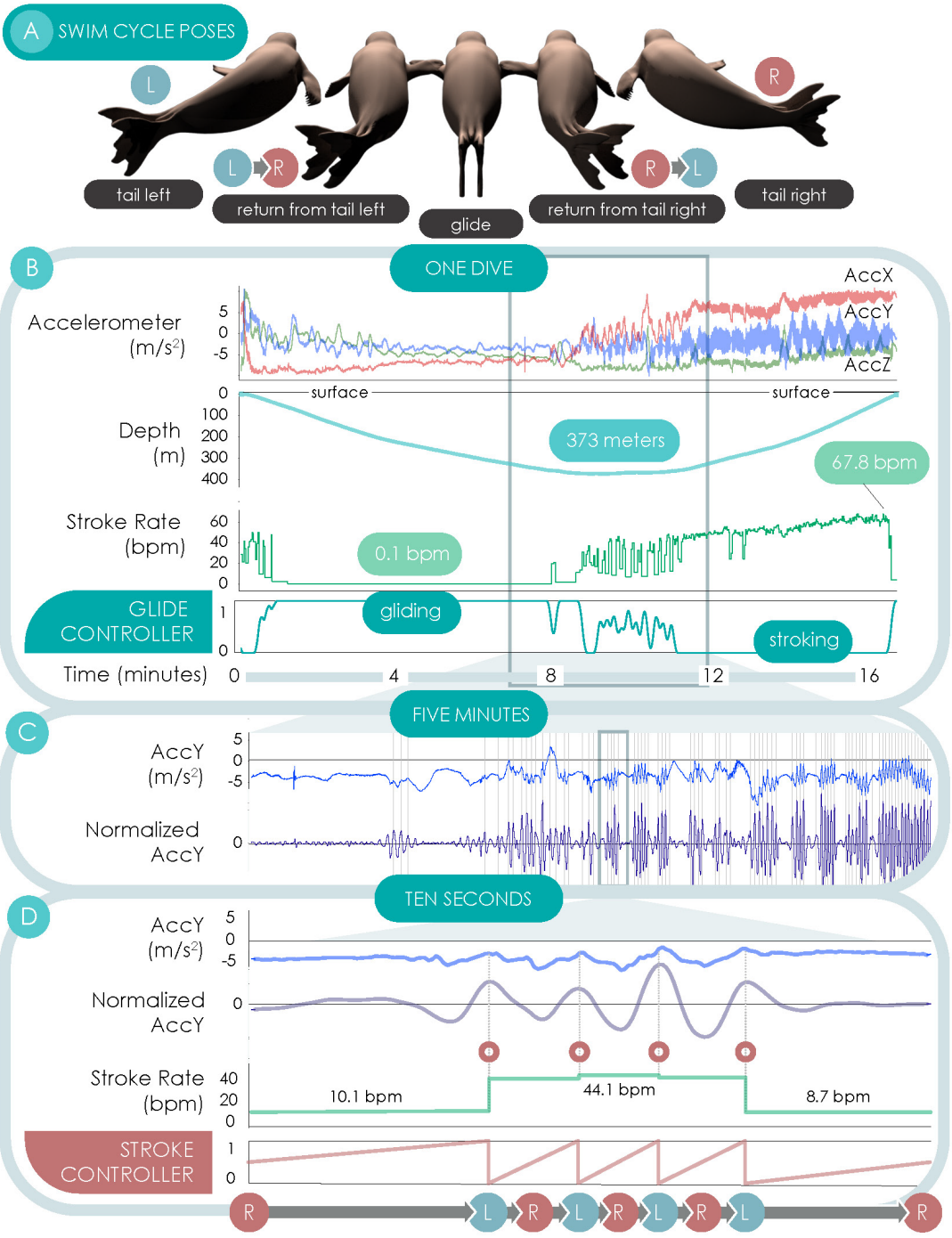
A SWIM CYCLE POSES
L
R
tail left
L R
return from tail left
glide
R L
return from tail right
tail right
B
ONE DIVE
Accelerometer (m/s²)
5
0
-5
AccX
AccY
AccZ
Depth (m)
0
100
200
300
400
surface
surface
373 meters
67.8 bpm
Stroke Rate (bpm)
60
40
20
0
0.1 bpm
GLIDE CONTROLLER
1
0
gliding
stroking
Time (minutes)
0
4
8
12
16
C
FIVE MINUTES
AccY (m/s²)
5
0
-5
Normalized AccY
0
D
TEN SECONDS
AccY (m/s²)
5
0
-5
Normalized AccY
0
Stroke Rate (bpm)
40
20
0
10.1 bpm
44.1 bpm
8.7 bpm
STROKE CONTROLLER
1
0
R L R L R L R L R

Figure 3.8. Stroke rate data processing pipeline. Raw and processed swimming data for (A) one dive, (B) five minutes, and (C) ten seconds showing raw depth (m) and accelerometer data (g), smoothed and normalized y-axis accelerometer data (g; arbitrary scale), the results of our cyclic measurement peak detection (stroke rate [bpm]), and two generated metrics - the glide and stroke controllers (values 0 to 1) - that drive our animation.

3.3.4 *Linking physiology to animation*

3.3.4a *Sonifying the marine mammal heart*

The electrocardiogram (ECG) was recorded at 100 Hz using custom physiological loggers (UFI Instruments) for both elephant seals and narwhals. Exported data was processed for heartbeat detection in LabChart (narwhal data) and using custom MATLAB processing scripts (elephant seal data). QRS-detections were validated and confirmed using visual inspection and then converted to instantaneous heart rate for visualization. QRS-detection events were exported as a series of timestamps to be used for sonification. From these events, we calculated the interbeat interval to be used as a millisecond precision delay between heartbeat sounds. Extreme bradycardia of 2.9106 beats per minute was identified for narwhals after escaping from entanglement [58] (see Figure 3.9).

When sonifying large shifts from bradycardia below 3 beats per minute to surfacing heart rates over 60 beats per minute, it is insufficient to warp the playback speed of a sound file with multiple heartbeats at a set heart rate. Instead, we linked the onset of each heartbeat to the onset of a sound file with millisecond precision to present accurate and extreme shifts in heart rate. We took advantage of the high-temporal-precision neurophysiology toolbox PsychoPy to present these sounds [37]. Our script

plays a sound file and then waits for the exact duration of the interbeat interval before playing the subsequent heartbeat. We recorded these generated heartbeat sounds and then linked them to the animations of swimming and diving behavior (Figure 3.9).

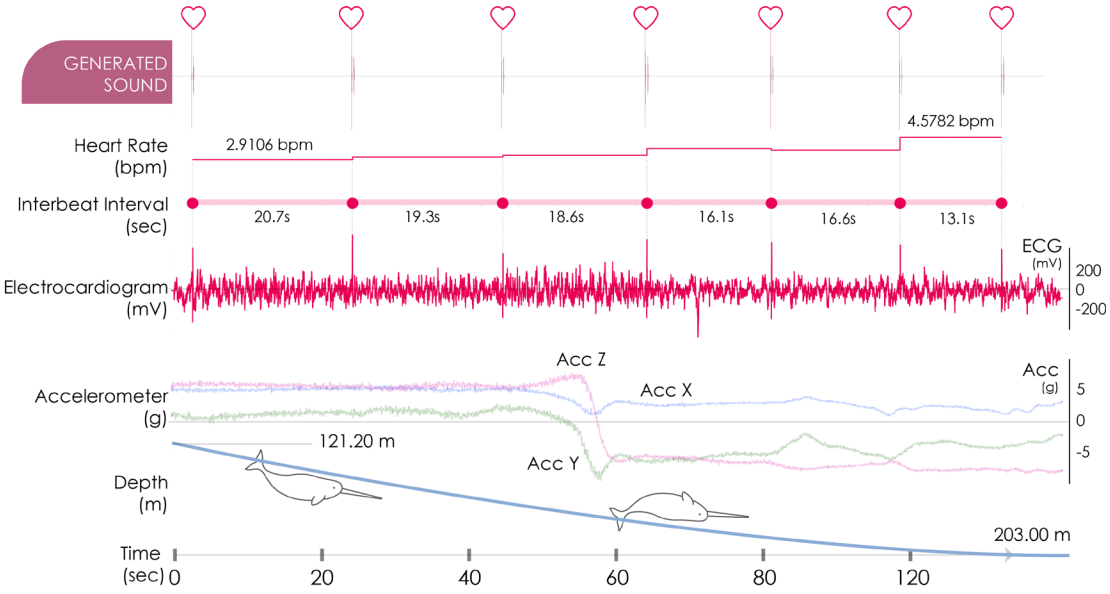

Figure 3.9. Linking physiology to sound. Raw tagging data (3-axis accelerometer [G-forces (g)], depth [meters (m)], and electrocardiogram [millivolts (mV)]) with peak detection analysis (heart rate [beats per minute (bpm)] and inter-beat interval [seconds (s)]), and resulting generated heartbeat waveform (arbitrary units). The animal demonstrates a very low bradycardia after release from net entanglement. Given the long duration between beats, this example demonstrates the utility of triggering heartbeat sounds at specific time points as opposed to warping the speed of existing human heart rate soundtracks.

3.3.5 *Editing and final production*

3.3.5a *Animating data streams and visualizing signals in 2D with line animations*

We visualized physiological data streams such as body condition and instantaneous heart rate as well as behavioral data streams such as GPS position, pitch, roll, heading, and depth using 2D line animations. Depending on the density of data

points and the desired flexibility of the animation, we either linked CSV data directly to the paths via a custom expression in Adobe After Effects (see GitHub and tutorials) or used a static vector graphic of a line chart [24,27]. In both cases, we generated trim paths along the path created by the data and tapered the stroke width to display the changes in data over time (Figure 3.10).

3.3.5b *Annotations, narration, and music*

We provided the context of each animation in the form of chart labels, narration, annotations, and captions. These narrations ensured that each graph is interpreted rapidly and properly. We believe that these verbal descriptions and context clues are essential to understand the science as well as the intended message of each animation. In addition to verbal descriptions, we worked with the musical composer Connor Vance to create musical scores to accompany and underscore the narrative arc of each animation. Musical instruments were selected to match the relative size of animals and frequency of motion. For example, lower register cellos were selected to portray slow movements of large whales and the vast ocean environment, while an ensemble of violins and swelling string glissandos accompanied the turbulence of a smaller elephant seal's tail moving through water. The musical accompaniment focused attention on certain movements, created a narrative arc, enhanced production quality, and fostered empathy between the audience and the animal protagonists.

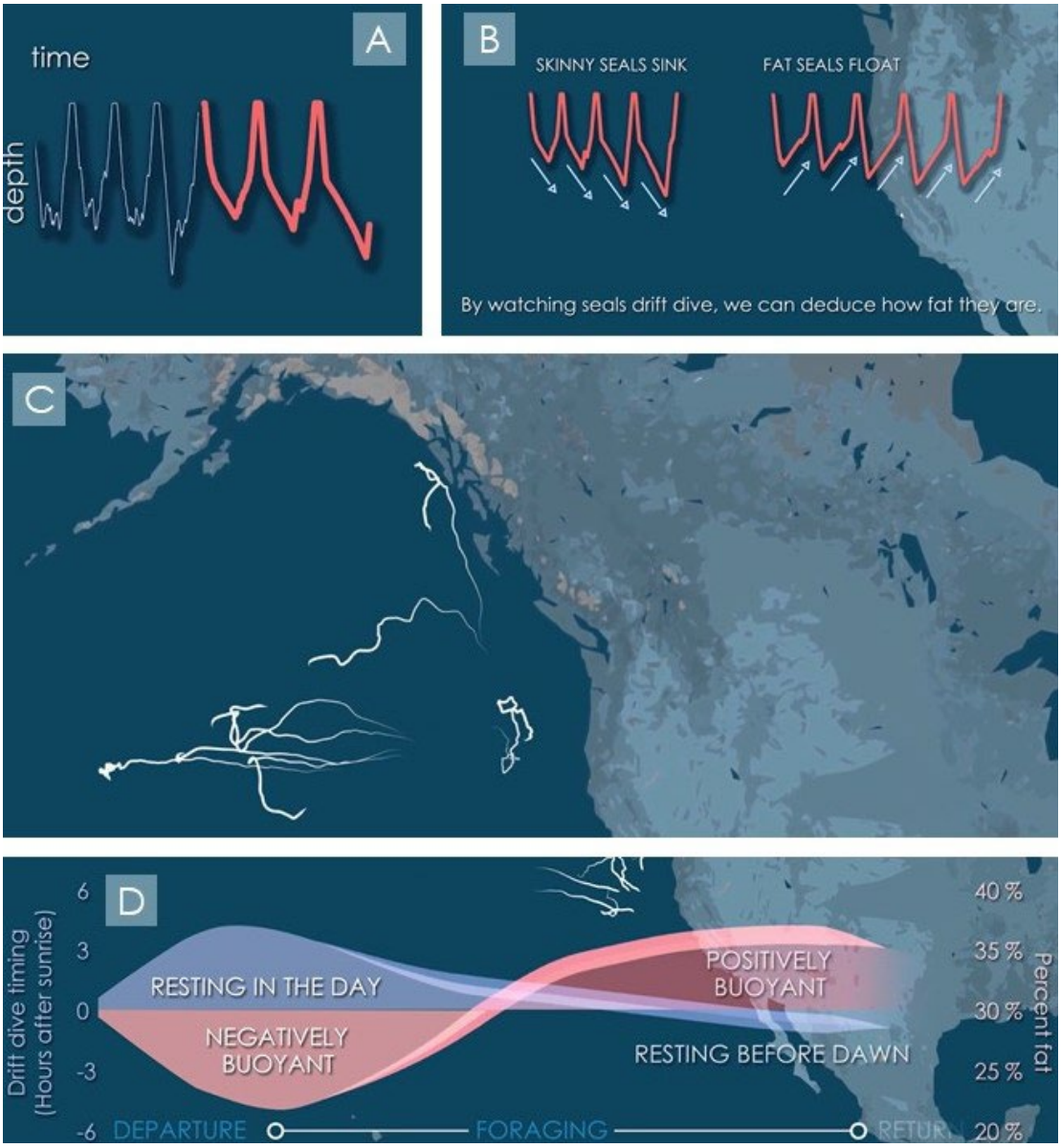

Figure 3.10. Three techniques for line animation with data in Adobe After Effects. (A & B) Flexible line animations of diving behavior generated using a custom expression in Adobe After Effects. This script links the control points of paths on the canvas to values from a CSV containing down sampled diving data. (C) Line animations demonstrating the migratory paths of female northern elephant seals across the Pacific generated using KML data from geolocation tags. (D) Tapered line animations with shaded areas based on a figure generated in R and assembled in

Adobe Illustrator, showing a shift in predator avoidance behavior associated with internal body condition [3,4,26].

3.4 DISCUSSION & OUTCOMES

Our animations addressed the four tasks outlined in Sect. 2 by establishing a creative pipeline for high-impact animations that reach a target audience to promote desired outcomes in education and conservation (Figure 3.2). By visualizing the invisible underwater behavior of marine mammals, we aim to create evocative animations which foster connection, empathy, and compassion between humans and the natural world. Our 3D humpback animation illustrates the risk-reduction benefit of ropeless fishing gear to humpback whales cooperatively foraging on the ocean floor. Our 2D elephant seal animation follows a cohort of seals halfway across the Pacific as they weigh risk and reward based on their rapidly changing internal and external environments [4]. Our 3D elephant seal animation shows diving behavior and physiology to better understand their fear response to natural killer whale predators. Our 3D narwhal animation tells the story of its human-caused paradoxical fear response, which involves a pronounced decrease in heart rate during escape, to help us recognize our role and impact on marine mammals.

Our goals with this framework were to incorporate raw tagging data to control animations that facilitate research as well as clearly communicate scientific results to maximize their reach and impact. As a tool for research and data exploration, our team worked closely with biologists to generate hypotheses about the synergistic effects of disturbance on physiology and behavior. Our tool serves to unite disparate data

streams across space and time, from shifts in heart rate and orientation which occur within seconds and across individual dives to large scale movements during seven-month foraging trips. Our animations consolidate data across space, time, physiology, and behavior to facilitate the identification and characterization of responses critical to survival. While we explore marine mammal animal-borne sensors in the present study, our pipeline can be broadly applied for other animal systems in studies of functional anatomy, ecophysiology, and movement ecology.

In our capacity as communicators, these animations targeted three key audiences: scientists in the fields of biologging, ecology, biology, and physics, the general public, and policymakers who can translate this research into legislative protections. Our *Lightscapes of Fear* animation, which accompanied the publication of a scientific article, reached these three key audiences and increased the paper's accessibility, reach, and visibility. Our tweet sharing the animation alongside the paper received over 100,000 views, with more than half of the comments specifically citing the animation. The article received a high attention score, scoring in the top 5% of all research outputs scored by Altmetric, with 311 tweet mentions and over 490,000 followers. In our process posts of other animations, we have had engagement from veterinarians as well as activists and policymakers. These metrics demonstrate that short, cinematic, and informative animations can increase the accessibility of scientific results and promote the conservation of marine mammals.

Beyond creating tools for data visualization, it is important to facilitate the implementation of new tools. We taught a wide range of animation skills to over a hundred scientists through a series of "Animation for Science Communication" workshops and created an online learning center with workshop recordings [24]. These workshops included specialized and advanced topics such as 3D-track visualization and custom scripting in Maya and Adobe After Effects and covered powerful built-in animation tools in PowerPoint. We continued this educational outreach through a data visualization collective in Winter 2021 that united students from various academic departments, including Astronomy & Astrophysics, Art: Games & Playable Media, Ecology & Evolutionary Biology, and Computational Media to create animations and data visualizations for science communication [25]. We have facilitated several animations inspired by our workshops by providing technical, design, and narrative advice [19,38,49]. Our GitHub repository and webpage offer in-depth tutorials for working with our custom scripts [24, 27]. Through educational outreach, we are creating forums for scientists to seek guidance on designing and sharing compelling stories with their data. We argue that by equipping biologists to leverage industry animation tools, we can expedite complex data analysis, promote science communication outcomes, foster empathy and compassion for the natural world, and better serve the ecosystems we aim to protect.

3.5 **ACKNOWLEDGMENTS**

The authors wish to thank the numerous field researchers involved in collecting and analyzing this data. This work was supported in part by the National Marine Sanctuary Foundation, the Volgenau Foundation, the Office of Naval Research (Grants #N00014-13-10808 and #N00014-17-1-2737 to T.M.W.), and the National Science Foundation (Grant #1656283).

3.6 AUTHOR CONTRIBUTIONS

J.K.B. (candidate): conceptualization, funding acquisition, methodology, validation, visualization, project administration, software, data curation, formal analysis, resources, investigation, writing- original draft, writing- review and editing. N.K.B.: methodology, writing- review and editing. A.G.F.: conceptualization, writing- review and editing. G.M., P.J.P., C.W., M.H., A.H., H.K., R.S.B., A.S.F., D.W.: data collection, writing- review and editing. T.M.W. & D.P.C.: funding acquisition, project supervision, writing- review and editing. All authors read and approved the final manuscript and approved its use in the dissertation.

3.7 REFERENCES

1. S. K. Adamczak, A. Pabst, W. A. McLellan, and L. H. Thorne. Using 3d models to improve estimates of marine mammal size and external morphology. *Frontiers in Marine Science*, 6:334–1–12, 2019.
2. Y. Akiyama, T. Akamatsu, M. H. Rasmussen, M. R. Iversen, T. Iwata, Y. Goto, K. Aoki, and K. Sato. Leave or stay? Video-logger revealed foraging efficiency of humpback whales under temporal change in prey density. *PLOS ONE*, 14(2):e0211138, 2019.

3. R. S. Beltran and J. M. Kendall-Bar. Risk versus reward on the high seas- Skinny elephant seals trade safety for sustenance. *The Conversation*, 2021. https://tinyurl.com/y5msn73z, [Online; accessed 202105-17].

4. R. S. Beltran, J. M. Kendall-Bar, E. Pirotta, T. Adachi, Y. Naito, Takahashi, J. Cremers, P. W. Robinson, D. E. Crocker, and D. P. Costa. Lightscapes of fear: How mesopredators balance starvation and predation in the open ocean. *Science Advances*, 7(12):eabd9818, 2021.

5. M. A. Bolstad. Large-scale cinematic visualization using universal scene description. In *Proc. Symposium on Large Data Analysis and Visualization (LDAV)*, pp. 1–2, 2019.

6. K. Borkiewicz, A. Christensen, H.-N. Kostis, G. Shirah, and R. Wyatt. Cinematic scientific visualization: The art of communicating science. In *ACM SIGGRAPH Courses*, pp. 1–273. 2019.

7. D. Cade, A. Friedlaender, J. Calambokidis, and J. Goldbogen. Kinematic diversity in rorqual whale feeding mechanisms. *Current Biology*, 26(19):2617–2624, 2016.

8. CharacterArtDirector. 3d seal, 2012. https://www.turbosquid. com/3d-models/maya-sea/655525, [Online; accessed 2021-05-17].

9. D. E. Crocker, B. J. L. Boeuf, and D. P. Costa. Drift diving in female northern elephant seals: implications for food processing. *Canadian Journal of Zoology*, 75(1):27–39, 2008.

10. M. S. Earle. See-through narwhal, 2019. https://sketchfab.com/ models/f4432157c6fc4cffa04b25c525e86728, [Online; accessed 2021-05-25].

11. M. M. S. Education. 3d skeleton of a harbour seal (phoca vitulina), 2018. https://www.youtube.com/watch?v=aUCQ_9odsbc&t=1s, [Online; accessed 2021-05-17].

12. Facts in Motion. 5 amazing facts you didn't know about sperm whales, 2017. https://www.youtube.com/watch?v=CJBw5RrFggw, [Online; accessed 2021-05-17].

13. M. A. Fedak, P. Lovell, and B. J. Mcconnell. Mamvis: A marine mammal behaviour visualization system. *The Journal of Visualization and Computer Animation*, 7(3):141–147, 1996.

14. A. G. Forbes. Articulating media arts activities in art-science contexts. *Leonardo*, 48(4):330–337, 2015.

15. A. G. Forbes, T. Hollerer, and G. Legrady. Behaviorism: A framework¨ for dynamic data visualization. *IEEE Transactions on Visualization and Computer Graphics*, 16(6):1164–1171, 2010.

16. J. Goldbogen, D. Cade, A. Boersma, J. Calambokidis, S. KahaneRapport, P. Segre, A. Stimpert, and A. Friedlaender. Using digital tags with integrated video and inertial sensors to study moving morphology and associated function in large aquatic vertebrates. *The Anatomical Record*, 300(11):1935–1941, 2017.

17. J. Goldbogen, J. Calambokidis, D. Croll, J. Harvey, K. M. Newton, E. Oleson, G. Schorr, and R. Shadwick. Foraging behavior of humpback whales: Kinematic and respiratory patterns suggest a high cost for a lunge. *Journal of Experimental Biology*, 211(23):3712–3719, 2008.

18. S. A. Gordine, M. Fedak, and L. Boehme. Fishing for drifts: Detecting buoyancy changes of a top marine predator using a step-wise filtering method. *Journal of Experimental Biology*, 218(23):3816–3824, 2015.

19. L. Gullikson. Drought alterations of invertebrate communities in headwater streams, 2021. https://www.youtube.com/watch?v=DX_ rFi2eojY&t=2s, [Online; accessed 2021-05-24].

20. A. Hill, C. Churchouse, and M. F. Schober. Seeking new ways to visually represent uncertainty in data: What we can learn from the fine arts. In *Proc. IEEE VIS Arts Program (VISAP)*, pp. 1–8, 2018.

21. D. J. Irschick, J. Martin, U. Siebert, J. H. Kristensen, P. T. Madsen, and F. Christiansen. Creation of accurate 3d models of harbor porpoises (Phocoena phocoena) using 3d photogrammetry. *Marine Mammal Science*, 37(2):482–491, 2021.

22. T. Jeanniard-du Dot, A. W. Trites, J. P. Y. Arnould, J. R. Speakman, and C. Guinet. Flipper strokes can predict energy expenditure and locomotion costs in free-ranging northern and Antarctic fur seals. *Scientific Reports*, 6(1):33912, 2016.

23. M. Johnson. Measuring the orientation and movement of marine animals using inertial and magnetic sensors - a tutorial. *Fine-scale animal movement workshop*, p. 22, 2011.

24. J. Kendall-Bar. Art for science communication, 2020. https://www.jessiekb.com/artforscicomm, [Online; accessed 2021-05-18].

25. J. Kendall-Bar. Data visualization collective, 2021. https://www. jessiekb.com/data-visualization-collective, [Online; accessed 2021-05-18].

26. J. Kendall-Bar. Skinny seals sacrifice safety for sustenance, 2021. https://www.youtube.com/watch?v=x3ugpT1ej0M, [Online; accessed 2021-05-18].

27. J. Kendall-Bar. *Visualizing Life in the Deep: Code repository for visualizing marine mammal tag data*. 2021. https://github.com/jmkendallbar/VisualizingLifeintheDeep, [Online; accessed 2021-06-01].

28. M. Lang. The snail and the whale, 2019. https://www.imdb.com/title/tt9303756/, [Online; accessed 2021-05-17].

29. J. Liem, C. Perin, and J. Wood. Structure and empathy in visual data storytelling: Evaluating their influence on attitude. *Computer Graphics Forum*, 39(3):277–289, 2020.

30. J. L. Maresh, T. Adachi, A. Takahashi, Y. Naito, D. E. Crocker, M. Horning, T. M. Williams, and D. P. Costa. Summing the strokes: Energy economy in northern elephant seals during large-scale foraging migrations. *Movement Ecology*, 3(1):1–16, 2015.

31. D. W. McClune. Joining the dots: Reconstructing 3d environments and movement paths using animal-borne devices. *Animal Biotelemetry*, 6(1):5, 2018.

32. B. I. McDonald and P. J. Ponganis. Deep-diving sea lions exhibit extreme bradycardia in long-duration dives. *Journal of Experimental Biology*, 217(9):1525–1534, 2014.

33. MotionCow. 3d humpback whale model, 2011. [Online; accessed 2021-05-17].

34. M. Nava. ABZU, 2016.ˆ https://abzugame.com, [Online; accessed 2021-05-17].

35. G. Oliver. Visualizing the tracking and diving behavior of marine mammals: A case study. In *Proc. IEEE Visualization*, pp. 397–399, 1995.

36. Oregon State University eCampus. Sperm whale dive, 3d simulation, 2015. https://www.youtube.com/watch?v=CJP8jC1SikQ, [Online; accessed 2021-05-17].

37. J. Peirce, J. R. Gray, S. Simpson, M. MacAskill, R. Hochenberger,¨ H. Sogo, E. Kastman, and J. K. Lindeløv. Psychopy2: Experiments in behavior made easy. *Behavior Research Methods*, 51(1):195–203, 2019.

38. M. Penland. Collateral damage: Bycatch in tuna fisheries, 2021. https://meganuwu.github.io/Shark-bycatch-project. github.io/, [Online; accessed 2021-05-24].

39. E. Pirotta, C. G. Booth, D. P. Costa, E. Fleishman, S. D. Kraus, D. Lusseau, D. Moretti, L. F. New, R. S. Schick, L. K. Schwarz, S. E. Simmons, L. Thomas, P. L. Tyack, M. J. Weise, R. S. Wells, and J. Harwood. Understanding the population consequences of disturbance. *Ecology and Evolution*, 8(19):9934–9946, 2018.

40. N. H. Riche, C. Hurter, N. Diakopoulos, and S. Carpendale. *Datadriven storytelling*. CRC Press, 2018.

41. P. Robinson. Time-latitude-longitude to KML, 2021. https://www.mathworks.com/matlabcentral/fileexchange/ 37406-time-latitude-longitude-to-kml, [Online; accessed 2021-05-20].

42. F. Samsel. Art-science-visualization collaborations: Examining the spectrum. *Proc. IEEE VIS Arts Program (VISAP)*, 2013.

43. F. Samsel, L. Bartram, and A. Bares. Art, affect and color: Creating engaging expressive scientific visualization. In *Proc. IEEE VIS Arts Program (VISAP)*, pp. 1–9, 2018.

44. V. Schmidt, T. C. Weber, D. N. Wiley, and M. P. Johnson. Underwater tracking of humpback whales (megaptera novaeangliae) with high-frequency pingers and acoustic recording tags. *IEEE Journal of Oceanic Engineering*, 35(4):821–836, 2010.

45. L. K. Schwarz, S. Villegas-Amtmann, R. S. Beltran, D. P. Costa, C. Goetsch, L. Huckst¨ adt, J. L. Maresh, and S. H. Peterson. Compar-¨ isons and uncertainty in fat and adipose tissue estimation techniques: The northern elephant seal as a case study. *PLOS ONE*, 10(6):e0131877, 2015.

46. E. Segel and J. Heer. Narrative visualization: Telling stories with data. *IEEE transactions on visualization and computer graphics*, 16(6):1139– 1148, 2010.

47. M. Sener, S. Levy, J. E. Stone, A. J. Christensen, B. Isralewitz, R. Patterson, K. Borkiewicz, J. Carpenter, C. N. Hunter, Z. Luthey-Schulten, et al. Multiscale modeling and cinematic visualization of photosynthetic energy conversion processes from electronic to cell scales. *Parallel Computing*, 102:102698, 2021.

48. B. Steinheider and G. Legrady. Interdisciplinary collaboration in digital media arts: A psychological perspective on the production process. *Leonardo*, 37(4):315–321, 2004.

49. N. Taylor. Communicating ocean research effectively promotional video, 2021. https:// youtube.com/watch?v=LI4pcamUvg0, [Online; accessed 2021-05-24].

50. P. Tyack. Acoustic playback experiments to study behavioral responses of free-ranging marine animals to anthropogenic sound. *Marine Ecology Progress Series*, 395(1938):187–200, 2009.

51. V. Vesna. Toward a third culture: Being in between. *Leonardo*, 34(2):121–125, 2001.

52. K. von Ompteda. Data manifestation: Merging the human world & global climate change. In *Proc. IEEE VIS Arts Program (VISAP)*, pp. 1–8, 2019.

53. J. N. Waite, W. J. Schrader, J.-A. E. Mellish, and M. Horning. Threedimensional photogrammetry as a tool for estimating morphometrics and body mass of

steller sea lions (Eumetopias jubatus). *Canadian Journal of Fisheries and Aquatic Sciences*, 64(2):296–303, 2007.

54. C. Ware, R. Arsenault, M. Plumlee, and D. Wiley. Visualizing the underwater behavior of humpback whales. *IEEE Computer Graphics and Applications*, 26(4):14–18, 2006.

55. C. Ware, D. N. Wiley, A. S. Friedlaender, M. Weinrich, E. L. Hazen, A. Bocconcelli, S. E. Parks, A. K. Stimpert, M. A. Thompson, and K. Abernathy. Bottom side-roll feeding by humpback whales (megaptera novaeangliae) in the southern gulf of maine, U.S.A. *Marine Mammal Science*, 30(2):494–511, 2014.

56. D. Wiley, C. Ware, A. Bocconcelli, D. Cholewiak, A. Friedlaender, M. Thompson, and M. Weinrich. Underwater components of humpback whale bubble-net feeding behaviour. *Behaviour*, 148(5/6):575–602, 2011.

57. T. M. Williams. The evolution of cost efficient swimming in marine mammals: Limits to energetic optimization. *Philosophical Transactions of the Royal Society B: Biological Sciences*, 354(1380):193–201, 1999.

58. T. M. Williams, S. B. Blackwell, B. Richter, M. H. S. Sinding, and M. P. Heide-Jørgensen. Paradoxical escape responses by narwhals (Monodon monoceros). *Science*, 358(6368):1328–1331, 2017.

SYNTHESIS

DISSERTATION SUMMARY

My dissertation includes three related components. Chapter 1 describes the design and fabrication of a non-invasive animal-borne electronic biologging tag that records sleep in wild northern elephant seals. This chapter details and reviews my process and recommendations to guide scientists as they develop new tools that investigate brain and heart functions in wild animals. Chapter 2 describes the deployment of this sleep tag on seals at sea to compare their sleep patterns with those of seals on land and in the lab. I used patterns in a relatively small, high-resolution EEG dataset to estimate sleep in hundreds of time-depth records across a rich, 20-year dataset. The need to feed dictates sleep time in seals at sea, confining sleep to 2 h per day over several months. While at sea, their extreme physiology allows seals to sleep underwater during long breath holds, where their sleep state dictates their three-dimensional motion. To unravel the biomechanics of sleep, I developed a custom visualization framework (Chapter 3) to visualize the underwater behavior and physiology of marine mammals. This allowed me to discover the morphology of a "sleep spiral" where seals shift from slow-wave sleep to rapid-eye movement sleep and become paralyzed. Upon transitioning to REM sleep, the seals lose control of their posture, turn upside down, and begin to spin. Sleep paralysis at depth, even in the presence of predators, suggests that their extreme physiology frees them from

constraints most prey face, by allowing them to sleep far from predators. My dissertation provides technology, analytical and visualization techniques that bring hidden behaviors and physiology to life as scientists explore the physiological extremes of the natural world.

IMPLICATIONS & FUTURE DIRECTIONS

I plan to expand the tools and techniques developed as part of my dissertation to facilitate behavioral and physiological research across multiple study systems –seals, sea lions, narwhals, humpback whales, blue whales, and humans. I am currently modifying the EEG device I created during my dissertation to measure clinical and subclinical seizures in California sea lions. Domoic acid toxicosis can result in acute and chronic epilepsy in sea lions, closely resembling the presentation of human mesial temporal lobe epilepsy. Therefore, research involving long-term monitoring of seizures and the exploration of experimental epilepsy treatments have potential benefits for sea lion conservation and translational medicine. Compared to mouse models, the sea lion brain is larger, and its epileptic pathology more closely matches that of human mesial temporal lobe epilepsy. Similarly, understanding sleep apnea in elephant seals can elucidate the physiology and limitations of wild animals and shed light on human pathologies such as obstructive sleep apnea and oxygen-related injury.

These comparative studies are currently limited by our ability to efficiently interpret, visualize, and compare these disparate study systems. I hope to build a

comprehensive framework for physiological data visualization that allows direct comparisons between parallel data streams, to better understand the ecological and evolutionary constraints animals face in their natural environments and the parallels with human physiology. Comparative physiology research can flourish at the intersection of science, engineering, and art, where software tools that advance scientific knowledge within and across study systems provide a platform for translational research, leveraging the threads that connect humans to the natural world.